1973

Close-coupling Calculations For Massive Ion - Hydrogen Atom Collisions Inthe Linear-trajectory Model

Alfred Zakhele Msezane

CLOSE COUPLING CALCULATIONS FOR MASSIVE ION-HYDROGEN ATOM COLLISIONS IN THE LINEAR TRAJECTORY MODEL

by

ALFRED ZAKHELE MSEZANE
Department of Physics

Submitted in partial fulfillment
of the requirements for the degree of
Doctor of Philosophy

Faculty of Graduate Studies
The University of Western Ontario
London, Canada
March, 1973

ABSTRACT

The Wilets and Gallaher (1966) formulation of H^+ - H collision has been generalized to the case of the heavy ion-atomic hydrogen collision. The resulting coupled differential equations have been solved and a computer program has been constructed to extract numerical results.

Calculations for the specific example of He^{2+} - H collision have been carried out using both eigenfunction and pseudo-state expansion bases. Charge transfer, excitation and ionization cross sections are presented and compared with other theoretical calculations and experimental measurements where these are available.

It is further shown that an eigenfunction expansion basis is unlikely to reproduce the 1.2° experiments of Keever et al. (1966) in a calculation involving a four-state approximation.

ACKNOWLEDGEMENTS

The author is highly indebted to his faculty supervisor, Dr. D. F. Gallaher, for his ideas and excellent supervision throughout the investigation of the problem.

Discussions with and suggestions by Dr. J. D. Bessis, Service de Physique Théorique, Centre d'Etudes Nucleaires de Saclay, France, who has been a visiting professor at the University of Western Ontario during 1971-1972, are highly appreciated. Sincere gratitude is extended to Dr. D. Rapp for making available to us his prepublication results on the He^{2+} - H collisions.

Thanks are due to the Physics Department for providing the facilities to carry out this investigation and to the Computing Centre for providing the computing facilities.

The author expresses gratitude to the advisory committee, and to those who directly or indirectly contributed towards the preparation of the thesis.

Finally, I wish to thank my wife for her support and for checking the equations and Mrs. C. Evans for her expert typing of the thesis.

TABLE OF CONTENTS

LIST OF TABLES

LIST OF FIGURES

CHAPTER I
INTRODUCTION

In recent years extensive theoretical investigations of the collision between protons and hydrogen atoms have been carried out using coupled channel calculations (see for example Wilets and Gallaher 1966, Gallaher and Wilets 1968, Cheshire 1968, Cheshire et al 1970 and Gaussorgues and Salin 1971). It is the purpose of this thesis to obtain a mathematical formulation, numerical methods and a computer program for the general case of the collision between a heavy ion with a hydrogen atom. Numerical results are sought for the specific case of an α-particle scattered from a hydrogen atom.

We have chosen a heavy ion as our projectile to study both charge transfer and direct excitation of the hydrogen atom using the non-relativistic semi-classical impact parameter model of Bates (1958). The model assumes the heavy ion and the proton move in straight line trajectories with constant relative velocity. In this thesis the incident ion is assumed to retain its structure throughout the encounter. Hereafter, the heavy ion will be referred to as "unstructured". Thus we are dealing with only three

bodies; the ion, the proton and the electron. The hydrogen atom is initially in the ground state or in any one of its excited states.

The collision between a heavy ion and a hydrogen atom yields in general charge transfer, excitation of the atom and ionization. Cross sections for these processes can be calculated in principle and measured experimentally in some cases. In charge transfer the final state consists of an electron bound to the ion plus a proton. Excitation of the atom arises when the final state is composed of an excited hydrogen atom and the ion. For the computation of cross sections for these processes, the electronic wave function is therefore expanded about the ion and the proton. These then constitute the two centres.

In order to assess the validity of a particular theoretical model it is essential to have as few variables in the model as possible. Then any disagreement between the calculated cross sections and the experimentally determined cross sections must reflect the inadequacy of the particular model. The hydrogen atom is the simplest atomic system, consisting only of one electron bound to a proton. The bound-state wave functions are well known and the system is mathematically simple to handle. Consequently, the hydrogen atom can be utilized as a convenient target for testing theoretical models which deal with charge transfer and direct excitation of an atom. Any uncertainty in the calculated cross sections can be

attributed to the inadequacy of the approximation employed, assuming all numerical computations have been performed correctly.

The specific case of He^{2+} - H collision yields the following possible results:

$$He^{2+} + H(1s) \rightarrow H^{+} + He^{+}(1s, 2s, \ldots) \qquad (a)$$

$$He^{2+} + H(1s) \rightarrow He^{2+} + H(2s, 2p, \ldots) \qquad (b)$$

$$He^{2+} + H(1s) \rightarrow He^{2+} + H^{+} + e^{-} \qquad (c)$$

These processes are respectively described as charge transfer, direct excitation and ionization; the initial state of the hydrogen atom need not necessarily be the ground state. Elastic scattering is a special case of direct excitation in which no energy is transferred to the active electron.

Throughout the thesis multi-state will mean inclusion of two or more states on either or both centres in the expansion of the electronic wave function. Theoretical calculations in a multi-state approximation for process (a) are few and, to our knowledge, none for reactions (b) and (c) in the energy range under consideration. Computing difficulties are mainly responsible for the lack of both a large number of and more extensive calculations in ion-atom collisions; these difficulties arise chiefly from matrix elements involving oscillatory momentum transfer terms and also from the large number of coupled differential equations which result when the expansion of the total

electronic wave function contains many eigenstates. In what follows we merely state without details what has been accomplished so far in the calculation of the charge transfer process for the He^{2+} - H collision.

The development of detailed charge transfer computations began with Oppenheimer (1928) and Brinkman and Kramers(1930), who employed the first Born approximation to evaluate charge transfer cross sections by assuming the relevant interaction potential to be that between the incident ion and the atomic electron. The theory of non-resonance charge transfer for α-particles colliding with atomic hydrogen was almost non-existent until Schiff (1954) used the first Born approximation in the energy range 100 keV - 1 Mev of the incident α-particle to evaluate charge exchange cross sections for reaction (a), taking the projectile-electronic interaction as the effective interaction. Using a two-state calculation, McCarroll and McElroy (1962) evaluated charge transfer cross sections for the non-resonance reaction

$$He^{2+} + H(1s) \rightarrow H^{+} + He^{+}(1s)$$

and McElroy (1963) obtained capture cross sections for the asymmetric accidental resonance process

$$He^{2+} + H(1s) \rightarrow H^{+} + He^{+}(2s \text{ or } 2p).$$

McElroy took into consideration momentum transfer to the active electron, partially included distortion and neglected back-coupling from the final to the initial state.

Basu et al (1967) calculated charge transfer to the n=1 and n=2 levels of He^{+} in a multi-state approximation

but neglected the important momentum transfer terms. Macomber and Webb (1967) pointed out the importance of back-coupling and the full distortion term in a two-state calculation of charge transfer cross sections. Coleman and Trelease (1968) evaluated charge exchange in the impulse approximation. They included only continuum states in the expansion of the total electronic wave function.

The most extensive calculation of charge transfer reported to date in a multi-state approximation taking into consideration momentum transfer, back-coupling and the full distortion term but neglecting rotational coupling has been carried out by Malaviya (1969).

The number of experiments available on charge exchange, direct excitation and ionization to focus the course of theoretical development is very small, in fact almost non-existent in some cases. The measurement of the total capture cross section for the accidental resonance reaction

$$He^{2+} + H(1s) \rightarrow H^{+} + He^{+}(2s \text{ or } 2p)$$

has been performed by Fite et al (1962), who covered the energy range 0.1 - 36 keV for the incident α-particle. Keever and Everhart (1966) measured the capture probability in the collision process

$$^{3}He^{2+} + H \rightarrow {}^{3}He^{+} + H^{+}$$

in the energy region 2 - 100 keV of the projectile.

Now that we have presented briefly the state of theoretical treatment on the subject of charge exchange

from the collision of α-particles with hydrogen atoms and none on direct excitation and ionization, let us state unambiguously what, in our opinion, are some of the remaining problems which require consideration. The sequence does not necessarily represent the order of importance nor urgency.

(i) Calculation of ionization and direct excitation of the active electron to various states of the target atom still remains.

(ii) According to Bates and McCarroll (1962) rotational-coupling effects which cause transitions among states with different m-values but the same $\ell \neq 0$ become important at low velocity of the α-particle and therefore should be considered in a multi-state calculation.

(iii) McElroy has predicted that for sufficiently high velocities of the incident α-particle, capture should occur more readily into the ground state of the He^+ ion, that is the $He^+(1s)$ state is more highly populated than the other states of He^+. Consequently, the transition to the ground state of He^+ should be considered in the calculation.

(iv) Expanding the total electronic wave function in terms of eigenstates is valid as long as the nuclear-nuclear separation distance R(t) is large. However, as $R(t) \to 0$ the adequacy of this expansion deteriorates. To fix our minds, consider a heavy

ion at infinity approaching atomic hydrogen. When R(t) is large enough the charge densities of the ions centred about each nucleus are well defined and distinct. Therefore the electron which is initially associated with the proton sees or feels two well defined charge distributions. As the ions approach each other and R(t) becomes smaller, the charge distributions associated with each nucleus begin to overlap. Consequently, the electron no longer sees the two distinct ions. When $R(t) \to 0$ and if there were enough binding energy to bind the two ions together, then the α-particle (the particular incident heavy ion in which we are interested) plus the proton would form the nucleus of ^5Li. The resulting atom would be doubly ionized ^5Li. This progression from one extreme to the other, reflects our ideas embodied in the solution of the collision problem under examination. The ion could still collide with the hydrogen atom with the electron perceiving the charge distributions about the distinct nuclei. This will depend upon the impact parameter. Following Cheshire et al. (1970) and incorporating the ideas already presented, we shall employ pseudo-states in an attempt to simulate the collision problem in a more realistic manner. These pseudo-states are unphysical and are chosen such that they have a

strong overlap with the intermediate states of Li^{++} only if the projectile is an α-particle and thus simulate the molecular features at small separations.

In the following chapters we shall attempt to take into account the preceding effects when we solve the scattering problem. At this juncture it may be worth-while to present the outline of the thesis. Chapters II and IV respectively entail mathematical development of and numerical methods for the solution of the general case of the scattering between a heavy ion and atomic hydrogen. In Chapter III, the general collision equations are reduced to the two-state expressions of McElroy (1963); some of the effects already mentioned are elucidated and deficiencies in previous theories for the specific case of α-particles colliding with atomic hydrogen are brought out. Numerical results are presented and compared with those of available experiments and previous theories in Chapter V. Finally, Chapter VI is devoted to the conclusion.

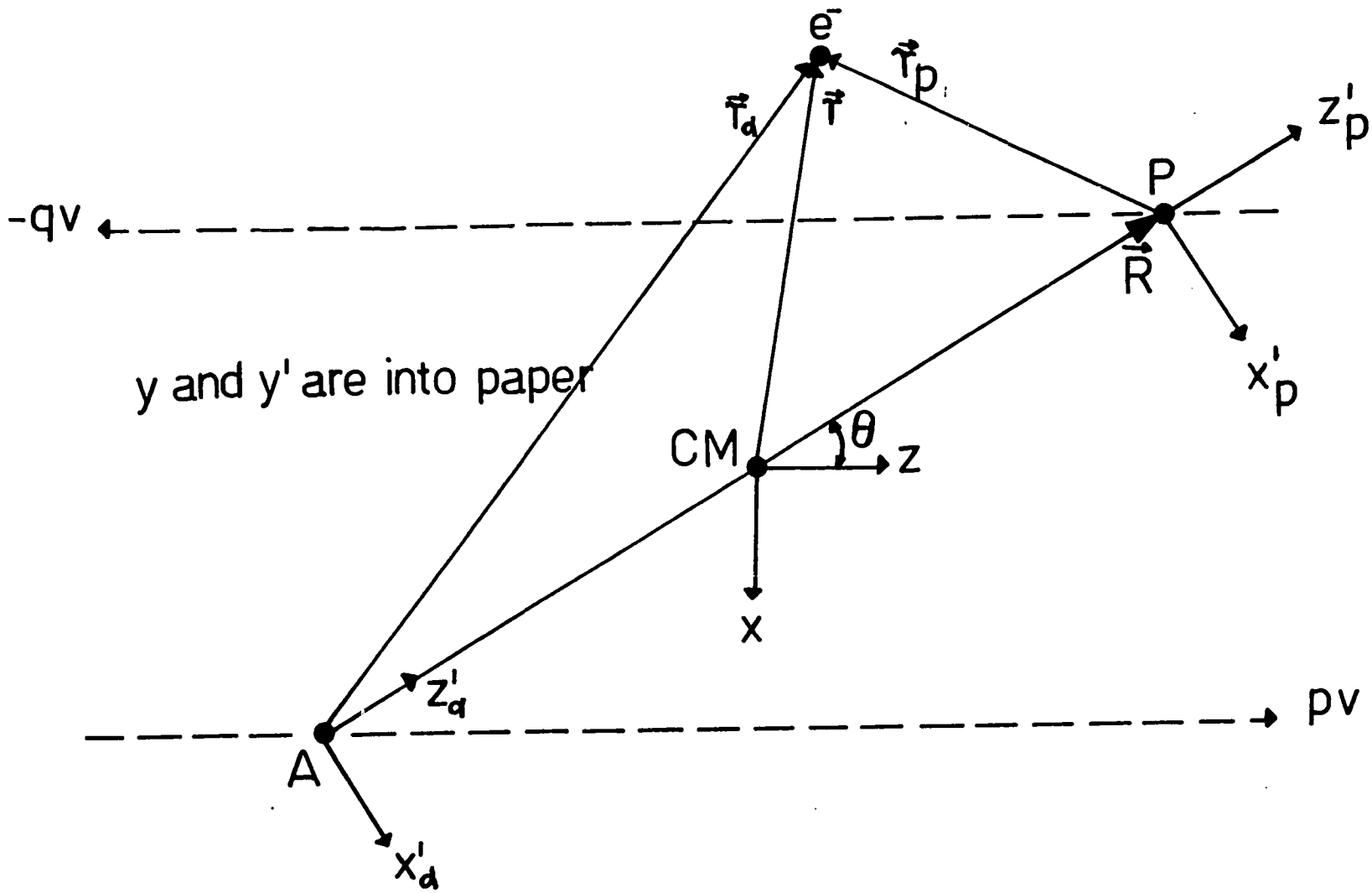

Fig. 2.1. Coordinate Representation of the Collision.

CHAPTER II

THEORY AND FORMALISM

2.2. The Coordinate System

The coupled differential equations for the scattering amplitudes to be derived shortly represent the general case of the collision of an unstructured heavy ion of charge Z and mass M with atomic hydrogen in a multi-state approximation using a double-centred expansion for the total electronic wave function. Atomic units (a.u.) will be employed throughout the thesis unless otherwise specified. In this system of units $\hbar = 1$, the electron mass, $m = 1$ and the electron charge, $e = 1$. The unit of length is the Bohr radius of the hydrogen atom $a_o = \hbar^2/me^2 = 0.529\text{Å}$ and the unit of energy is twice the Rydberg defined by $\frac{e^2}{a_o} = 27.2$ eV.

The frame of reference for the scattering problem is shown in Figure 2.1 and is labelled in anticipation of numerical calculations in which an α-particle is substituted for the heavy ion. In Figure 2.1, A represents the position of the ion and P that of the proton whose mass is m_p. The vector $\overline{R}$, the internuclear separation between the nuclei, is related to the vector $\overline{\rho}$, the impact parameter by

$$\overline{R} = \overline{\rho} + \overline{v}t \qquad (2.1)$$

where $\overline{v}$ is the velocity of the projectile in the laboratory coordinate system, and t is the collision time such that at $t = 0$, A and P are closest to each other.

The position vector of the electron (e^-) relative to the centre-of-mass (CM) of the ion-proton system is denoted by $\bar{r}$. The vectors $\bar{r}_\alpha$ and $\bar{r}_p$ represent respectively the positions of the electron from A and P, and are given by

$$\bar{r}_\alpha = \bar{r} + p\bar{R} \qquad (2.2)$$

$$\bar{r}_p = \bar{r} - q\bar{R}$$

where

$$p = \frac{m_p}{M+m_p}$$

$$q = \frac{M}{M+m_p}$$

and

$$p + q = 1 .$$

The coordinate system xyz, fixed at the CM of the nuclei, consists of x and z in the collision plane while y is perpendicular to the plane. $x'_\alpha y'_\alpha z'_\alpha$ and $x'_p y'_p z'_p$, two rotating coordinate systems centred respectively on A and P, are chosen with $y'_\alpha = y'_p = y$, z'_α and z'_p along the internuclear line. The angle between the z-axis and $\bar{R}$ is determined by

$$\rho = R \sin\theta \qquad (2.3)$$

and ϕ denotes the corresponding azimuthal angle of the electron relative to the collision plane. θ'_α, ϕ'_α are the polar and azimuthal angles of the electron relative to A and θ'_p, ϕ'_p the same angles relative to P.

2.2 The Coupled Differential Equations

Having defined the reference frame for the collision problem, we now proceed with the derivation of the coupled differential equations for the scattering amplitudes. For convenience let us adopt at once Einstein's summation convention

in which summation over repeated indices is implied.

Following Bates (1958) the electronic wave function which allows for the energy and momentum associated with the translational motion of the active electron relative to the projectile and is variationally correct (Geltman, 1965, page 203) can be written in a two-centred expansion. The true electronic wave function which can be represented by an expansion over a denumerably infinite number of discrete states and a non denumerably infinite number of continuum states will in practice be represented by a variational trial function because of the truncation of this expansion after a finite number of terms. Thus one writes for the electronic wave function

$$\Psi(\bar{r},t) = a_k(t)W_k(\bar{r}_p,t) + b_k(t)U_k(\bar{r}_\alpha,t) \qquad (2.4)$$

In this expansion

$$U_k(\bar{r}_\alpha,t) = u_k(\bar{r}_\alpha)\ e^{ivpz}\ e^{-iE_k^\alpha t}$$

$$W_k(\bar{r}_p,t) = w_k(\bar{r}_p)\ e^{-ivqz}\ e^{-iE_k^p}$$

and the total energies E^α and E^p are given by

$$E^\alpha = \varepsilon^\alpha + \tfrac{1}{2}(pv)^2$$

$$E^p = \varepsilon^p + \tfrac{1}{2}(qv)^2$$

where $u_k(\bar{r}_\alpha)$ and $w_k(\bar{r}_p)$ the eigenfunctions with eigenenergies ε_k^α and ε_k^p of the respective operators $H^\alpha = -\frac{\nabla^2}{2} - \frac{Z}{r_\alpha}$ and $H^p = -\frac{\nabla^2}{2} - \frac{1}{r_p}$, satisfy the equations

$$\left(-\frac{\nabla^2}{2} - \frac{Z}{r_\alpha}\right) u_k(\bar{r}_\alpha) = \varepsilon_k^\alpha \; u_k(\bar{r}_\alpha)$$

$$\left(-\frac{\nabla^2}{2} - \frac{1}{r_p}\right) w_k(\bar{r}_p) = \varepsilon_k^p \; w_k(\bar{r}p) \qquad (2.5)$$

with $\varepsilon_n = -\frac{Z^2}{2n^2}$ and the set of quantum numbers(n&lm) are represented by k. The expansion coefficients a_k and b_k are time dependent and in the limit $t \to +\infty$ determine the probabilities of excitation of the target atom and charge transfer to the projectile. The terms e^{-ivqz} and e^{ivpz} (momentum transfer terms) take account of the translational motion of the electron when associated with the target proton or with the projectile ion respectively.

In general, the expansion (2.4) should include a summation over discrete states and integration over the continuum. According to Coleman and Trelease (1968), a good wave function for the electron should include the most important bound states together with the continuum. This remark coupled with the observed slow convergence of the expansion (2.4) when applied to protons scattering from hydrogen atoms (Wilets and Gallaher 1966) has prompted us to employ pseudo-states to achieve a more realistic representation of the collision problem at both large and small separation distances of the nuclei.

Our interest lies in the solution of the time dependent Schrödinger equation,

$$H\,\bar{\Psi}(\bar{r}, t) = i\,\frac{\partial}{\partial t}\;\bar{\Psi}(\bar{r}, t) \qquad (2.6)$$

with the complete Hamiltonian given by

$$H(t) = -\frac{\nabla^2}{2} - \frac{1}{r_p} - \frac{Z}{r_\alpha} + \frac{Z}{R} \quad .$$

H depends parametrically upon the time through R [equations (2.1) and (2.2)]. The Coulomb term $\frac{Z}{R}$ which describes the interaction between the nuclei may be included or omitted without affecting the final probabilities (Gallaher, Ph.D. thesis). In this calculation we have omitted it. Hence H will be taken without the $\frac{Z}{R}$ term as

$$H(t) = -\frac{\nabla^2}{2} - \frac{1}{r_p} - \frac{Z}{r_\alpha} \qquad (2.7)$$

Therefore, the immediate task is the solution of (2.6) with the Hamiltonian (2.7) for the amplitudes a_k and b_k, and thence to determine the probabilities of excitation of the target atom and charge exchange to the projectile as $t \to +\infty$. To accomplish this purpose, let us write for conciseness and convenience,

$$\hat{\varepsilon}_k \equiv \varepsilon_k^\alpha, \quad \varepsilon_k \equiv \varepsilon_k^p$$

and

$$(\alpha) \equiv (\bar{r}_\alpha, t), \quad (p) \equiv (\bar{r}_p, t)$$

so that

$$U_k(\alpha) \equiv U_k(\bar{r}_\alpha, t), \quad W_k(p) \equiv W_k(\bar{r}_p, t)$$

and

$$u_k(\bar{\alpha}) \equiv u_k(\bar{r}_\alpha), \quad w_k(\bar{p}) \equiv w_k(\bar{r}_p) \quad .$$

Operating upon $W_k(p)$ with H, we obtain

$$HW_k(p) = \left(-\frac{\nabla^2}{2} - \frac{1}{\gamma_p} - \frac{Z}{\gamma_\alpha}\right)\left(w_k(\bar{p})\ e^{-ivqz}\right)e^{-iE_k^p t}$$

$$= \left(-\frac{\nabla^2}{2} - \frac{1}{\gamma_p} - \frac{Z}{\gamma_\alpha}\right)\left(w_k(\bar{p})\right) \cdot e^{-ivqz}\ e^{-iE_k^p t}$$

$$- \left(\nabla w_k(\bar{p}) \cdot \nabla e^{-ivqz}\right)\ e^{-iE_k^p t} - \left(\frac{\nabla^2}{2}\ e^{-ivqz}\right)\cdot w_k(\bar{p}) e^{-iE_k^p t}\ ,$$

which after some manipulation reduces to

$$HW_k(p) = (E_k^p - \frac{Z}{\gamma_\alpha})W_k(p) + iqv[\frac{\partial}{\partial z}\ w_k(\bar{p})]e^{-ivqz}e^{-iE_k^p t} \quad (2.8).$$

In order to evaluate the quantities $i\frac{\partial}{\partial t}\ W_k(p)$ and $i\frac{\partial}{\partial t}\ U_k(\alpha)$, let us represent $i\frac{\partial}{\partial t}$ in terms of the rotating coordinate systems for each centre.

For the centre P one can write:

$$\begin{aligned} x_p' &= x \cos\theta + z \sin\theta \\ y_p' &= y \\ z_p' &= z \cos\theta - x \sin\theta - qR \end{aligned} \qquad (2.9a)$$

so that

$$\begin{aligned} \dot{x}_p' &= (-x \sin\theta + z \cos\theta)\ \dot{\theta} \\ &= (z_p' + qR)\ \dot{\theta} \\ \dot{z}_p' &= (-z \sin\theta - x \cos\theta)\ \dot{\theta} - q\dot{R} \\ &= -x_p'\ \dot{\theta} - q\dot{R} \end{aligned} \qquad (2.9b)$$

and consequently

$$\frac{\partial}{\partial t} = \dot{x}_p'\ \frac{\partial}{\partial x_p'} + \dot{z}_p'\ \frac{\partial}{\partial z_p'}\ . \qquad (2.9c)$$

Similar expressions can be obtained for the centre A:

$$\begin{aligned} x'_\alpha &= x \cos\theta + z \sin\theta \\ y'_\alpha &= y \\ z'_\alpha &= z \cos\theta - x \sin\theta + pR \end{aligned} \tag{2.9d}$$

with

$$\begin{aligned} \dot{x}'_\alpha &= (-x \sin\theta + z \cos\theta)\,\dot{\theta} \\ &= (z'_\alpha - pR)\,\dot{\theta} \\ \dot{z}'_\alpha &= (-z \sin\theta - x \cos\theta)\,\dot{\theta} + p\dot{R} \\ &= -x'_\alpha\,\dot{\theta} + p\dot{R} \end{aligned} \tag{2.9e}$$

and therefore we may also write

$$\frac{\partial}{\partial t} = \dot{x}' \frac{\partial}{\partial x'_\alpha} + \dot{z}'_\alpha \frac{\partial}{\partial z'_\alpha} \quad . \tag{2.9f}$$

The operation $i\frac{\partial}{\partial t} W_k(p)$ leads to

$$i\frac{\partial}{\partial t} W_k(p) = i\frac{\partial}{\partial t}\left[w_k(\bar{p}) e^{-ivqz}\, e^{-iE_k^p t}\right]$$

$$= E_k^p W_k(p) + i\left[\dot{x}'_p \frac{\partial}{\partial x'_p} + \dot{z}'_p \frac{\partial}{\partial z'_p}\right] w_k(\bar{p}) \cdot e^{-ivqz}\, e^{-iE_k^p t}$$

where $\frac{\partial}{\partial t}$ has been represented in terms of the rotating coordinate system for the centre P. Employing expressions (2.9b), we obtain for the preceding equation

$$i\frac{\partial}{\partial t} W_k(p) = E_k^p W_k(p) + i\left[(z'_p + qR)\,\dot{\theta}\,\frac{\partial}{\partial x'_p}\right.$$

$$\left. + (-x'_p\,\dot{\theta} - q\dot{R})\,\frac{\partial}{\partial z'_p}\right] w_k(\bar{p}) \cdot e^{-ivqz}\, e^{-iE_k^p t}$$

$$= E_k^p W_k(p) + i\dot{\theta}\left[z'_p \frac{\partial}{\partial x'_p} - x'_p \frac{\partial}{\partial z'_p}\right] w_k(\bar{p}) \cdot e^{-ivqz}\, e^{iE_k^p t}$$

$$+ iq\left[R\dot{\theta}\frac{\partial}{\partial x'_p} - \dot{R}\,\frac{\partial}{\partial z'_p}\right] w_k(\bar{p}) \cdot e^{-ivqz}\, e^{-iE_k^p t} \tag{2.10}$$

By exploiting the relations

$$\dot{R} = -v \cos\theta$$

$$\dot{\theta} = v \sin\theta / R$$

which may easily be derived from (2.1) and (2.3), one reorganizes (2.10) to the form

$$i\frac{\partial}{\partial t}W_k(p) = E_k^p W_k(p) - \dot{\theta}\ell_p W_k(p) + iq[v \sin\theta \frac{\partial}{\partial x_p'} + v \cos\theta \frac{\partial}{\partial z_p'}] W_k(\bar{p}) \cdot e^{-ivqz} e^{-iE_k^p t}$$

The orbital angular momentum operator ℓ_y' denoted by ℓ_p and given by

$$\ell_y' = -i [z_p' \frac{\partial}{\partial x_p'} - x_p' \frac{\partial}{\partial z_p'}]$$

operates here only upon $w_k(\bar{p})$.

From (2.9a)

$$\frac{\partial}{\partial z_p} = \frac{\partial z_p'}{\partial z} \frac{\partial}{\partial z_p'} + \frac{\partial x_p'}{\partial z} \frac{\partial}{\partial x_p'}$$

$$= \cos\theta \frac{\partial}{\partial z_p'} + \sin\theta \frac{\partial}{\partial x_p'} .$$

Therefore,

$$i\frac{\partial}{\partial t}W_k(p) = E_k^p W_k(p) - \dot{\theta}\ell_p W_k(p) + iqv(\frac{\partial}{\partial z}w_k(\bar{p})) e^{-ivqz} e^{-iE_k^p t} \quad (2.11)$$

A combination of (2.8) and (2.11) with some further manipulation leads to the more convenient form

$$[H - i\frac{\partial}{\partial t}] W_k(p) = [-\frac{Z}{\gamma_\alpha} + \dot{\theta}\ell_p] W_k(p) \quad (2.12)$$

When H is applied to the function $U_k(\alpha)$ we obtain the expression

$$H\, U_k(\alpha) = [E_k^\alpha - \frac{1}{r_p}]U_k(\alpha) - ipv\frac{\partial}{\partial z}u_k(\bar{\alpha}) \cdot e^{ivpz}\, e^{-iE_k^\alpha t}$$

which, following exactly the same procedure that led to (2.12) and employing the appropriate expression in (2.9) for the centre A, can be reduced to

$$[H - i\frac{\partial}{\partial t}]\, U_k(\alpha) = [-\frac{1}{r_p} + \dot{\theta}\ell_\alpha]\, U_k(\alpha) \qquad (2.13)$$

We note that in (2.13) ℓ_α operates only upon $u_k(\bar{\alpha})$, where in this case

$$\ell_\alpha = -i[z'_\alpha \frac{\partial}{\partial x'} - x'_\alpha \frac{\partial}{\partial z'_\alpha}] \quad .$$

The terms $\dot{\theta}\ell_p$ and $\dot{\theta}\ell_\alpha$ give rise to what is known as "rotational coupling" which is caused by the rotation of the internuclear line about the centre P or A and these terms have been neglected by previous investigators studying He^{2+} - H collisions.

To obtain the desired coupled differential equations, we differentiate (2.4) with respect to the time and find

$$i\frac{\partial}{\partial t}\,\bar{\Psi}(\bar{r},t) = i\,\dot{a}_k W_k(p) + a_k\, i\frac{\partial}{\partial t}\, W_k(p)$$

$$+ i\,\dot{b}_k\, U_k(\alpha) + b_k\, i\frac{\partial}{\partial t}\, U_k(\alpha)$$

$$\equiv H\,\bar{\Psi}(\bar{r},t).$$

Utilizing (2.12) and (2.13), and remembering that summation over k is implied, we recover the more meaningful and convenient form of the coupled differential equations for the amplitudes

$$i\,\dot{a}_k\,W_k(p) + i\,\dot{b}_k\,U_k(\alpha)$$

$$= a_k\left[-\frac{Z}{\gamma_\alpha} + \dot{\theta}\ell_p\right] W_k(p)$$

$$+ b_k\left[-\frac{1}{\gamma_p} + \dot{\theta}\ell_\alpha\right] U_k(\alpha) \qquad (2.14)$$

2.3 The Matrix Elements and the Coupled Differential Equations

In order to obtain the matrix elements of the operators appearing in (2.14) and, hence the coupled differential equations which are amenable to solution, let us write the complex conjugate of $W_k(p)$ and $U_k(\alpha)$:

$$W_k^*(p) = w_k(\bar{p})\; e^{ivqz}\; e^{iE_k^p t}$$

$$U_k^*(\alpha) = u_k^*(\bar{\alpha})\; e^{-ivpz}\; e^{iE_k^\alpha t}\ .$$

Multiplying (2.14) from the left by $W_{k'}^*(p)$ and integrating over all space we obtain for the left hand side of (2.14)

$$i\,\dot{a}_k \int d\bar{\gamma}\; w_{k'}^*(\bar{p}) e^{ivqz} e^{iE_{k'}^p t}\, w_k(\bar{p}) e^{-ivqz}\; e^{-iE_k^p t}$$

$$+ i\,\dot{b}_k \int d\bar{\gamma}\; w_{k'}^*(\bar{p}) e^{ivqz} e^{iE_{k'}^p t}\, u_k(\bar{\alpha}) e^{ivpz} e^{-iE_k^\alpha t}$$

$$= i\,\dot{a}_k\;\langle k'P|Pk\rangle\; e^{i\varepsilon_{k'k}t} + i\,\dot{b}_k \langle k'P|e^{ivz}|\alpha k\rangle e^{i(q-p)\frac{v^2}{2}t}$$

$$\times\; e^{i\varepsilon_{k'\hat{k}}t} \qquad (2.15)$$

where $\varepsilon_{k'k} = \varepsilon_{k'} - \varepsilon_k$, $\varepsilon_{k'\hat{k}} = \varepsilon_{k'} - \hat{\varepsilon}_k$

and $\varepsilon_k \equiv \varepsilon_k^p$, $p + q = 1$, $\hat{\varepsilon}_k \equiv \varepsilon_k^\alpha$.

After similar multiplication and integration, each term on the right hand side of (2.14) can be written separately in

a more compact and obvious notation as

$$a_k \int d\bar{\gamma}\, W^*_{k'}(p)\, [-\frac{Z}{\gamma_\alpha} + \dot{\theta}\ell_p]\, W_k(p)$$

$$= a_k \int d\bar{\gamma}\, [w^*_{k'}(\bar{p})(-\frac{Z}{\gamma_\alpha} + \dot{\theta}\ell_p) w_k(\bar{p})]\, e^{+i(\varepsilon_{k'} - \varepsilon_k)t}$$

$$= a_k\, [\langle k'P|(\dot{\theta}\ell_p - \frac{Z}{\gamma_\alpha})|Pk\rangle]\, e^{i\varepsilon_{k'k}t} \qquad (2.16)$$

and

$$b_k \int d\bar{\gamma}\, W^*_{k'}(p)\, [-\frac{1}{\gamma_p} + \dot{\theta}\ell_\alpha]\, U_k(\alpha)$$

$$= b_k[\langle k'P|e^{ivz}(\dot{\theta}\ell_\alpha - \frac{1}{\gamma_p})|\alpha k\rangle]\, e^{i(q-p)\frac{v^2}{2}t}\, e^{i\varepsilon_{k'\hat{k}}t} \qquad (2.17)$$

where we have used

$$(qv)^2/2 - (pv)^2/2 = \frac{v^2}{2}[q^2 - p^2] = \frac{v^2}{2}(q - p).$$

Finally, from expressions (2.15), (2.16) and (2.17) we obtain

$$i\,\dot{a}_k\langle k'P|Pk\rangle e^{i\varepsilon_{k'k}t} + i\,\dot{b}_k\langle k'P|e^{ivz}|\alpha k\rangle e^{i(q-p)\frac{v^2}{2}t}\, e^{i\varepsilon_{k'\hat{k}}t}$$

$$= a_k[\langle k'P|(\dot{\theta}\ell_p - \frac{Z}{\gamma_\alpha})|Pk\rangle]\, e^{i\varepsilon_{k'k}t}$$

$$+ b_k[\langle k'P|e^{ivz}(\dot{\theta}\ell_\alpha - \frac{1}{\gamma_p})|\alpha k\rangle]\, e^{i(q-p)\frac{v^2}{2}t}\, e^{i\varepsilon_{k'\hat{k}}t} \qquad (2.18)$$

Similarly by multiplying (2.14) by $U^*_{k'}(\alpha)$ and proceeding exactly as before we obtain

$$i\,\dot{a}_k\langle k'\alpha|e^{-ivz}|Pk\rangle e^{i(p-q)\frac{v^2}{2}t}\, e^{i\varepsilon_{\hat{k}'k}t}$$

$$+ i\,\dot{b}_k\langle k'\alpha|\alpha k\rangle\, e^{i\varepsilon_{\hat{k}'k}t}$$

$$= a_k\langle k'\alpha|e^{-ivz}[\dot{\theta}\ell_p - \frac{Z}{\gamma_\alpha}]|Pk\rangle e^{i(p-q)\frac{v^2}{2}t}\, e^{i\varepsilon_{\hat{k}'k}t}$$

$$+ b_k\langle k'\alpha|[\dot{\theta}\ell_\alpha - \frac{1}{\gamma_p}]|\alpha k\rangle\, e^{i\varepsilon_{\hat{k}'\hat{k}}t} \qquad (2.19)$$

Equations (2.18) and (2.19) represent the forms of (2.14) we wanted and they will be solved for the amplitudes a_k and b_k as $t \to \infty$. These equations are cumbersome to handle as they stand. We shall therefore express (2.18) and (2.19) in a more compact and easy to manipulate form as

$$i\, P_{k'k}\, \dot{a}_k + i\, S_{k'k}\, \dot{b}_k = Q_{k'k}\, a_k + R_{k'k}\, b_k$$

$$i\, T_{k'k}\, \dot{a}_k + i\, L_{k'k}\, \dot{b}_k = M_{k'k}\, a_k + N_{k'k}\, b_k \qquad (2.20)$$

or identically

$$i\, P\, \dot{a} + i\, S\, \dot{b} = Qa + Rb$$

$$i\, T\, \dot{a} + i\, L\, \dot{b} = Ma + Nb \qquad (2.21)$$

where the time dependent matrix elements are given by

$$P_{k'k} \equiv \langle k'P | Pk \rangle\, e^{i\varepsilon_{k'k}t}$$

$$= \int d\bar{\gamma}\, w^*_{k'}(\bar{\gamma}_p)\, w_k(\bar{\gamma}_p)\, e^{i\varepsilon_{k'k}t}$$

$$S_{k'k} \equiv \langle k'P | e^{ivz} | \alpha k \rangle\, e^{i(q-p)\frac{v^2}{2}t}\, e^{i\varepsilon_{k'\hat{k}}t}$$

$$= \int d\bar{\gamma}\, w^*_{k'}(\bar{\gamma}_p)\, e^{ivz}\, u_k(\bar{\gamma}_\alpha)\, e^{i(q-p)\frac{v^2}{2}t}\, e^{i(\varepsilon_{k'}-\hat{\varepsilon}_k)t}$$

$$Q_{k'k} \equiv \langle k'P | [\dot{\theta}\ell_p - \frac{Z}{\gamma_\alpha}] | Pk \rangle\, e^{i\varepsilon_{k'k}t}$$

$$= \int d\bar{\gamma}\, w^*_{k'}(\bar{\gamma}_p)[\dot{\theta}\ell_p - \frac{Z}{\gamma_\alpha}]\, w_k(\bar{\gamma}_p)\, e^{i\varepsilon_{k'k}t}$$

$$R_{k'k} \equiv \langle k'P | e^{ivz}[\dot{\theta}\ell_\alpha - \frac{1}{\gamma_p}] | \alpha k \rangle\, e^{i(q-p)\frac{v^2}{2}t}\, e^{i\varepsilon_{k'\hat{k}}t}$$

$$= \int d\bar{\gamma}\, w^*_{k'}(\bar{\gamma}_p)\, e^{ivz}[\dot{\theta}\ell_\alpha - \frac{1}{\gamma_p}]\, u_k(\bar{\gamma}_\alpha)\, e^{i(q-p)\frac{v^2}{2}t}\, e^{i\varepsilon_{k'}\hat{k}t}$$

$$T_{k'k} \equiv \langle k'\alpha | e^{-ivz} | Pk \rangle \; e^{-i(q-p)\frac{v^2}{2}t} \; e^{i\varepsilon\hat{k}'k t}$$

$$= \int d\bar{\gamma} \; u^*_{k'}(\bar{\gamma}_\alpha) \; e^{-ivz} \; w_k(\bar{\gamma}_p) \; e^{-i(q-p)\frac{v^2}{2}t} \; e^{i\varepsilon\hat{k}'k t}$$

$$L_{k'k} \equiv \langle k'\alpha | \alpha k \rangle \; e^{i\varepsilon\hat{k}'\hat{k}t}$$

$$= \int d\bar{\gamma} \; u^*_{k'}(\bar{\gamma}_\alpha) \; u_k(\bar{\gamma}_\alpha) \; e^{i\varepsilon\hat{k}'\hat{k}t}$$

$$M_{k'k} \equiv \langle k'\alpha | e^{-ivz}[\dot{\theta}\ell_p - \frac{Z}{\gamma_\alpha}] | Pk \rangle \; e^{-i(q-p)\frac{v^2}{2}t} \; e^{i\varepsilon\hat{k}'k t}$$

$$= \int d\bar{\gamma} \; u^*_{k'}(\bar{\gamma}_\alpha) e^{-ivz}[\dot{\theta}\ell_p - \frac{Z}{\gamma_\alpha}] \; w_k(\bar{\gamma}_p) \; e^{-i(q-p)\frac{v^2}{2}t} \; e^{i\varepsilon\hat{k}'k t}$$

$$N_{k'k} \equiv \langle k'\alpha | [\dot{\theta}\ell_\alpha - \frac{1}{\gamma_p}] | \alpha k \rangle \; e^{i\varepsilon\hat{k}'\hat{k}t}$$

$$= \int d\bar{\gamma} \; u^*_{k'}(\bar{\gamma}_\alpha)[\dot{\theta}\ell_\alpha - \frac{1}{\gamma_p}] \; u_k(\bar{\gamma}_\alpha) \; e^{i\varepsilon\hat{k}'\hat{k}t} \qquad (2.22)$$

For convenience we factorize the matrix elements in (2.22) and write them as

$$P_{k'k} = \hat{P}_{k'k} \; e^{i\varepsilon k'k t}$$

$$S_{k'k} = \hat{S}_{k'k} \; e^{i(q-p)\frac{v^2}{2}t} \; e^{i\varepsilon k'\hat{k}t}$$

$$Q_{k'k} = \hat{Q}_{k'k} \; e^{i\varepsilon k'k t}$$

$$R_{k'k} = \hat{R}_{k'k} \; e^{i(q-p)\frac{v^2}{2}t} \; e^{i\varepsilon k'\hat{k}t}$$

$$T_{k'k} = \hat{T}_{k'k} \; e^{-i(q-p)\frac{v^2}{2}t} \; e^{i\varepsilon\hat{k}'k t}$$

$$L_{k'k} = \hat{L}_{k'k} \; e^{i\varepsilon\hat{k}'\hat{k}t}$$

$$M_{k'k} = \hat{M}_{k'k}\, e^{-i(q-p)\frac{v^2}{2}t}\, e^{i\varepsilon\hat{k}'k t}$$

$$N_{k'k} = \hat{N}_{k'k}\, e^{i\varepsilon\hat{k}'k t}$$

where the spatial elements are given by

$$\hat{P}_{k'k} = \delta_{k'k}$$

$$\hat{Q}_{k'k} = \langle k'P|[\dot{\theta}\ell_p - \frac{Z}{\gamma_\alpha}]|Pk\rangle$$

$$\hat{S}_{k'k} = \langle k'P|e^{ivz}|\alpha k\rangle$$

$$\hat{R}_{k'k} = \langle k'P|e^{ivz}[\dot{\theta}\ell_\alpha - \frac{1}{\gamma_p}]|\alpha k\rangle \qquad (2.22a)$$

$$\hat{T}_{k'k} = \langle k'\alpha|e^{-ivz}|Pk\rangle$$

$$\hat{L}_{k'k} = \delta_{k'k}$$

$$\hat{M}_{k'k} = \langle k'\alpha|e^{-ivz}[\dot{\theta}\ell_p - \frac{Z}{\gamma_\alpha}]|Pk\rangle$$

$$\hat{N}_{k'k} = \langle k'\alpha|[\dot{\theta}\ell_\alpha - \frac{1}{\gamma_p}]|\alpha k\rangle$$

The two matrix equations in (2.21) can be combined into a single coupled matrix equation. Thus

$$i\begin{pmatrix} P & S \\ T & L \end{pmatrix}\begin{pmatrix} \dot{a} \\ \dot{b} \end{pmatrix} = \begin{pmatrix} Q & R \\ M & N \end{pmatrix}\begin{pmatrix} a \\ b \end{pmatrix} \qquad (2.23)$$

or

$$i\begin{pmatrix} \dot{a} \\ \dot{b} \end{pmatrix} = \begin{pmatrix} P & S \\ T & L \end{pmatrix}^{-1}\begin{pmatrix} Q & R \\ M & N \end{pmatrix}\begin{pmatrix} a \\ b \end{pmatrix} \qquad (2.24)$$

and finally;

$$i\dot{A} = W A \qquad (2.25$$

or $\quad i\dot{A}_k = W_{kk'} A_{k'}$

where $A = \binom{a}{b}$ is a column matrix and W is a 2n x 2n time dependent matrix with n being the dimension of either a_k or b_k. Extreme care must be exercised when handling the coupled differential equations (2.25). In order to obtain a solution to these equations for the amplitudes A_k, we write the $W_{kk'}$ as a product of two quantities: one in which the time does not appear explicitly and another with explicit time dependence. With this separation of the $W_{kk'}$ the integration scheme designed by Wilets and Gallaher (1966) may then be applied in principle to effect the solution of (2.25). A number of authors have attempted to solve the coupled equations (2.25) or variations thereof in various approximations, which we shall discuss in Chapter III.

2.4 Time Dependence of the $W_{kk'}$

We want to express the coupled differential equations (2.25) such that the $W_{kk'}$ are written in the manner of the equations preceding (2.22a). Thus

$$i\dot{A} = W A$$

where $W_{kk'} = \hat{W}_{kk'} \cdot E_{kk'}(t)$. The explicit time dependence of the $W_{kk'}$ is now carried by $E_{kk'}(t)$. The $\hat{W}_{kk'}$ are implicit function of time through R(t). We shall encounter this time dependence when we consider numerical solutions to (2.25). To write the $W_{kk'}$ in the form $W_{kk'} = \hat{W}_{kk'} \cdot E_{kk'}(t)$ we make use of (2.21).

Operating upon the first of those equations from the left with P^{-1} (the inverse of the matrix P) and upon the second equation with T^{-1}, we eliminate $\dot{a}_k$ from the resulting equations and obtain:

$$i[P^{-1}S - T^{-1}L]\dot{b} = [P^{-1}Q - T^{-1}M]a + [P^{-1}R - T^{-1}N]b$$

or

$$i\,\dot{b} = D^{-1}B\,a + D^{-1}C\,b$$

and finally,

$$i\,\dot{b} = X\,a + Y\,b \tag{2.26}$$

where

$$X = D^{-1}B,\quad Y = D^{-1}C$$

$$D = P^{-1}S - T^{-1}L,\quad B = P^{-1}Q - T^{-1}M$$

and

$$C = P^{-1}R - T^{-1}N\ .$$

The elimination of $\dot{b}_k$ from (2.21) leads to the following expression for $\dot{a}_k$

$$i\,\dot{a} = D_1^{-1}\ B_1\,a + D_1^{-1}\ C_1\,b$$

or

$$i\,\dot{a} = X_1\,a + Y_1\,b \tag{2.27}$$

with

$$X_1 = D_1^{-1}\ B_1\ ,\quad Y_1 = D_1^{-1}\ C_1$$

$$D_1 = S^{-1}P - L^{-1}T,\quad B_1 = S^{-1}Q - L^{-1}M$$

and

$$C_1 = S^{-1}R - L^{-1}N.$$

Equations (2.26) and (2.27) can be brought together and written thus

$$i\begin{pmatrix}\dot{a}\\ \dot{b}\end{pmatrix} = \begin{pmatrix}X_1 & Y_1\\ X & Y\end{pmatrix}\begin{pmatrix}a\\ b\end{pmatrix} \tag{2.28}$$

The form of the coupled differential equations represented by (2.28) is convenient as long as one is interested in

extracting the explicit time dependence of W. However, for numerical computation (2.24) is preferred over (2.28) because the latter entails more matrices that require numerical inversion than the former.

We have expressed the matrix D as

$$D = P^{-1}S - T^{-1}L$$

so that from the definitions of P and S

$$(P^{-1}S)_{\alpha k'} = \hat{P}^{-1}_{\alpha k} e^{i\varepsilon_{\alpha k} t} \hat{S}_{kk'} e^{i\varepsilon_{k}\hat{k}'t} e^{i(q-p)\frac{v^2}{2}t}$$

$$= (\hat{PS})_{\alpha k'} e^{i\varepsilon_{\alpha}\hat{k}'t} e^{i(q-p)\frac{v^2}{2}t} .$$

Similarly from the definitions of T and L

$$(T^{-1}L)_{\alpha k'} = (\hat{TL})_{\alpha k'} e^{i\varepsilon_{\alpha}\hat{k}'t} e^{i(q-p)\frac{v^2}{2}t} .$$

Therefore

$$D_{kk'} = \hat{D}_{kk'} e^{i\varepsilon_{k}k't} e^{i(q-p)\frac{v^2}{2}t} \qquad (2.29)$$

Now $B = P^{-1}Q - T^{-1}M$ and $C = P^{-1}R - T^{-1}N$ and by choice of normalization P is merely $\delta_{kk'}$ so that the time dependence of B is the same as that of Q. C has the same time dependence carried by R. One can easily show that the time dependence of $T^{-1}M$ is the same as that of $P^{-1}Q$ and the time dependence of $T^{-1}N$ is the same as that of $P^{-1}R$.

Consequently, $B_{kk'} = \hat{B}_{kk'} e^{i\varepsilon_{k}k't}$ and

$C_{kk'} = \hat{C}_{kk'} e^{i\varepsilon_{k}\hat{k}'t} e^{i(q-p)\frac{v^2}{2}t}$ so that

$$X_{\alpha k'} \equiv (D^{-1}B)_{\alpha k'}$$

$$= \hat{D}^{-1}_{\alpha k}\, e^{i\varepsilon\hat{\alpha}k t}\, e^{-i(q-p)\frac{v^2}{2}t}\, \hat{B}_{kk'}\, e^{i\varepsilon_{kk'}t}$$

or

$$X_{kk'} = \hat{X}_{kk'}\, e^{i\varepsilon\hat{k}k't}\, e^{-i(q-p)\frac{v^2}{2}t}$$

and (2.30)

$$Y_{kk'} \equiv (D^{-1}C)_{kk'}$$

$$= \hat{Y}_{kk'}\, e^{i\varepsilon\hat{k}\hat{k}'t}$$

where

$$\hat{X}_{kk'} = \hat{D}^{-1}_{k\alpha}\, \hat{B}_{\alpha k'}$$

$$\hat{Y}_{kk'} = \hat{D}^{-1}_{k\alpha}\, \hat{C}_{\alpha k'}$$

and summation over repeated indices is implied.

From the definition of $D_1 = S^{-1}P - L^{-1}T$ and the relationship $L^{-1} = L(L_{kk'} = \delta_{kk'})$, we obtain

$$(D_1)_{kk'} = (\hat{D}_1)_{kk'}\, e^{i\varepsilon\hat{k}k't}\, e^{-i(q-p)\frac{v^2}{2}t},$$

which has the same time dependence as $(P^{-1}S)^{-1}$. The time dependence of C_1 is the same as that of N.

Thus

$$(C_1)_{kk'} = (\hat{C}_1)_{kk'}\, e^{i\varepsilon\hat{k}\hat{k}'t}.$$

Similarly M carries the same time dependence as B_1 so that

$$(B_1)_{kk'} = (\hat{B}_1)_{kk'}\, e^{i\varepsilon\hat{k}k't}\, e^{-i(q-p)\frac{v^2}{2}t}.$$

Therefore

$$(D_1^{-1}B_1)_{\alpha k'} = (\hat{D}_1^{-1})_{\alpha k}\, e^{i\varepsilon_{\alpha\hat{k}}t}\, e^{i(q-p)\frac{v^2}{2}t}\, (\hat{B}_1)_{kk'}\, e^{i\varepsilon_{\hat{k}k'}t} \times e^{-i(q-p)\frac{v^2}{2}t}$$

$$(D_1^{-1}B_1)_{kk'} = (\hat{X}_1)_{kk'}\, e^{i\varepsilon_{kk'}t}$$

and

$$(D_1^{-1}C_1)_{\alpha k'} = (\hat{D}_1^{-1})_{\alpha k} e^{i\varepsilon_{\alpha\hat{k}}t}\, e^{i(q-p)\frac{v^2}{2}t} (\hat{C}_1)_{kk'}\, e^{i\varepsilon_{\hat{k}\hat{k}'}t}$$

$$(D_1^{-1}C_1)_{kk'} = (\hat{Y}_1)_{kk'}\, e^{i\varepsilon_{k\hat{k}'}t}\, e^{i(q-p)\frac{v^2}{2}t}\ .$$

X_1 and Y_1 can now be expressed as

$$(X_1)_{kk'} = (\hat{X}_1)_{kk'}\, e^{i\varepsilon_{kk'}t}$$

and (2.31)

$$(Y_1)_{kk'} = (\hat{Y}_1)_{kk'}\, e^{i\varepsilon_{k\hat{k}'}t}\, e^{i(q-p)\frac{v^2}{2}t}\ .$$

The use of (2.30) and (2.31) enables us to extract the explicit time dependence of the matrices in (2.28). Thus

$$i\begin{pmatrix}\dot{a}_k\\ \dot{b}_k\end{pmatrix} = \begin{pmatrix}(\hat{X}_1)_{kk'}\, e^{i\varepsilon_{kk'}t} & (\hat{Y}_1)_{kk'} e^{i\varepsilon_{k\hat{k}'}t} e^{i(q-p)\frac{v^2}{2}t}\\ \hat{X}_{kk'}\, e^{i\varepsilon_{\hat{k}k'}t}\, e^{-i(q-p)\frac{v^2}{2}t} & \hat{Y}_{kk'} e^{i\varepsilon_{\hat{k}\hat{k}'}t}\end{pmatrix}\begin{pmatrix}a_{k'}\\ b_{k'}\end{pmatrix} \tag{2.32}$$

and consequently the expression for W becomes

$$W_{kk'} = \hat{W}_{kk'} \cdot E_{kk'}(t)$$

where

$$\hat{W}_{kk'} = \left[\begin{pmatrix}\hat{P} & \hat{S}\\ \hat{T} & \hat{L}\end{pmatrix}^{-1}\begin{pmatrix}\hat{Q} & \hat{R}\\ \hat{M} & \hat{N}\end{pmatrix}\right]_{kk'}$$

and (2.33)

$$E_{kk'}(t) = \begin{pmatrix} e^{i\varepsilon_{kk'}t} & e^{i\varepsilon_{k\hat{k}'}t} & e^{i(q-p)\frac{v^2}{2}t} \\ e^{i\varepsilon_{\hat{k}k'}t} & e^{-i(q-p)\frac{v^2}{2}t} & e^{i\varepsilon_{\hat{k}\hat{k}'}t} \end{pmatrix}$$

The results in (2.33) are general and exact; they represent a convenient form for the $W_{kk'}$ which will be used in the numerical solution for the amplitudes to determine the probabilities for excitation of the target H atom and charge transfer to the projectile and, hence the respective cross sections. It should be noted that equations (2.33) have no other connotation except that represented by (2.32).

2.5 Unitarity

The preservation of the normalization (unitarity) of the electronic wave function represented in (2.4) fulfils a useful purpose. In our calculation conservation of probability serves as an invaluable check upon both programming errors and incorrect numerical integration of the coupled differential equations for the amplitudes. To establish the unitarity condition one requires the explicit evaluation of the normalization integral, $\int d\bar{\gamma}\ \bar{\Psi}^*\ \bar{\Psi}$ which should equal unity.

Using the definition of $\bar{\Psi}$ in (2.4) one obtains

$$\int d\bar{\gamma}\ \bar{\Psi}^*(\bar{\gamma},t)\ \bar{\Psi}(\bar{\gamma},t)$$

$$= \int d\bar{\gamma}[a_k^*, W_{k'}^*(p) + b_{k'}^* U_{k'}^*(\alpha)][a_k W_k(p) + b_k\ U_k(\alpha)] \quad (2.34)$$

(the explicit summation over k and k' here has been suppressed.)

We have expressed the functions $W_k(p)$ and $U_k(\alpha)$ as

$$W_k(p) = w_k(\bar{p})\, e^{-ivqz}\, e^{-iE_k^p t}$$

$$U_k(\alpha) = u_k(\bar{\alpha})\, e^{ivpz}\, e^{-iE_k^\alpha t}$$

so that

$$\int d\bar{\gamma}\, W^*_{k'}(p)\, W_k(p) = \int d\bar{\gamma}\, U^*_{k'}(\alpha)\, U_k(\alpha) = \delta_{k'k}$$

and

$$\int d\bar{\gamma}\, U^*_{k'}(\alpha)\, W_k(p) = \int d\bar{\gamma}\, u^*_{k'}(\bar{\alpha})\, e^{-ivpz}\, e^{iE^\alpha_{k'}t}\, w_k(\bar{p}) e^{-ivqz} e^{-iE_k^p t}$$

$$= \langle k'\alpha | e^{-ivz} | pk \rangle\, e^{-i(q-p)\frac{v^2}{2}t}\, e^{i\varepsilon \hat{k}'k t} \qquad (2.35)$$

where $\varepsilon_{k\hat{k}'} = \varepsilon_k - \hat{\varepsilon}_{k'}$ and $p^2 - q^2 = -(q-p)$.

The expression on the right hand side of (2.35) is nothing but $T_{k'k}$ [see equations (2.22)]. Therefore, equation (2.35) may be rewritten as

$$\int d\bar{\gamma}\, U^*_{k'}(\alpha)\, W_k(p) = T_{k'k} \,.$$

Similarly the relationship

$$\int d\bar{\gamma} W^*_{k'}(p)\, U_k(\alpha) = \langle k'P | e^{ivz} | \alpha k \rangle e^{i(q-p)\frac{v^2}{2}t}\, e^{i\varepsilon_{k'}\hat{k}t}$$

can be established and further expressed as

$$\int d\bar{\gamma}\, W^*_{k'}(p)\, U_k(\alpha) = S_{k'k} = T^*_{kk'} \,.$$

The unitarity condition [equation (2.34)] now reduces to

$$\int d\bar{\gamma}\, \bar{\Psi}^*(\bar{\gamma},t)\, \bar{\Psi}\,(\bar{\gamma},t) = [a^*_{k'}a_k + b^*_{k'}b_k]\, \delta_{k'k}$$

$$+ a^*_{k'}b_k\, S_{k'k} + b^*_{k'}a_k\, T_{k'k} \,.$$

Introducing the summation sign explicitly, one finally writes

$$\int d\bar{\gamma}\ \bar{\Psi}^*(\bar{\gamma},t)\ \bar{\Psi}\ (\bar{\gamma},t) = \sum_k [|a_k|^2 + |b_k|^2] + \sum_{kk'} a_k^*, b_k\ S_{k'k}$$

$$+ \sum_{kk'} b_k^*, a_k\ T_{k'k} \qquad (2.36)$$

Equation (2.36) represents the unitarity condition to be satisfied by the electronic wave function and we employ it extensively in numerical computations for checking the acceptability of the calculated amplitudes a_k and b_k. Ideally, the summation represented by equation (2.36) should equal to unity before and after a computation.

One may also express the unitarity preservation condition by differentiating the preceding relation $\int d\bar{\gamma}\ \bar{\Psi}^*\ \bar{\Psi} = 1$ with respect to time. This finally gives a matrix equation expressing a relationship which must hold among various matrix elements which in other contexts has proven useful. It was not employed, however, in this thesis.

It may be pointed out that, because of time reversal invariance and detailed balance holding for this process an interesting check of the calculations could be made by "running the computer program backwards"; that is, starting at $t = -T_{max}$ with the amplitudes a_k and b_k appropriate to a given process one could ascertain whether the proper initial conditions $a_k\ (-\ T_{max}) = \delta_{1k}$ and $b_k\ (-\ T_{max}) = 0$ are recoverable at $t = +\ T_{max}$. This would impose a very stringent criterion on the calculation.

CHAPTER III

PREVIOUS SOLUTIONS

3.1 Introduction

In the previous chapter, we presented in general terms the mathematical formulation of the collision between an unstructured massive ion and atomic hydrogen. For the discussion of previous theoretical calculations and comparison with experimental results, we have selected explicitly an α-particle for the projectile. This chapter is therefore concerned mainly with the scattering of an α-particle by a hydrogen atom. Some of the calculations we shall consider do not necessarily involve a direct solution or manipulation of (2.25) in which Z is set equal to 2(the charge of the He^{2+} ion) and M equals 4; they, however, entail a solution of some kind for the He^{2+} - H collision problem.

To facilitate the discussion of previous theoretical solutions of the collision between an α-particle and a hydrogen atom and to avoid unnecessary reproduction of some expressions, let us rewrite (2.25)

$$i \dot{A} = W A \tag{3.1a}$$

with

$$W_{kk'} = \begin{pmatrix} P & S \\ T & L \end{pmatrix}^{-1}_{k\alpha} \begin{pmatrix} Q & R \\ M & N \end{pmatrix}_{\alpha k'} \qquad (3.1b)$$

and

$$A_k = \begin{pmatrix} a_k \\ b_k \end{pmatrix}$$

where the time dependent matrices on the right hand side of (3.1b) are defined in (2.22). Several calculations involving the collision of mainly protons with hydrogen atoms in various approximations to evaluate cross sections have been carried out using a differential equation resembling (3.1) or variants of it. Wilets and Gallaher (1966) were the first to apply (3.1) in a slightly different formulation to protons incident upon hydrogen atoms using a multi-state approximation to evaluate among other things charge transfer and direct excitation cross sections. Cheshire et al. (1970) applied the Wilets and Gallaher version of (3.1) to protons colliding with hydrogen atoms by replacing the eigenstates in (2.22) with pseudo-states. Recently, Gaussorgues and Salin (1971) have employed the Wilets and Gallaher formulation without the momentum transfer terms to the scattering of protons by hydrogen atoms to determine charge transfer differential cross sections. These are but a few examples of studies which involve the direct solution of (3.1) or variations of it for the specific case of proton-hydrogen collisions. They are intended to show that (3.1) is indeed general and therefore applicable in principle to the collision of an unstructured heavy ion with atomic hydrogen. The

availability of some experimental measurements and theoretical computations resulted in the selection of the α-particle as projectile for obtaining numerical results from the general formulation.

Dealing with proton-hydrogen scattering has the additional advantage of symmetry which is absent in the general case. In fact, Wilets and Gallaher ingeniously exploited symmetry arguments to reduce considerably the complexity of the problem, thereby reducing the cost of computing which remains a stumbling block towards a complete theoretical analysis of problems of this nature. In what follows we discuss previous solutions to (3.1) or variants of it as well as other approaches relevant to He^{2+} - H scattering to establish how much has been accomplished thus far and to what extent these results are reliable.

3.2 Previous Solutions of He^{2+} - H Collision

(a) McElroy (1963)

He solved the collision problem between an incident α-particle and a hydrogen atom which is initially in the ground state in a two-state approximation. While taking account partially of distortion he neglected back-coupling from the final to the initial state, which according to Macomber and Webb (1967) is not important at α-energies above about 100keV provided the correct distortion term is used. The inclusion of only the ground state of H in the expansion of the total electronic wave function limited

McElroy to the calculation of charge transfer to any one of the He^+ states considered.

With the necessary approximations we shall extract the equations of McElroy from (3.1) and, in the process, the meaning of distortion and back-coupling both of which are fully accounted for in our formulation will follow naturally. Towards this end, it is convenient to employ (2.21) rather than (3.1). Therefore, remembering that the matrix elements $P_{kk'}$ and $L_{kk'}$ are each merely $\delta_{kk'}$ and that $S = T^*$ in (2.22), we reduce (2.21) to McElroy's equations with the additional approximation that all $\dot{\theta}$-dependent terms in (2.22) are set equal to zero and that all terms not involving the initial or final states are omitted. Consequently, setting $P = L = I$ and premultiplying the second equation in (2.21) by T^{-1}, one obtains

$$\begin{aligned} i\,\dot{a} + i\,S\,\dot{b} &= Q\,a + R\,b \\ i\,a + i\,T^{-1}\dot{b} &= T^{-1}Ma + T^{-1}N\,b \end{aligned} \tag{3.2}$$

The elimination of $\dot{a}_k$ from (3.2) and some manipulation leads to

$$i(1 - TS)\dot{b} = (M - TQ)a + (N - TR)b \tag{3.3}$$

Similarly, by eliminating $\dot{b}_k$ from (2.21) one obtains

$$i(1 - ST)\dot{a} = (Q - SM)a + (R - SN)b \tag{3.4}$$

It must be stressed that the two-state approximation of McElroy does not involve intermediate states; it contains only the initial and final states concerned. Therefore, identifying (3.3) and (3.4) with McElroy's equations and

denoting the initial state by i and the final state by j, (3.3) and (3.4) become in his notation

$$i(1 - |S_{ij}|^2)\dot{a}_i = (C_{ii} - S_{ij}h_{ji})a_i + (h_{ij} - S_{ij}C_{jj})b_j \times e^{-i(\varepsilon_j^{\alpha}-\varepsilon_i^{p})t}$$

and (3.5)

$$i(1 - |S_{ij}|^2)\dot{b}_j = (C_{jj} - S_{ji}h_{ij})b_j + (h_{ji} - S_{ji}C_{ii})a_i \times e^{-i(\varepsilon_i^{p}-\varepsilon_j^{\alpha})t}$$

where the matrix elements in (3.5) do not depend upon the time directly and are identified as

$$\begin{aligned} S_{ij} &= \int \phi_i^*(\gamma_p)\ \phi_j(\gamma_\alpha)\ e^{ivz}\ d\tau \\ S_{ji} &= \int \phi_j^*(\gamma_\alpha)\ \phi_i(\gamma_p)\ e^{-ivz}\ d\tau \\ h_{ij} &= -\int \phi_i^*(\gamma_p)\ \phi_j(\gamma_\alpha)\gamma_p^{-1}\ e^{ivz}\ d\tau \\ h_{ji} &= -2\int \phi_j^*(\gamma_\alpha)\ \phi_i(\gamma_p)\gamma_\alpha^{-1}\ e^{-ivz}\ d\tau \\ C_{ii} &= -2\int \phi_i^*(\gamma_p)\ \phi_i(\gamma_p)\gamma_\alpha^{-1}\ d\tau \\ C_{jj} &= -\int \phi_j^*(\gamma_\alpha)\ \phi_j(\gamma_\alpha)\gamma_p^{-1} d\tau\ . \end{aligned} \tag{3.6}$$

The absence of the terms containing $\dot{\theta}$ in (3.6) is a manifestation of the neglect of rotational coupling. To what extent rotational coupling effects influence both charge transfer and excitation cross sections has not previously been investigated for this problem in a multi-state expansion of the total electronic wave function.

McElroy solved (3.5) with the initial boundary conditions

$$a_i(-\infty) = 1 \qquad (3.7)$$
$$b_j(-\infty) = 0 \quad ;$$

which represent the binding of the active electron to the proton initially. In the final state the electron is bound to the α-particle to form He^+(2s or 2p). Equations (3.5) are reduced further by making the following substitutions:

$$a_i = a_{oi}\, e^{-i\int_{-\infty}^{t}\alpha_i dt} \qquad (3.8)$$
$$b_j = b_{oj}\, e^{-i\int_{-\infty}^{t}\beta_j dt}$$

so that

$$\dot{a}_i = \dot{a}_{oi}\, e^{-i\int_{-\infty}^{t}\alpha_i dt} - i\,\alpha_i a_i$$

and (3.9)

$$\dot{b}_j = \dot{b}_{oj}\, e^{-i\int_{-\infty}^{t}\beta_j dt} - i\,\beta_i b_j$$

Substituting (3.8) and (3.9) into (3.5) and simplifying, one obtains

$$i\,\dot{a}_{oi} = \frac{(h_{ij}-S_{ij}C_{jj})}{1-|S_{ij}|^2}\, b_{oj}\, e^{-i(\varepsilon_j^{\alpha}-\varepsilon_i^{p})t}\, e^{i\delta_{ij}} \qquad (3.10)$$

$$i\,\dot{b}_{oj} = \frac{(h_{ji}-S_{ji}C_{ii})}{1-|S_{ij}|^2}\, a_{oi}\, e^{-i(\varepsilon_i^{p}-\varepsilon_j^{\alpha})t}\, e^{-i\delta_{ij}} \qquad (3.11)$$

and, after integration of (3.11) over time from $-\infty$ to $+\infty$,

$$i\, b_{oj}(\infty) = \int_{-\infty}^{\infty} \frac{(h_{ji}-S_{ji}C_{ii})}{1-|S_{ij}|^2}\, e^{-i(\varepsilon_i^p-\varepsilon_j^\alpha)t}\, e^{-i\delta_{ij}}\, dt \quad (3.12)$$

where

$$\delta_{ij} = \int_{-\infty}^{t} (\alpha_i - \beta_j)\, dt \quad (3.13)$$

$$= \int_{-\infty}^{t} \frac{(C_{ii}-C_{jj}-S_{ij}h_{ji}+S_{ji}h_{ij})dt}{1-|S_{ij}|^2} \quad (3.14)$$

$$\simeq \int_{-\infty}^{t} (C_{ii} - C_{jj})\, dt \quad (3.15)$$

with

$$\alpha_i = \frac{C_{ii}-S_{ij}h_{ji}}{1-|S_{ij}|^2}$$

and

$$\beta_j = \frac{C_{jj}-S_{ji}h_{ij}}{1-|S_{ij}|^2}$$

McElroy integrated (3.11) with the approximation that $a_{oi}(t) = 1$ throughout the encounter which amounts to neglect of back-coupling. The distortion term δ_{ij} which is absent in the symmetric resonance process describes the distortion of the eigenenergies (Bates 1958) and this arises from the fact that the initial state consists of a neutral and a positive ion while the final state involves two positive ions moving in a repulsive Coulomb field. Adopting the expression (3.14) for δ_{ij} is equivalent to taking full account of distortion, whereas the approximation (3.15)

to δ_{ij} results in only partial consideration of distortion. For a discussion of the consequences of using both (3.14) and (3.15) on the charge transfer cross sections see Macomber and Webb (1967).

The probability of capture into state j occurring at some impact parameter ρ is

$$P(\rho,j) = |b_{oj}(\infty)|^2 \qquad (3.16)$$

with $b_{oj}(\infty)$ given by (3.12) and the cross section for charge transfer is

$$Q(i,j) = 2\pi\int_0^\infty P(\rho,j)\ \rho d\rho\ . \qquad (3.17)$$

It is of interest to observe that if δ_{ij} and S_{ij} are both set equal to zero in (3.12) one recovers the Brinkman and Kramers (1930) approximation in which they used the incident ion-electronic interaction as the interaction potential responsible for the charge transfer.

Both McCarroll and McElroy (1962) and McElroy (1963) employed (3.12) to study the non-resonance and the accidental resonance reactions given respectively by

$$He^{2+} + H(1s) \rightarrow He^{+}(1s) + H^{+} \qquad (3.17a)$$

and

$$He^{2+} + H(1s) \rightarrow He^{+}(2s,\ 2p) + H^{+} \qquad (3.17b)$$

Reactions (3.17a) and (3.17b) have been studied for the range of α-particle energies (50-1600keV) and (25-800keV) respectively. As can be seen from both (3.17a) and (3.17b) the computation of McElroy is an extension of the calculation of McCarroll and McElroy.

(b) Basu et al (1967)

They solved the collision problem for the range of α-particle energies (1 - 100keV) by using a variational method. The trial electronic wave function is expanded in terms of the ground state of H and the He^+ states under consideration enabling one to calculate only charge transfer to the different states of He^+ included in the expansion of the total electronic wave function. A serious objection to their calculation is the omission of momentum transfer terms at all energies of the incident α-particle considered. According to Malaviya (1969) momentum transfer terms remain important down to α-particle speeds of about 0.1 a.u. (see also Bates and McCarroll 1962). Therefore, the calculation though a multi-state one does not represent a significant improvement over the previous attempts.

(c) Coleman and Trelease (1968)

Coleman and Trelease employed the high energy impulse approximation in which they took account only of intermediate continuum states which, they claim, are likely to be important at high energies. The authors admit, however, that their results for the capture cross sections are unlikely to be correct at low energies because they neglected Coulomb repulsion in the final state. Consequently their results for the capture cross sections to the n = 2 level of He^+ are much lower than the experimental values of Fite et al. (1962) and of Pivovar et al. (1962). In fact any theory which neglects back-coupling and/or distortion is not expected to give

reliable results below impact energies of He^{2+} less than about 100keV (see Macomber and Webb 1967). According to Malaviya (1969) the capture cross sections to the n = 2 level of He^{+} calculated in the impulse approximation are less than his two-state or five-state results by a factor of approximately 3 (see results in Chapter V).

(d) Malaviya (1969)

The calculation by Malaviya of electron capture represents the first multi-state attempt towards the solution of the He^{2+} - H collision problem which takes complete account of the important effects of distortion and back-coupling as well as momentum transfer. Malaviya expanded the total electronic wave function in terms of travelling atomic orbitals representing H(1s), $He^{+}(2s)$, $He^{+}(2p_z)$ and $He^{+}(2p_x)$ states and called this a five-state approximation. This nomenclature is different from that employed here; in the four-state approximation used in most of the results of this thesis the four states 1s, 2s, $2p_0$, and $2p_1$ are included on each of the centres. In Malaviya's labelling, this would be called a ten-state approximation. Malaviya utilized energy difference arguments to neglect coupling to other states of H and to the $He^{+}(1s)$ state.

By comparing his two-state with his five-state results he concluded that for projectile energies greater than 25keV the inclusion of intermediate channels arising in part from the rotation of the internuclear line is not important. The results of Malaviya for electron capture

are in fair agreement with experiments (see Chapter V for results) except at low energies where the theoretical curves fall faster towards zero than the experimental curves. He attributed this deviation from experimental results as due partly to the use of atomic rather than molecular eigenfunctions.

As will be shown in the results our calculations contradict the conclusion that one can omit the transition to the ground state of He^+ in the computation of charge transfer without specifying the energy limit. Actually, as the energy of the incident α-particle approaches and exceeds about 800keV, the $He^+(1s)$ state tends to receive a greater population compared to the other states of He^+ in keeping with the theoretical predictions of McElroy (1963).

Further, we do not agree with Malaviya's observation that one can neglect rotational coupling. Our capture cross sections to the n = 2 level of He^+ tend to rise above Malaviya's at α-particle energies less than about 25keV, where Malaviya's results fall faster than the experimental findings.

One observes from the preceding presentation that no previous calculations exist on either excitation or ionization of the target atom or of resulting polarization of the target using α-particles as projectiles. It is therefore also a purpose of this thesis to estimate target polarizations and ionization cross sections, and to evaluate excitation cross sections.

CHAPTER IV

NUMERICAL METHODS

4.1 Introduction

For the complete integration of the coupled differential equations (2.25) we shall employ the method of Wilets and Gallaher (1966) (hereafter called W-G) but with major modifications. The scheme of integrating the coupled differential equations for the amplitudes from $t \to -\infty$ to $t \to +\infty$ may be broken into three main sections.

First, the spatial matrix elements represented by equations (2.22a) are all integrated in a prolate elliptic coordinate system. The particular matrix elements $\hat{Q}_{kk'}$ and $\hat{N}_{kk'}$ may then be integrated either analytically or numerically as desired while the remaining spatial matrix elements ($\hat{S}_{kk'}$, $\hat{R}_{kk'}$, $\hat{T}_{kk'}$ and $\hat{M}_{kk'}$) are of necessity evaluated numerically; for this the Gauss-Laguerre and the Gauss-Legendre quadrature methods have been adopted. Subsequently, by (2.33), the $\hat{W}_{kk'}$ are then determined and stored at each point of a coarse mesh.

Next, utilizing these $\hat{W}_{kk'}$ and a five point Lagrange interpolation formula, the time integration over a fine mesh with limits $(-T_{max}, +T_{max})$ is effected via a fourth order Adams-Moulton predictor-corrector method using the Runge-Kutta formula of the same order as starter.

Finally, the resulting amplitudes are extrapolated from $t = +T_{max}$ to $t \to +\infty$ by Cheshire's procedure (1968).

4.2 Choice of Method for Integration of Coupled Equations

The overall integration scheme of W-G having been applied successfully for the solution of the $H^+ - H$ collision problem was a natural choice for evaluating the matrix elements in (2.22a) as well as for time integrating the coupled differential equations for the amplitudes from $t = -T_{max}$ to $t = +T_{max}$ over the fine mesh. Unfortunately the application of that scheme in all its details has proven unsuitable for this problem. We, however, retained its underlying overall basis.

Before providing an explanation in detail of why the W-G method as it stood was unsuccessful in this work, we must emphasize that it is not the intention of the author to examine critically the conditions and range of validity of the total W-G integration scheme; we are merely stating an observation and attempt to provide a reasoned explanation for the failure of that approach when applied without modifications to the present problem. In fact, the purpose of this section is to guide future workers against the blind use of the W-G method as it stands if their problem should be similar to this one.

In general, the formulation employed by W-G for numerically integrating the spatial matrix elements which enter into the expression for the $\hat{W}_{kk'}$ is not recommended

especially when one deals with wave functions that are generally more compact than hydrogenic wave functions (such as pseudo-state wave functions). The validity of the results obtained by their approach will depend upon, among other things, the magnitude of the coefficients of R(t) appearing in the exponentially decaying terms in the wave functions. In general, a large R(t) will diminish the reliability of these results.

To apply the time integration scheme of W-G to the differential equation for the amplitudes, let us recast (2.25) into a second order differential equation involving only one amplitude, say b(t). For the reduction of (2.25) to this second order equation, we utilize (2.21). Without much labour, (2.21) can be transformed into

$$\ddot{b} - iw\dot{b} - ivb = 0 \qquad (4.1)$$

$$a = \rho\dot{b} + \beta b$$

or replacing b(t) by X(t)

$$\ddot{X} + n\dot{X} + mX = 0 \qquad (4.2)$$

$$a = \rho\dot{X} + \beta X$$

where, in this section only, the time dependent matrices w, v, ρ, and β are defined as

$$w = P_2^{-1}[i\,\dot{P}_2 + T_2 - L_2] \qquad (4.3)$$

$$v = P_2^{-1}[\dot{T}_2 + i\,N_2]$$

$$n = -iw \qquad \rho = i\,P_2$$

$$m = -iv \qquad \beta = T_2$$

with

$$P_2 = P_1^{-1}S_1 \qquad T_2 = P_1^{-1}T_1$$

$$L_2 = M_1^{-1}L_1 \qquad N_2 = M_1^{-1}N_1$$

and

$$P_1 = P^{-1}Q - T^{-1}M \qquad T_1 = T^{-1}N - P^{-1}R$$

$$S_1 = P^{-1}S - T^{-1}L \qquad M_1 = Q^{-1}P - M^{-1}T \qquad (4.4)$$

$$L_1 = M^{-1}L - Q^{-1}S \qquad N_1 = Q^{-1}R - M^{-1}N$$

The matrices without subscripts in (4.4) are identified as those appearing in (2.22). To obtain the matrices w and v, one therefore has to invert numerically (it should be noted that the matrices containing the momentum transfer terms $e^{\pm ivz}$ have not yet been obtained in closed form) a rather large number of matrices. This process of numerical inversion is in general long and time consuming and should be avoided where possible. Consequently this introduces an argument against the procedure we are outlining.

To solve (4.2) for X(t) and thence a(t), let us expand both X(t) and $\dot{X}(t)$ in a Taylor series. Thus

$$X(t+\Delta t) = X(t) + \Delta t\, \dot{X}(t) + \frac{(\Delta t)^2}{2!}\ddot{X}(t) + \frac{(\Delta t)^3}{3!}\dddot{X}(t) + \ldots$$

and (4.5)

$$\dot{X}(t+\Delta t) = \dot{X}(t) + \Delta t X(t) + \frac{(\Delta t)^2}{2!}\dddot{X}(t) + \frac{(\Delta t)^3}{3!}\ddddot{X}(t) + \ldots$$

The Taylor series is truncated after the $(\Delta t)^3$ term; making the scheme correct to order $(\Delta t)^4$.

From (4.2)

$$\ddot{X} = -n\dot{X} - mX$$

and by differentiation with respect to time one obtains

$$\dddot{X} = (-\dot{n} - m + n^2)\dot{X} + (-\dot{m} + nm)X \tag{4.6}$$

and

$$\ddddot{X} = (-\ddot{n} - 2\dot{m} + n\dot{n} + 2\dot{n}n + mn - n^3 + nm)\dot{X}$$

$$+ (m^2 - n^2m - \ddot{m} + 2\dot{n}m + n\dot{m})X$$

It must be borne in mind that the matrices n and m as well as their time derivatives are evaluated at time t and they do not commute. Both n and m and their derivatives are also expanded in Taylor series

$$n(t + \tfrac{\Delta t}{2}) \simeq n(t) + (\tfrac{\Delta t}{2})\dot{n}(t) + \frac{(\Delta t/2)^2}{2!}\ddot{n}(t)$$

$$\dot{n}(t+\tfrac{\Delta t}{2}) \simeq \dot{n}(t) + (\tfrac{\Delta t}{2})\ddot{n}(t)$$

$$\ddot{n}(t+\tfrac{\Delta t}{2}) \simeq \ddot{n}(t)$$

$$m(t+\tfrac{\Delta t}{2}) \simeq m(t) + (\tfrac{\Delta t}{2})\dot{m}(t) + \frac{(\Delta t/2)^2}{2!}\ddot{m}(t)$$

$$\dot{m}(t+\tfrac{\Delta t}{2}) \simeq \dot{m}(t) + (\tfrac{\Delta t}{2})\ddot{m}(t)$$

$$\ddot{m}(t+\tfrac{\Delta t}{2}) \simeq \ddot{m}(t) \quad .$$

Solving for n(t), m(t) and their respective time derivatives we obtain

$$n(t) \simeq n(t+\tfrac{\Delta t}{2}) - (\tfrac{\Delta t}{2})\dot{n}(t+\tfrac{\Delta t}{2}) + \frac{(\Delta t)^2}{8}\ddot{n}(t+\tfrac{\Delta t}{2})$$

$$\dot{n}(t) \simeq \dot{n}(t+\tfrac{\Delta t}{2}) - (\tfrac{\Delta t}{2})\ddot{n}(t+\tfrac{\Delta t}{2}) \tag{4.7a}$$

$$\ddot{n}(t) \simeq \ddot{n}(t+\tfrac{\Delta t}{2})$$

and

$$m(t) \simeq m(t+\tfrac{\Delta t}{2}) - (\tfrac{\Delta t}{2})\dot{m}(t+\tfrac{\Delta t}{2}) + \frac{(\Delta t)^2}{8}\ddot{m}(t+\tfrac{\Delta t}{2})$$

$$\dot{m}(t) \simeq \dot{m}(t+\tfrac{\Delta t}{2}) - (\tfrac{\Delta t}{2})\ddot{m}(t+\tfrac{\Delta t}{2}) \qquad (4.7b)$$

$$\ddot{m}(t) \simeq \ddot{m}(t+\tfrac{\Delta t}{2}) \quad .$$

(4.7a) and (4.7b) are then substituted into (4.6) and the resulting expressions are used in (4.5). After a lengthy but straightforward calculation one obtains the amplitude X and its first derivative at time t + Δt in terms of X(t) and $\dot{X}(t)$. Thus we find

$$X(t+\Delta t) = \left\{\Delta t - \frac{(\Delta t)^2}{2!}n + \frac{(\Delta t)^3}{3!}\left[\frac{\dot{n}}{2} - m + n^2\right]\right.$$

$$\left. + \frac{(\Delta t)^4}{4!}\left[-\frac{\ddot{n}}{2} - n\dot{n} + mn - n^3 + nm\right]\right\}_{t+\frac{\Delta t}{2}} \dot{X}(t)$$

$$+ \left\{1 - \frac{(\Delta t)^2}{2!}m + \frac{(\Delta t)^3}{3!}\left[\frac{\dot{m}}{2} + nm\right]\right.$$

$$\left. + \frac{(\Delta t)^4}{4!}\left[-\frac{\ddot{m}}{2} - n\dot{m} + m^2 - n^2 m\right]\right\}_{t+\frac{\Delta t}{2}} X(t) \qquad (4.8)$$

and

$$\dot{X}(t+\Delta t) = \left\{1 - \Delta t n + \frac{(\Delta t)^2}{2!}\left[-m + n^2\right] + \frac{(\Delta t)^3}{3!}\left[-\frac{\ddot{n}}{4} - \frac{n\dot{n}}{2} - \frac{\dot{m}}{2} + \frac{\dot{n}n}{2} + mn - n^3 + nm\right]\right.$$

$$+ \frac{(\Delta t)^4}{4!}\left[-\frac{\ddot{m}}{2} + \frac{\ddot{n}n}{2} - m\dot{n} + n^2\dot{n} + \frac{n\ddot{n}}{2} + \dot{m}n - \dot{n}n^2 - mn^2 + n^4 - nmn + m^2 - n^2 m\right.$$

$$\left.\left. + \dot{n}m\right]\right\}_{t+\frac{\Delta t}{2}} \dot{X}(t) + \left\{-\Delta t m + \frac{(\Delta t)^2}{2!}nm + \frac{(\Delta t)^3}{3!}\right.$$

$$\left[-\frac{\ddot{m}}{4} - \frac{n\dot{m}}{2} + m^2 - n^2 m + \frac{\dot{n}m}{2}\right] + \frac{(\Delta t)^4}{4!}\left[\frac{n\ddot{m}}{2} - m\dot{m} + n^2\dot{m} + \frac{\ddot{n}m}{2} + \dot{m}m - \dot{n}nm\right.$$

$$\left.\left. - mnm + n^3 m - nm^2\right]\right\}_{t+\Delta t/2} X(t) \quad .$$

Both the matrices and their time derivatives in (4.8) are now evaluated at time $(t + \Delta t/2)$. Thus, knowing X and $\dot{X}$ at time t, one calculates the matrices and their time derivatives at time $(t + \Delta t/2)$ and consequently obtains $X(t + \Delta t)$ and $\dot{X}(t + \Delta t)$ through the stepping formula (4.8). The boundary conditions are

$$a_k(-\infty) = \delta_{1k} \text{ and } X_k(-\infty) \equiv b_k(-\infty) = 0 \qquad (4.9)$$

so that from (4.2)

$$\dot{X}_k(-\infty) = \rho^{-1}_{kk'}(-\infty)\, a_{k'}(-\infty)$$

$$= \rho^{-1}_{k1}(-\infty) \quad .$$

These boundary conditions have the effect of placing the active electron in the 1s-state of the target hydrogen atom at $t = -\infty$. The charge transfer probability at this time is thus effectively zero.

Without much difficulty the matrices n and m can be expressed in the form [see for example equation (2.32)]

$$n(t) = \hat{n}\, e^{i\hat{w}t}$$

$$m(t) = \hat{m}\, e^{i\hat{w}t}. \qquad (4.10)$$

The time dependence of $\hat{n}$ and $\hat{m}$ arises parametrically through R(t), the internuclear separation.

Differentiating (4.10) with respect to time we obtain

$$\dot{n}(t) = (\dot{\hat{n}} + i\hat{w}\hat{n})\, e^{i\hat{w}t}$$

$$\dot{m}(t) = (\dot{\hat{m}} + i\hat{w}\hat{m})\, e^{i\hat{w}t} \qquad (4.11a)$$

and

$$\ddot{\hat{n}}(t) = (\ddot{\hat{n}} + 2i\hat{w}\dot{\hat{n}} - \hat{w}^2\hat{n})\, e^{i\hat{w}t}$$

$$\ddot{\hat{m}}(t) = (\ddot{\hat{m}} + 2i\hat{w}\dot{\hat{m}} - \hat{w}^2 m)\, e^{i\hat{w}t} \qquad (4.11b)$$

The scheme of W-G can now be applied to (4.8) to obtain $X(t = T_{max})$, with the matrices given in (4.10) and their derivatives in (4.11a) and (4.11b). Thence, in principle, $a(t = T_{max})$ could be calculated from the second equation in (4.2). A major practical difficulty with this method of solution occurs when one attempts to calculate the time derivatives of the matrices $\hat{n}$ and $\hat{m}$ numerically. In this calculation the variation in the matrix elements $\hat{n}_{kk'}$ and $\hat{m}_{kk'}$ as the internuclear separation R(t) changes is not necessarily smooth. In fact for some energies and impact parameters (especially small ones) these variations are quite rapid, in particular as $R(t) \to 0$. This makes numerical differentiation very difficult and therefore unreliable. Accurate values of $\dot{\hat{n}}(t)$, $\dot{\hat{m}}(t)$, $\ddot{\hat{n}}(t)$ and $\ddot{\hat{m}}(t)$ are essential for dependable results. For the H^+ - H collision problem, the wave functions are not as compact as in this case. Therefore one might expect the scheme to work quite well in the H^+ - H collision problem.

Since our aim is to obtain, among other things, both excitation and charge transfer cross sections within a reasonable computing time, we were unable to employ (4.2) to evaluate the amplitude a(t) at either $t = T_{max}$ or $t \to +\infty$ (assymptotically) for the following simple reason. Some elements of the matrices ρ and β were quite large ($\sim 10^8$) at

either $t = T_{max}$ or $t \to +\infty$; now we know from probability conservation requirements that no single element of either $a_k(t)$ or $b_k(t)$ may exceed unity. Consequently, the computer must be capable of handling numbers to about twelve significant figures if, for example, one requires that the amplitudes be calculated correctly to four significant figures. When these calculations are effected, one has always to bear in mind the cost of computing (in terms of time or dollars). Even with as good a machine as the CDC 6600 we could not get reliable results at reasonable costs! Consequently, we abandoned the method as being quite impracticable.

One was able to avoid numerical differentiation by expressing the time derivatives of the matrices in terms of the matrices n and m. The only objection to this method of solution is that one winds up with long and complicated expressions for the time derivatives of the matrices. Consequently, accuracy improves but computer time rises considerably. For the type of calculation we are pursuing, one would only be content with great accuracy for the least computer time! The failure to realize this ideal forced us to abandon the procedure outlined.

4.3 Evaluation of the Matrix Elements

The evaluation of the matrix elements in (2.22a) and the subsequent determination from (2.32) of the $\hat{W}_{kk'}$ which are required for the time integration of the coupled differential equations represent the necessary steps towards

the solution of (2.25) for the amplitudes and, consequently, the calculation of charge transfer and excitation cross sections of the target atom. Let us rewrite for convenience the matrix elements in (2.22a)

$$\begin{aligned}
\hat{P}_{kk'} &= \hat{L}_{kk'} = \delta_{kk'} \\
\hat{Q}_{kk'} &= \langle kP|\dot{\theta}\ell_p|Pk'\rangle - \langle kP|\frac{Z}{\gamma_\alpha}Pk' \\
\hat{N}_{kk'} &= \langle k\alpha|\dot{\theta}\ell_\alpha|\alpha k'\rangle - \langle k\alpha|\frac{1}{\gamma_p}|\alpha k'\rangle \\
\hat{S}_{kk'} &= \langle kP|e^{ivz}|\alpha k'\rangle \\
\hat{T}_{kk'} &= \langle k\alpha|e^{-ivz}|Pk'\rangle \\
\hat{R}_{kk'} &= \langle kP|e^{ivz}\dot{\theta}\ell_\alpha|\alpha k'\rangle - \langle kP|e^{ivz}\frac{1}{\gamma_p}|\alpha k'\rangle \\
\hat{M}_{kk'} &= \langle k\alpha|e^{-ivz}\dot{\theta}\ell_p|Pk'\rangle - \langle k\alpha|e^{-ivz}\frac{Z}{\gamma_\alpha}|Pk'\rangle.
\end{aligned} \tag{4.12}$$

The matrix elements $\hat{Q}_{kk'}$ and $\hat{N}_{kk'}$ are of the standard molecular structure integrals and can be obtained in closed analytical form. The others that involve the momentum tranfer terms $e^{\pm ivz}$ have to be calculated numerically because we have not yet discovered analytic expressions for them. Fortunately, the existence of an interdependence among them reduces their actual computation to only the four matrices: $\hat{N}$(or $\hat{Q}$), $\hat{S}$ (or $\hat{T}$), $\hat{R}$ and $\hat{M}$. The remaining two $\hat{Q}$ and $\hat{T}$ are deduced from $\hat{N}$ and $\hat{S}$ respectively. Since $\hat{N}$ is expressible in terms of R(t), the nuclear separation, the substitution $R(t) \rightarrow \frac{R(t)}{2}$ leads to a correct expression for the second term in the expression for $\hat{Q}$. $\hat{T}$ may be extracted from $\hat{S}$ by making use of the relation

$$\hat{S}_{kk'} = \hat{T}^*_{k'k} \tag{4.13}$$

which follows directly from (4.12).

The preparation of the four matrices $\hat{N}$, $\hat{S}$, $\hat{R}$ and $\hat{M}$ for numerical integration is achieved by following the integration procedure of Gallaher (Ph.D. thesis) in which integration over the azimuthal angle ϕ' is performed first and summation over the magnetic quantum number m is reduced to only positive (including zero) values, leaving two dimensional integrals which may then be evaluated numerically. To exploit the method, one first expresses the terms containing the operators ℓ_α and ℓ_p in the expressions for $\hat{R}$ and $\hat{M}$ in terms of $\hat{S}$ and $\hat{T}$.

Writing $\ell_\alpha \equiv (\ell_{y'})_\alpha$

$$= \frac{\ell'^{+} - \ell'^{-}}{2i}$$

and

$\ell_p \equiv (\ell_{y'})_p$, and remembering that the operation of ℓ_α is upon only $|\alpha k'\rangle$ and of ℓ_p is confined to only $|Pk'\rangle$, one obtains the following expressions for the elements $\langle kP|\dot{\theta}\, e^{ivz}\, \ell_\alpha|\alpha k'\rangle$ and $\langle k\alpha|\dot{\theta}\, e^{-ivz}\, \ell_p|Pk'\rangle$:

$$\langle kP|\dot{\theta}\, e^{ivz}\, \ell_\alpha|\alpha k'\rangle$$

$$= \dot{\theta}\langle kP|e^{ivz}\left[\frac{\ell'^{+} - \ell'^{-}}{2i}\right]|\,\alpha k'\rangle$$

$$= \frac{\dot{\theta}}{2i}\Big\{\sqrt{(\ell'-m')(\ell'+m'+1)}\;\langle kP|e^{ivz}|\alpha k'+1\rangle$$

$$-\sqrt{(\ell'+m')(\ell'-m'+1)}\;\langle kP|e^{ivz}|\alpha k'-1\rangle\Big\}$$

$$= \frac{\dot{\theta}}{2i}\left\{ \sqrt{(\ell'-m')(\ell'+m'+1)}\ \hat{S}_{kk'+1} - \sqrt{(\ell'+m')(\ell'-m'+1)}\ \hat{S}_{kk'-1} \right\} \tag{4.14}$$

and

$$\langle k\alpha | \dot{\theta}\ e^{-ivz} \ell_p | Pk' \rangle$$

$$= \dot{\theta} \langle k\alpha | e^{-ivz} \left[\frac{\ell'^{+} - \ell'^{-}}{2i} \right] | Pk' \rangle$$

$$= \frac{\dot{\theta}}{2i}\left\{ \sqrt{(\ell'-m')(\ell'+m'+1)}\ \hat{T}_{kk'+1} - \sqrt{(\ell'+m')(\ell'-m'+1)}\ \hat{T}_{kk'-1} \right\}$$

where $(k' \pm 1)$ means $(n', \ell', m' \pm 1)$.

Similarly, one also writes

$$\langle kP | \dot{\theta} \ell_p | Pk' \rangle = \frac{\dot{\theta}}{2i}\left\{ \sqrt{(\ell'-m')(\ell'+m'+1)}\ \delta_{kk'+1} - \sqrt{(\ell'+m')(\ell'-m'+1)}\delta_{kk'-1} \right\} \tag{4.15}$$

and

$$\langle k\alpha | \dot{\theta} \ell_\alpha | \alpha k' \rangle = \frac{\dot{\theta}}{2i}\left\{ \sqrt{(\ell'-m')(\ell'+m'+1)}\delta_{kk'+1} - \sqrt{(\ell'+m')(\ell'-m'+1)}\delta_{kk'-1} \right\}$$

The use of the abbreviations $C^{+}_{k'+1} \equiv \frac{1}{2i}\sqrt{(\ell'-m')(\ell'+m'+1)}$ and $C^{-}_{k'-1} \equiv \frac{1}{2i}\sqrt{(\ell'+m')(\ell'-m'+1)}$ leads to the four matrix elements being expressed more compactly as

$$\begin{aligned}
\hat{N}_{kk'} &= \dot{\theta}[C^{+}_{k'+1}\delta_{kk'+1} - C^{-}_{k'-1}\delta_{kk'-1}] - \langle k\alpha | \frac{1}{\gamma_p} | \alpha k' \rangle \\
\hat{S}_{kk'} &= \langle kP | e^{ivz} | \alpha k' \rangle \\
\hat{R}_{kk'} &= \dot{\theta}[C^{+}_{k'+1}\hat{S}_{kk'+1} - C^{-}_{k'-1}\hat{S}_{kk'-1}] - \langle kP | e^{ivz} \frac{1}{\gamma_p} | \alpha k' \rangle \\
\hat{M}_{kk'} &= \dot{\theta}[C^{+}_{k'+1}\hat{T}_{kk'+1} - C_{k'-1}\hat{T}_{kk'-1}] - \langle k\alpha | e^{-ivz} \frac{Z}{\gamma_\alpha} Pk' \rangle
\end{aligned} \tag{4.16}$$

where the matrix $\hat{T}$ is not independent of $\hat{S}$; the dependence

being given by (4.13). One immediately observes that the evaluation of the matrix elements in (4.12) has been reduced to the calculation of essentially the four sets of matrix elements: $\langle k\alpha|\frac{1}{\gamma_p}|\alpha k'\rangle$, $\langle kP|e^{ivz}|\alpha k'\rangle$, $\langle kP|e^{ivz}\frac{1}{\gamma_p}|\alpha k'\rangle$ and $\langle k\alpha|e^{-ivz}\frac{Z}{\gamma_\alpha}|Pk'\rangle$.

Therefore the integration over ϕ' can now be performed and the Gallaher (Ph.D. thesis) scheme followed to reduce the above four sets of matrix elements to two dimensional integrals in preparation for numerical integration.

We first consider the elements $\langle k\alpha|\frac{1}{\gamma_p}|\alpha k'\rangle$ which may be integrated analytically. Nevertheless, we shall illustrate how they may be computed numerically; they might as well be evaluated in a similar manner to the rest which can be calculated only by numerical methods at the present time. Therefore integration over the angle ϕ' reduces $\langle k\alpha|\frac{1}{\gamma_p}|\alpha k'\rangle$ to

$$\langle k\alpha|\frac{1}{\gamma_p}|\alpha k'\rangle = NV_{kk'}\delta_{mm'} \tag{4.17}$$

where the elements $NV_{kk'}$ are two dimensional integrals which will be evaluated by transforming over to confocal elliptic coordinates. From Appendix A

$$\xi R(t) = \gamma_\alpha + \gamma_p, \quad \eta R(t) = \gamma_\alpha - \gamma_p$$

so that

$$\gamma_\alpha = (\xi + \eta)\frac{R(t)}{2}, \quad \gamma_p = (\xi - \eta)\frac{R(t)}{2}$$

where the coordinate ξ is analogous to a radial coordinate and η to the cosine of an angular coordinate. The Jacobian

of the transformation from (ρ', ϕ', z') to (ξ, ϕ', η) coordinates is

$$J(\rho',\phi',z' \rightarrow \xi, \phi', \eta) = \left(\frac{R}{2}\right)^3 (\xi^2-\eta^2) .$$

Thus

$$\rho' d\rho' d\phi' dz' = \left(\frac{R}{2}\right)^3 (\xi^2-\eta^2) d\xi d\eta d\phi'$$

$$= \left(\frac{R}{2}\right) \gamma_\alpha \gamma_p \, d\xi d\eta d\phi'$$

where

$$\rho' = \sqrt{x'^2 + y'^2} \qquad \text{and } R \equiv R(t).$$

To utilize computer time more efficiently, we construct a general integration scheme which will be employed to calculate numerically all the matrix elements needed. To this end, a transformation of the integration variable ξ (the limits on ξ, η and ϕ' are: $1 \leq \xi < \infty$, $-1 \leq \eta \leq +1$ and $0 \leq \phi' \leq 2\pi$) to another variable with limits $(0,\infty)$ is effected so as to avail ourselves of the Gauss-Laguerre quadrature method. To change the limits of integration of ξ from $(1, \infty)$ to $(0, \infty)$, one sets

$$x = \xi R = \gamma_\alpha + \gamma_p$$

and defines the new variable y in terms of x as

$$y = x - R$$

$$= \xi R - R$$

so that

$$dy = R \, d\xi .$$

Therefore $\int_1^\infty d\xi \, F(\xi) = \int_0^\infty dy/R \, F(y)$

where F is some unspecified function and

$$\xi = y/R + 1.$$

Consequently,

$$\langle k\alpha|\frac{1}{\gamma_p}|\alpha k'\rangle=\delta_{mm'}\int_0^{\infty}\int_{-1}^{+1}\frac{FA(k)FA(k')}{\gamma_p}\left(\frac{R}{2}\right)\gamma_\alpha\gamma_p\,\frac{dy}{R}\,d\eta \qquad (4.18)$$

where the FA(k) are properly normalized bound state eigenfunctions of He^+. In this thesis the bound state eigenfunctions for both He^+ and H are normalized to 4π for $m = 0$ and to 2π for $m \neq 0$.

The Gauss-Laguerre (for the variable y) and the Gauss-Legendre (for the variable η) formulas may now be applied to (4.18). The form (4.18) is easy to program since it entails merely reading in the correct wave functions and the rest involves only simple calculations for the computer.

However, the computation of the exchange type elements:

$$\langle k\alpha|e^{ivz}|Pk'\rangle,\ \langle k\alpha|e^{ivz}/\gamma_p|Pk'\rangle \text{ and } \langle kP|e^{-ivz}\,\frac{Z}{\gamma_\alpha}|\alpha k'\rangle$$

is not straightforward. To calculate these elements, one exploits the invariance of $H \equiv -\frac{\nabla^2}{2} - \frac{Z}{\gamma_\alpha} - \frac{1}{\gamma_p} + \frac{Z}{R}$ with respect to reflection through the collision plane ($\phi \to -\phi$) to obtain the following correspondence for the total electronic wave function

$$\Psi(\gamma, \theta, \phi, t) = \Psi(\gamma, \theta, -\phi, t).$$

Consequently, retaining only the angular part of $\Psi(\bar{\gamma}, t)$, one obtains

$$\sum_m A_{n\ell m}(t)\ Y_{\ell m}(\theta,\phi) = \sum_m A_{n\ell m}(t)\ Y_{\ell m}(\theta,-\phi) \qquad (4.19)$$

where the sum is over values of m ranging from $-\ell$ to $+\ell$. However, the summation over k in (2.4) allows only positive values of k. Following Gallaher (Ph.D. Thesis) the sum over m may be reduced to only values of $m \geq 0$.

The spherical harmonics satisfy the relation

$$Y^*_{\ell m}(\theta,\phi) = (-)^m Y_{\ell -m}(\theta,\phi)$$

or $$Y_{\ell -m}(\theta,\phi) = (-)^m Y^*_{\ell m}(\theta,\phi)$$

so that

$$\sum_m A_{n\ell m}(t)\, Y_{\ell m}(\theta,\phi) = \sum_m A_{n\ell m}(t)\, (-)^m\, Y^*_{\ell m}(\theta,\phi).$$

Therefore

$$A_{n\ell -m}(t) = (-)^m A_{n\ell m}(t) \,. \tag{4.20}$$

Thus the modified spherical harmonics $\mathcal{Y}_{\ell m}(\theta',\phi')$ can now be defined as

$$\mathcal{Y}_{\ell m}(\theta',\phi') = \begin{cases} Y_{\ell o}(\theta',\phi') & , \ m=o \\ \dfrac{1}{\sqrt{2}}\left[Y_{\ell m}(\theta',\phi') + (-)^m Y_{\ell -m}(\theta',\phi')\right] & , \ m>o \end{cases} \tag{4.21}$$

and have the proper normalization

$$\int \mathcal{Y}^*_{\ell m}(\theta',\phi')\, \mathcal{Y}_{\ell' m'}(\theta',\phi')\, d\Omega' = \delta_{\ell\ell'}\, \delta_{mm'}.$$

Further, a representation of e^{ivz} in terms of the rotating coordinate system is necessary for the reduction of the exchange type matrices to two dimensional integrals. Expressing z in terms of z' and ρ' as

$$z = z' \cos\theta + \rho' \cos\phi' \sin\theta$$

we obtain the following expression for e^{ivz}:

$$e^{ivz} = e^{ivz'\cos\theta}\, e^{iv\sqrt{x'^2+y'^2}\,\cos\phi'\,\sin\theta} .$$

Therefore, the exchange matrix elements involve an integration over ϕ' of the form

$$\int_0^{2\pi} d\phi'\; e^{i(m-m')\phi'}\; e^{iv\rho'\cos\phi'\sin\theta}$$

$$= 2\pi\, i^{|m-m'|}\, J_{|m-m'|}(v\rho'\sin\theta)$$

where $J_m(x)$ is the ordinary Bessel function of the first kind of order m and argument x. A series expansion of $J_m(x)$ which converges for all finite values of x exists and is given by

$$J_{+m}(x) = \left(\frac{x}{2}\right)^m \sum_{j=0}^{\infty} \frac{(-)^j}{j!\Gamma(j+m+1)} \left(\frac{x}{2}\right)^{2j} .$$

Asymptotic forms of $J_m(x)$ for small and large arguments are given by (see Jackson 1962)

$$J_m(x) \xrightarrow[x\to 0]{} \frac{1}{\Gamma(m+1)} \left(\frac{x}{2}\right)^m \qquad \text{for } x << 1,$$

and

$$J_m(x) \xrightarrow[x\to\infty]{} \sqrt{\frac{2}{\pi x}}\; \cos\left(x-\frac{m\pi}{2}-\frac{\pi}{4}\right) \qquad \text{for } x >> 1.$$

$J_{-m}(x)$ and $J_m(x)$ are related by

$$J_{-m}(x) = (-)^m J_m(x) .$$

Consequently, we are now faced essentially with the evaluation of the two dimensional integrals for the exchange matrix elements of the types

$$SV_{kk'}(\tfrac{1}{2}) \equiv (kP|e^{ivz'\cos\theta}\, i^{|m\mp m'|} J_{|m\mp m'|}(v\rho'\sin\theta)|\alpha k')$$

$$RV_{kk'}(\tfrac{1}{2}) \equiv (kP|e^{ivz'\cos\theta}\, \frac{i^{|m\mp m'|}}{\gamma_p} J_{|m\mp m'|}(v\rho'\sin\theta)|\alpha k')$$

$$MV_{kk'}(\tfrac{1}{2}) \equiv (k\alpha|e^{-ivz'\cos\theta}\, i^{|m\mp m'|} \frac{Z}{\gamma_\alpha} J_{|m\mp m'|}(v\rho'\sin\theta)|Pk')$$

where $(\tfrac{1}{2})$ indicates the m, m' combinations $\binom{m-m'}{m+m'}$

and $|k\beta) \Leftrightarrow R_{n\ell}(\gamma_\beta)\, \Theta_{\ell m}(\theta'_\beta) \times \begin{cases} 1 & \text{for } m=0 \\ 2^{-1/2} & \text{for } m>0 \end{cases}$.

in which the $\Theta_{\ell m}(\theta'_\beta)$ are the normalized associated Legendre functions $P^m_\ell(\theta'_\beta)$. From the definition of the modified spherical harmonics $\mathcal{Y}_{\ell m}(\theta',\phi')$ (equations 4.21) and the fact that summation is now only over $m \geq o$, a typical matrix element will contain angular integrals of the form:

$$\begin{array}{ll}
\int d\Omega [Y^*_{\ell m} + (-)^m Y^*_{\ell -m}][Y_{\ell' m'} + (-)^{m'} Y_{\ell' -m'}], & \begin{array}{l} m>0 \\ m'>0 \end{array} \\
\int d\Omega [Y^*_{\ell m} + (-)^m Y^*_{\ell -m}] Y_{\ell' o}, & \begin{array}{l} m>0 \\ m'=0 \end{array} \\
\int d\Omega\ Y^*_{\ell o} [Y_{\ell' m'} + (-)^{m'} Y_{\ell' -m'}], & \begin{array}{l} m=0 \\ m'>0 \end{array} \\
\int d\Omega\ Y^*_{\ell o}\ Y_{\ell' o}\ , & \begin{array}{l} m=0 \\ m'=0 \end{array}
\end{array} \qquad (4.22)$$

Introducing the notation σ_m where

$$\sigma_m = \begin{cases} 0\ , & m = 0 \\ 1\ , & m > 0 \end{cases}$$, one recognizes

that the ϕ' integration in (4.22) can be represented for

all m and m' combinations as

$$\int d\phi' [e^{-im\phi'} + e^{im\phi'}][e^{im'\phi'} + e^{-im'\phi'}] , \qquad \begin{matrix} m>0 \\ m'>0 \end{matrix}$$

$$\int d\phi' [e^{-im\phi'} + e^{im\phi'}] , \qquad \begin{matrix} m>0 \\ m'=0 \end{matrix}$$

$$\int d\phi' [e^{im'\phi'} + e^{-im'\phi'}] , \qquad \begin{matrix} m=0 \\ m'>0 \end{matrix}$$

$$\int d\phi' , \qquad \begin{matrix} m=0 \\ m'=o \end{matrix}$$

Consequently, the two dimensional integrals of interest are expressible in the more general form:

$$(kP|e^{ivz}|\alpha k') = (1+\sigma_m\sigma_{m'})SV_{kk'}(1)+(\sigma_m+\sigma_{m'})SV_{kk'}(2)$$

$$(kP|e^{ivz}/\gamma_p|\alpha k') = (1+\sigma_m\sigma_{m'})RV_{kk'}(1)+(\sigma_m+\sigma_{m'})RV_{kk'}(2)$$

$$(k\alpha|e^{-ivz}\frac{Z}{\gamma_\alpha}|Pk') = (1+\sigma_m\sigma_{m'})MV_{kk'}(1)+(\sigma_m+\sigma_{m'})MV_{kk'}(2) \qquad (4.23)$$

These expressions can now be integrated numerically with care over the variables y and η after the manner of equation (4.18) and the resultant expressions used in (4.16) to obtain all the spatial matrix elements required in the calculation of the $\hat{W}_{kk'}$. The η integration was effected by means of the Gauss-Legendre method with the number of pivots and weights being allowed to vary with R(t) because there is no difficulty in obtaining sufficient accuracy with only a few points for small R(t) than for large R(t). A ten point Gauss-Laguerre method gives acceptable results

for the y integration. Consequently Gallaher (not yet published) has developed a method whereby the η integration can be performed analytically thereby reducing numerical integration to only over the y variable. This will, without doubt, reduce computing time considerably.

4.4 Time Integration of the Coupled Differential Equation

It should be remembered that the integration of the coupled differential equations (2.25) for the amplitudes proceeds from some large negative time ($-T_{max}$) to a large positive time ($+T_{max}$) such that the boundary conditions are valid there. The elements $\hat{N}_{kk'}$, $\hat{Q}_{kk'}$, $\hat{S}_{kk'}$, $\hat{T}_{kk'}$, $\hat{R}_{kk'}$, $\hat{M}_{kk'}$ as well as $\hat{W}_{kk'}$ have been evaluated for some R(t). Therefore, by implication (see derivation of the coupled differential equations in Chapter II) the calculation of the $\hat{W}_{kk'}$ was for negative time only. However, the $\hat{W}_{kk'}$ are needed for $t > o$ also. We therefore establish a relationship between the $\hat{W}_{kk'}$ ($t > o$) and the $\hat{W}_{kk'}$ ($t < o$). To accomplish this the spatial matrices which determine the $\hat{W}_{kk'}$ for $t > o$ have to be known.

We have seen that $R \cos\theta = -vt$ and $R \sin\theta = \rho$, where $R = \sqrt{\rho^2+(vt)^2}$. For negative times θ varies from near zero ($t = -T_{max}$) to near $\frac{\pi}{2}$ ($t = o$). Positive times corresponding to θ values ranging from $\frac{\pi}{2}$ ($t = o$) to near π($t = +T_{max}$) so that for positive times $\cos(\pi-\theta) = \frac{vt}{R}$ and $\sin(\pi-\theta) = \frac{\rho}{R}$. Therefore $\cos\theta$ is the only quantity that changes

as the time progresses from negative to positive values. Consequently, the only matrix elements affected by the transition from $t < o$ to $t > o$ are those containing $e^{ivz'\cos\theta}$. Thus it is necessary to determine the correspondence between $(kP|e^{ivz}|\alpha k')_{t<o}$ and $(kP|e^{ivz}|\alpha k')_{t>o}$.

We have previously shown that

$$(kP|e^{ivz}|\alpha k')_{t>o} = \chi_{mm'}SV_{kk'}(1) + \gamma_{mm'}SV_{kk'}(2)$$

with $\chi_{mm'} = 1 + \sigma_m\sigma_{m'}$ and $\gamma_{mm'} = \sigma_m+\sigma_{m'}$.

Denoting by θ^- the angle corresponding to $t < o$ and considering only $SV_{kk'}(1)$ (the use of $SV_{kk'}(2)$ will give the same results) we have

$$SV_{kk'}(1) \equiv (kP|e^{ivz'\cos\theta^-}{}_i{}^{|m-m'|}J_{|m-m'|}(v\rho'\sin\theta^-)|\alpha k')_{t<o}$$

$$= (kP|e^{-ivz'\cos\theta^-}{}_i{}^{|m-m'|}J_{|m-m'|}(v\rho'\sin\theta^-)|\alpha k')_{t>o}$$

But $(kP|e^{-ivz'\cos\theta^-}{}_i{}^{|m-m'|}J_{|m-m'|}(v\rho'\sin\theta^-)|\alpha k')_{(t>o)}$

$$= (-)^{|m-m'|}(kP|e^{ivz'\cos\theta^-}{}_i{}^{|m-m'|}J_{|m-m'|}(v\rho'\sin\theta^-)|\alpha k')^*_{(t>o)}$$

Therefore

$$SV_{kk'}(1)[t>o] = (-)^{|m-m'|}SV^*_{kk'}(1)\ [t<o]$$

and in general

$$(kP|e^{ivz}|\alpha k')_{t>o} = (-)^{|m-m'|}(kP|e^{ivz}|\alpha k')^*_{t<o} \qquad (4.25)$$

Thus, it immediately follows that all the elements containing the momentum transfer terms will transform according to (4.25).

The corresponding expression for the $\hat{W}_{kk'}(t>o)$ is obtained by exploiting equation 2.32). Thence the trans-

formation of $(\hat{Y}_1)_{kk'}$ to positive times shall be deduced. The reflection of the spatial matrix elements $\hat{X}_{kk'}$, $(\hat{X}_1)_{kk'}$ and $\hat{Y}_{kk'}$ from t<o to t>o will follow the same procedure as for $(\hat{Y}_1)_{kk'}$. For this section only, the substitutions $\hat{F}_{kk'} \equiv (\hat{Y}_1)_{kk'}$ and $\hat{G}_{kk'} \equiv (\hat{X}_1)_{kk'}$ will minimize confusion in the notation. The $(\hat{Y}_1)_{kk'}$ were defined as (see equations preceding (2.31)).

$$(\hat{Y}_1)_{kk'} = (\hat{D}_1^{-1}\hat{C}_1)_{kk'}$$

$$= [\hat{S}^{-1}\hat{P}-\hat{L}^{-1}\hat{T}]^{-1}_{k\alpha}\,[\hat{S}^{-1}\hat{R}-\hat{L}^{-1}\hat{N}]_{\alpha k'}$$

The matrices $\hat{P}$, $\hat{L}$ and $\hat{N}$ are independent of $\cos\theta^-$ and from (4.25)

$$\hat{S}^{-1}(t>o) = (-)^{|m-m'|}\,\hat{S}^{-1*}(t<o)$$

so that

$$\hat{T}(t>o) = (-)^{|m-m'|}\,\hat{T}^{*}\,(t<o)$$

and

$$\hat{R}(t>o) = (-)^{|m-m'|}\,\hat{R}^{*}(t<o)$$

Thus

$$\hat{F}_{kk'}(t>o) = (-)^{|m-m'|}(\hat{Y}_1)^{*}_{kk'}$$

$$= (-)^{|m-m'|}\hat{F}^{*}_{kk'}\,(t<o)\ .$$

Let us now consider carefully the spatial matrix $\hat{X}_1$ which has been defined as

$$\hat{X}_1 = \hat{D}_1^{-1}\hat{C}_1$$

$$= (\hat{S}^{-1}\hat{P} - \hat{L}^{-1}\hat{T})^{-1}(\hat{S}^{-1}\hat{Q} - \hat{L}^{-1}\hat{M})$$

and writing $\hat{G}$ for $\hat{X}_1$, we obtain

$$\hat{G}_{kk'}(t>o) = [(\hat{S}^{-1*}\hat{P}-\hat{L}^{-1}\hat{T}^{*})^{-1}_{k\alpha}(\hat{S}^{-1*}\hat{Q}-\hat{L}^{-1}\hat{M}^{*})_{\alpha k'}]_{t<o}$$

From the expression for $\hat{N}_{kk'}$ [see equations (4.16)], one may represent $\hat{N}_{kk'}$ as

$$\hat{N}_{kk'} = (-)^{|m-m'|}\hat{N}^{*}_{kk'} \qquad \text{and also write}$$

$$\hat{Q}_{kk'} = (-)^{|m-m'|}\hat{Q}^{*}_{kk'} .$$

Therefore the expression for $\hat{G}_{kk'}(t>o)$ now becomes

$$\hat{G}_{kk'}(t>o) = (-)^{|m-m'|}[(\hat{S}^{-1}\hat{P}-\hat{L}^{-1}\hat{T})^{-1}_{k\alpha}\ (\hat{S}^{-1}\hat{Q}-\hat{L}^{-1}\hat{M})_{\alpha k'}]^{*}_{t<o}$$

$$= (-)^{|m-m'|}\hat{G}^{*}_{kk'}\ (t<o).$$

Similarly, it can be shown without difficulty that

$$\hat{X}_{kk'}\ (t>o) = (-)^{|m-m'|}X^{*}_{kk'}\ (t<o)$$

and

$$\hat{Y}_{kk'}\ (t>o) = (-)^{|m-m'|}\hat{Y}^{*}_{kk'}\ (t<o)$$

Therefore, it follows from (2.32) that

$$\hat{W}_{kk'}(t>o) = (-)^{|m-m'|}\begin{pmatrix}\hat{G}^{*}_{kk'} & \hat{F}^{*}_{kk'}\\ \hat{X}^{*}_{kk'} & \hat{Y}^{*}_{kk'}\end{pmatrix}_{t<o}$$

$$= (-)^{|m-m'|}\ \hat{W}^{*}_{kk'}\ (t<o) \qquad (4.26)$$

It should be noted that one could obtain (4.26) directly from the $\hat{W}_{kk'}$ given in (2.33). Thus if one considers the relationship

$$\begin{pmatrix} \hat{Q} & \hat{R} \\ \hat{M} & \hat{N} \end{pmatrix}_{t>o} = \begin{pmatrix} \hat{Q} & (-)^{|m-m'|}\hat{R}^* \\ (-)^{|m-m'|}\hat{M}^* & \hat{N} \end{pmatrix}_{t<o}$$

with $\hat{Q} = (-)^{|m-m'|}\hat{Q}^*$ and $\hat{N} = (-)^{|m-m'|}\hat{N}^*$

so that

$$\begin{pmatrix} \hat{Q} & \hat{R} \\ \hat{M} & \hat{N} \end{pmatrix}_{t<o} = (-)^{|m-m'|}\begin{pmatrix} \hat{Q} & \hat{R} \\ \hat{M} & \hat{N} \end{pmatrix}^* ,$$

one immediately obtains (4.26) from the first equation in (2.33).

The elements $\hat{W}_{kk'}$ are evaluated and stored at constant intervals over a coarse trajectory time mesh determined by $\Delta T = \frac{T_{max}}{J_{max}-\frac{1}{2}}$, where JAY runs from 1 at $t = -T_{max}$ to J_{max} at $t = -\frac{\Delta T}{2}$, where $\Delta t = \frac{\Delta T}{L_{max}}$ (L_{max} being arbitrary) specifies the fine mesh. Thus knowing the $\hat{W}_{kk'}$ at each coarse mesh point JAY along the trajectory by means of a five point Lagrange interpolation formula, the values of the $\hat{W}_{kk'}$ corresponding to each Δt on the fine mesh can be calculated.

To be consistent with our purpose, we shall endeavour to make the time integration of the differential equation $i\dot{A}_k = W_{kk'}A_{k'}$ as general as possible. Necessary details will be provided in Chapter V in which results are presented for the specific case of the He^{2+} - H collision. The time integration of the differential equations for the amplitudes $A_k(t)$ from $-T_{max}$ to $+T_{max}$ over the fine mesh proceeds via

a fourth order Adams-Moulton formula with the Runge-Kutta method (Ralston, 1962) as starter. The Cheshire (1968) procedure is suitable for the extrapolation of the amplitudes from $t = +T_{max}$ to $t \to \infty$. This extrapolation method is more accurate than the previous approximate formulation used by W - G. Preservation of unitarity plays an essential role in determining the acceptability of calculated results and may be maintained within some predetermined value throughout the calculation; the check upon unitarity preservation being made at $t = \pm T_{max}$ and at $t \to \infty$. In this way spurious results may be checked and eliminated. A further more stringent check on unitarity preservation may be carried out by utilizing detailed balance and time reversal invariance arguments, however, these additional means of checking the results have not been implemented here (see Green (1965) and also McDowell and Coleman p. 192).

Defining the excitation cross section as Q_{DE} and the charge transfer cross section as Q_{EX} and remembering that $A_k(t) = \begin{pmatrix} a_k(t) \\ b_k(t) \end{pmatrix}$, we obtain

$$Q_{DE} = 2\pi \int_0^\infty \rho |a(\infty)|^2 d\rho$$

and (4.28)

$$Q_{EX} = 2\pi \int_0^\infty \rho |b(\infty)|^2 d\rho$$

It might be worthwhile to add here that for the case of the He^{2+}-H collision, it was observed that at large R(t) the spatial matrix elements $\hat{W}_{kk'}$ varied smoothly with JAY or

R(t). However, as R(t) became smaller the $\hat{W}_{kk}$, began to vary rapidly; the extent of the variation being dependent upon the impact parameter and the energy of the incident α-particle. This, therefore, necessitated the introduction of a variable parameter FNJ which divided the coarse interval between J1 and J1 + J2 according to the value of FNJ, where J1 + J2 = JMAX and J1 (or J2) is arbitrary. Gallaher and Wilets (1968) observed this same behaviour for the case of the H^+-H collision. Therefore there is no reason to believe the contrary for this general case. Anyway the computer program takes care of the rapid behaviour of the $\hat{W}_{kk}$, and FNJ may be set accordingly, depending on the value of the impact parameter ρ.

CHAPTER V

RESULTS AND DISCUSSION

5.1. Introduction

In this chapter we present numerical calculations for the collision between an α-particle and atomic hydrogen which is initially in the ground state. Computations have been carried out coupling the four eigenstates 1s, 2s, $2p_0$ and $2p_1$ ($2p_1 \equiv 2p_{\pm}$) and in some cases the four pseudo-states $\overline{1s}$, $\overline{2s}$, $\overline{2p_0}$, and $\overline{2p_1}$. In this chapter a pseudo-state will be represented as $\overline{nm}$ or $|\overline{nm}\rangle$, where n denotes the principal quantum number and m is either s or p and stands for either an s or p state. These calculations were obtained for kinetic energies of the incident α-particle in the laboratory reference frame from 6.3 keV to 4 Mev. For each of these energies considered, the direct and charge exchange probabilities $P_k(\rho, E)$ to each applicable state as well as the pseudo-direct and pseudo-exchange probabilities $\bar{P}_k(\rho, E)$ were calculated over the range of impact parameters necessary for numerical determination of the various cross sections. For a four-state calculation the P_k results consist of a set of eight numbers — the first four yield excitation results and the last four

correspond to charge transfer results. Therefore k ranges from 1 to $2K_{max}$.

Plots were obtained representing probabilities times impact parameter against impact parameter ρ for the range of energies under consideration. Initially rather arbitrary values of ρ were selected and these plots constructed. More values of ρ were introduced as deemed necessary to precisely determine the structure of these curves. Thus unnecessary computations were avoided. In general, some of the individual probabilities exhibited considerable structure at low energies and small impact parameters. However, at low energies the main contribution to the cross sections arises from relatively large values of ρ. Consequently, the rapid variations of the plots of $P_k(\rho, E)\rho$ against ρ were not too closely followed for small values of ρ where the contribution to the cross section is in any case small in this energy region. The high-energy behaviour of the variation of $P_k(\rho, E)\rho$ versus ρ necessitated more careful determination of the quantities $P_k(\rho, E)$ even at small impact parameters; small ρ values account for the major contribution to the cross section here.

The $P_k(\rho, E)$ and the $\overline{P}_k(\rho, E)$ were obtained from the amplitudes $A_k(t = +\infty)$ using the relationship

$$P_k(\rho, E) = |A_k(t = +\infty)|^2.$$

The $A_k(t = +\infty)$ are the asymptotic solutions of the coupled differential equations represented by (2.25). The substitution

of eigenstates or pseudo-states into the expansion of the electronic wave function determines the $P_k(\rho, E)$ or the $\overline{P}_k(\rho, E)$. The required asymptotic amplitudes $A_k(t = +\infty)$ were calculated by means of our computer program and the quantities $P_k(\rho, E)$ constructed as above. In most of the calculations performed, $P(\rho, E)$ was determined to an accuracy better than one per cent. However for energies of the projectile around 800 keV and greater charge transfer and excitation cross sections are small. Therefore the accuracy of $P(\rho, E)$ here depended upon the magnitude of the cross section for the particular charge transfer or excitation process concerned. At 4 Mev, for example, where both charge exchange and excitation of the target atom are small, $P(\rho, E)$ was evaluated to better than 0.1 per cent. Like Wilets and Gallaher (1966) and Gaussorgues and Salin (1971) we found that Z_{max} need not be unnecessarily large; a value of Z_{max} around 30 Bohr radii was more than adequate. Typical low energy numerical integration values were Z_{max} = 32 Bohr radii, FNJ = 2, J1 = 20, J2 = 15 for values of $\rho > 3$. For $\rho < 3$, J1 and J2 had to be adjusted accordingly. For some calculations, FNJ was set equal to 3 or even 4. A consistency check was carried out when ρ became very small (≤ 0.1) depending upon the energy. This is necessary because of the general difficulty of obtaining good unitarity checks at small ρ values.

Charge transfer cross sections and direct excitation cross sections were obtained from the $P_k(\rho, E)\rho$ versus ρ plots by numerical integration using Bode's rule (see Abramowitz and Stegun 1970, p. 889 and Hildebrand 1956). Where the plots displayed considerable structure, the interval of integration $\Delta\rho = \rho_i - \rho_{i-1}$ was reduced and the curves divided into suitable segments each with a maximum of eight or ten equidistant ρ values. For some of the curves that displayed logarithmic tails which diminished monotonically, the formula

$$\Delta A = \dot{y}_n(\rho_n - \rho_{n-1})/\ell n\ [\frac{y_{n-1}}{y_n}]$$

where $\dot{y}_n = P_n(\rho, E)\rho_n$ was employed to estimate the additional area beyond ρ_n (ρ_n being the final impact parameter in the integration).

The 2p polarization fractions $P_o^{2p}(E)$ were computed from both charge transfer and direct excitation cross sections from the formula due to Percival and Seaton (1958):

$$P_o^{2p} = \frac{\sigma_o - \sigma_1}{a\sigma_o + b\sigma_1}$$

where σ_o and σ_1 represent the $2p_o$ and $2p_1$ cross sections and the constants a and b are given for p states by a = 2.375 and b = 3.749.

The estimation of ionization cross sections is applicable to only those energies at which calculations of the cross sections (excitation and charge transfer) involved the utilization of pseudo-states. The implementation of

these pseudo-states is an artifice to try to allow for the continuum in the expansion; an estimate of ionization may consequently be extracted from such a calculation (for explicit form of the pseudo-states see 5.4.) One would reduce considerably the amount of labour in calculating cross sections for the three processes of charge transfer, excitation of the target atom and ionization if they could somehow be obtained simultaneously. If the pseudo-states include both bound and continuum portions then it should be possible to calculate ionization after excitation and charge transfer have been obtained. We would extract ionization cross sections as follows. Let $|n\ell\rangle_H$ be an eigenstate for the hydrogen atom and $|\overline{n\ell}\rangle_H$ the corresponding pseudo-state. Similarly, let $|n\ell\rangle_{He^+}$ denote a He^+ eigenstate and $|\overline{n\ell}\rangle_{He^+}$ the corresponding pseudo-state with n being the principal quantum number and ℓ standing for either an s or p state. Then the ionization cross section in this approximation is given by

$$\sigma_{ion}(E) = \sigma^{exct}_{1s-\overline{1s}} \left[1 - \sum_{n=1}^{\infty} \left| \underset{H}{<} \overline{1s} \,|\, ns\rangle_H \right|^2 \right]$$

$$+ \sigma^{exct}_{1s-\overline{2s}} \left[1 - \sum_{n=1}^{\infty} \left| \underset{H}{<} \overline{2s} \,|\, ns\rangle_H \right|^2 \right]$$

$$+ \sigma^{exct}_{1s-\overline{2p}} \left[1 - \sum_{n=2}^{\infty} \left| \underset{H}{<} \overline{2p} \,|\, np\rangle_H \right|^2 \right]$$

$$+ \sigma^{exch}_{1s-\overline{1s}} \left[1 - \sum_{n=1}^{\infty} \left| \underset{He^+}{<} \overline{1s} \,|\, ns\rangle_{He^+} \right|^2 \right]$$

$$+ \sigma^{exch}_{1s-\overline{2s}} \left[1 - \sum_{n=1}^{\infty} \left| \; {}_{He^+}\!\langle \overline{2s} | ns \rangle_{He^+} \right|^2 \right]$$

$$+ \sigma^{exch}_{1s-\overline{2p}} \left[1 - \sum_{n=1}^{\infty} \left| \; {}_{He^+}\!\langle \overline{2p} | ns \rangle_{He^+} \right|^2 \right]$$

$$+ \ldots \qquad (5.1)$$

The term involving the cross section $\sigma^{exct}_{1s-\overline{1s}}$ has no meaning because excitation of the hydrogen atom to its ground state makes no physical sense. One immediately sees that ionization cross sections can be calculated from the knowledge of the exchange cross sections σ^{exch} and excitation cross sections σ^{exct} when pseudo-states are employed. The problem here is how to choose the most advantageous pseudo-states. The lack of experimental observations on ionization cross sections leaves us without guidance.

5.2. Probability times impact parameter versus impact parameter plots.

In figures 5.1 to 5.16 we present plots of probability times impact parameter against impact parameter for the following energies of the incident α-particle: 6.3, 10, 15.81, 25, 40, 50, 100, 200, 400, 800, 3000, and 4000 keV. The impact parameter is measured in units of a_o, and the energies are measured in the laboratory reference frame. These impact energies were selected to facilitate comparison with other available theoretical calculations, in particular those of Malaviya (1969). Figures 5.1 to 5.4 inclusive represent calculations coupling pseudo-states whereas the rest of the plots, figures 5.5 to 5.16, are the results for

eigenstates. Both the pseudo-state results and the eigenstate results for an incident α-particle energy of 25 keV have already been presented at the 25th Annual Gaseous Electronic Conference (1972) and are included here for completeness. The evolution with energy of the magnitudes and shape of these figures represents the general behaviour in energy of the cross sections since the areas under the curves are a direct measure of the cross sections. Consequently we shall make a detailed analysis of these probability times impact parameter versus impact parameter plots.

In general, the pseudo-state results display more structure than the eigenstate calculations. The shapes of the pseudo-state results differ significantly from the eigenstate results at the same energies; however they have the same ρ-spread. An examination of the plots in figures 5.5 to 5.16 reveals certain general features. At low energies of the projectile the charge transfer process predominates over excitation of the H atom, the plots revealing structure and having an effective ρ spread of about 10 Bohr radii. The main contribution to charge transfer cross sections comes from values of $\rho > 1$ Bohr radius, mostly around 4 Bohr radii. Excitation of the H atom to individual states (2s, 2p) is small and displays rapid oscillations. Consequently the combined effect to the n=2 quantum level of H has been evaluated. To obtain reliable values for the cross sections to the different states of H for n=2, one would require to know the $P_k(\rho, E)$ for many

values of ρ. This general behaviour in the plots continues through 25 keV to about 200 keV where all the curves display a single preponderant peak. The excitation graphs reveal their maxima at approximately ρ = 4 Bohr radii for p states and at ρ somewhat less than 4 Bohr radii for the s state. The range of the charge transfer curves has diminished to about ρ = 5 Bohr radii. Meanwhile the ρ spread for the excitation curves has increased to about 10 Bohr radii. Therefore, in general, as the energy of the α-particle increases the charge exchange plots shrink in ρ spread and diminish in magnitude. The excitation plots, however, increase both in range and in magnitude.

At 800 keV, charge transfer to the $He^+(2s)$ ion still displays two distinct peaks; the dominant peak now having switched over to the smaller value of ρ. The 1s - 1s charge transfer process has become predominant over the rest of the exchange plots; most of the charge transfer probability now going to the ground state of the He^+ ion. This observation is consistent with the theoretical prediction of Bates and McCarroll (1962) who prognosticated that at high energies charge transfer to s states should dominate. The behaviour of the charge transfer plots at high energies contradicts the argument by Malaviya (1969) that charge transfer to the ground state can be omitted without specifying the energy range. At 800 keV the ρ spread of all the charge transfer plots has diminished to about ρ = 3 Bohr radii. On the other hand the excitation curve areas,

the 2p in particular, have increased in magnitude over those for the exchange plots while their range goes well beyond ρ = 10 Bohr radii. In fact these curves display the same behaviour as the radial probability density versus the distance from the nucleus plots given in Richtmyer et al. (1955) p. 211, Fig. 57. These curves reflect the strong coupling between the 2s and 2p states.

The behaviour at very high energy (4 Mev for example) of the plots for both charge transfer and excitation processes is anomalous. Charge transfer to the 2p level has become very small and therefore has not been plotted. The 1s - 2s charge exchange plot reveals two strong and distinct peaks with maxima at $\rho \simeq 0.5$ and $\rho \simeq 3.5$ Bohr radii. The magnitude and ρ spread of this curve exceed that of the same plot at 800 keV. The 1s-2p excitation plot has now acquired three peaks and has diminished in range. The 1s - 2s excitation curve, though maintaining the simgle peak it displayed at 400 keV through 800 keV with approximately the same ρ spread of about 2 Bohr radii, has decreased in range. This very high energy behaviour of the plots may reflect a deterioration of the impact parameter approximation at these energies.

5.3. Charge transfer cross sections and excitation cross sections.

Tables 5.1 and 5.2 represent both excitation cross sections and charge transfer cross sections when pseudo-states

and eigenstates were coupled. The 2p polarization fractions p_o^{2p} are also included in each of these tables. The pseudo-state results for the total capture cross sections are very similar to the corresponding eigenstate total capture cross section results. Quite generally the use of pseudo-states in the particular form chosen in this thesis cause a redistribution of the probability populations of the individual 2p sublevels (m=o and m=±1). The total cross sections to the n=2 quantum level appear to be independent of whether pseudo-states or eigenstates have been employed in the expansion.

For the process of excitation, both individual and total excitation cross sections turn out to be sensitive to whether eigenstates or pseudo-states are used. A comparison at corresponding energies of the excitation cross sections represented in tables 5.1 and 5.2 supports this claim.

From Rapp's calculation one sees that the inclusion of the $He^+(1s)$ in the expansion of the total electronic wave function depresses the H(2) cross section. One may then explain the dominance of the H(2) pseudo-state cross section over the H(2) eigenstate cross section at 800 keV. A good simulation of the collision at close encounters is essential at high energies because change transfer is confined to small values of impact parameters. Therefore if excitation is achieved also through coupling open channels of the H atom with the states of the He^+ ion in particular the ground state, then the use of pseudo-states should decrease the cross section further because the criterion for their choice was to give strong overlap with the states of the $^5Li^{++}$ ion which

for small impact parameters may be thought in some sense to be temporarily "formed" during the collision. We also note that the $P_k(\rho,E)\rho$ versus ρ plots for excitation at high energies are spread over broad regions of impact parameter. At low energies, however, the transition takes place via compound transitional states which may be some of the intermediate states of the $^5Li^{++}$ ion. The main contribution to these low energy cross sections comes from values of $\rho > 1$.

Perhaps a revealing way to assess with delicacy the effects of a particular pseudo-state basis choice upon the calculated cross sections would be to retain the first four hydrogenic eigenstates 1s, 2s, $2p_o$ and $2p_1$ and represent the 3s and 3p states in pseudo form.

In table 5.3, we have compared our present calculated results Q_p with the four-state results of Malaviya (1969) Q_M and the eight-state calculations of Rapp Q_R for charge transfer cross sections. The latter's prepublication results became available to us after we had completed our investigation. This explains the difference in some of the energies at which the calculations have been carried out. For some energies, Malaviya has not evaluated capture cross sections to the ground state; hence the blanks. In general the 1s-1s charge transfer cross section is small at low and moderate energies. Consequently charge transfer to the ground state of the He^+ ion is sensitive to the extent to which unitarity is conserved. Therefore cross sections to the $He^+(1s)$ ion have not been computed where unitarity was poorly preserved. There is generally fair agreement among the

three calculations for cross sections to $He^+(2s)$ except at energies of the projectile less than about 16 keV where Rapp's calculations exceed ours and Malaviya's in that order. For He^{2+} energies in excess of 25 keV, the results of Rapp exceed ours whereas Malaviya's are smaller and begin to rise above ours at 200 keV. For capture cross sections to the 2p level, the three calculations are in fair agreement except at 25 keV where our calculations are lower than Q_M or Q_R. At energies less than about 15 keV, Malaviya's capture cross sections to the 2p level fall faster than ours with decreasing energy. Above about 50 keV his total capture cross sections to the n = 2 level dominate ours persistently with agreement becoming closer as the energy increases. However, at 10 keV there is better agreement between Rapp's results and ours with the former's remaining above ours as the energy decreases.

In figure 5.17 we make a comparison between the results on capture cross sections to the second quantum level of the He^+ ion obtained in the present calculations and Malaviya's corresponding cross section results, the experimental measurements by Fite et al. (1962) and by Pivovar et al. (1962). As mentioned by Malaviya, the measurements by Fite et al. were carried out utilizing $^3He^{2+}$ ions and therefore, they were scaled to correspond to $^4He^{2+}$ ions. The cross sections presented by Pivovar et al. were experimentally for capture from H_2 molecules; the raw data being halved for the present case. The latter adjustment introduces an uncertainty and according to Tuan and Gerjuoy (1960) is not strictly justified. Also

included are the theoretical results of Coleman and Trelease (1968) using the impulse approximation, which are denoted by CT. At low energy, there is good agreement between our calculations and experiment. Between about 16 and 100 keV disagreement between theoretical results and experimental measurements persists. The high energy behavior of our calculations exhibits the same trend as Malaviya's. It must be noted that for readily visualizable comparison we merely plotted our results over those of Malaviya.

To facilitate comparison with the calculated total capture cross sections by Rapp and with the experimental measurements by Fite et al., we have plotted our results over the former's in figure 5.18. The extent of agreement between theory and experiment is obvious from the plots. Again here the measurements by Fite et al. were for the $^3He^{2+}$ ions. There is relatively good agreement between our calculation and Rapp's cross sections except between 15 and 25 keV where Rapp's results surpass ours. At high energies our results tend to agree with the seven-state calculation by Rapp. The apparent predominance of the experimentally determined total capture cross sections over the calculated total capture cross sections is to be expected. As one adds more and more states, the calculated cross sections would be expected to converge to some limit - perhaps (hopefully) the experimentally measured results! Around 20 keV the experimental points are rather scattered. Comparison with theoretical calculations would be facilitated if a curve with error bars was drawn through the experimental points.

In figure 5.19 we present plots of excitation cross sections against impact energy. For impact energies less than 25 keV we omitted the calculation of excitation cross sections to the individual states for the quantum level n=2. This is due to the difficulty of obtaining reliable computations for the cross sections for small energies. The calculation could be done if required, however. Our calculations for the excitation cross sections exceed those of Rapp considerably. We have found one possible explanation for this discrepancy: one of the time factors in the expansion for the electronic wave function employed by Rapp is erroneous (see for example McDowell and Coleman 1970, p. 157 equations 4.10.5 or Bates 1958 for the correct time factors). The time factor $\exp[i(q-p)\frac{v^2}{2}t]$ appearing in our equation (2.32) becomes incorrect in Rapp's formulation; so does the $E_{kk'}(t)$ given by the second equation in (2.33). To what extent this error affects the excitation cross sections we do not know. The error does not seem to be of any consequence for charge transfer calculations; there is reasonable agreement between our results and Rapp's. The only major difference is in the distribution of the probability populations of the individual 2p sublevels. There are unfortunately no experiments available with which to compare our polarization results.

An examination of Rapp's seven-state and eight-state calculations is quite revealing; the excitation cross sections

are sensitive to the inclusion or omission of the ground state of the He^+ ion. We have already pointed out that the choice of our pseudo-states affected excitation cross sections extensively even in cases where the main contribution to the cross sections came from relatively large values of ρ. If the impact energy is not too high, one can picture the excitation of the H atom as involving also the charge transfer process and thus coupling the states of the He^+ ion. Therefore in the manner of Cheshire (1968) we "see" the electron "hopping" to and from the He^{2+} ion as the α-particle passes the H atom with the electron eventually ending up in one of the higher states of the H atom — the hydrogen atom is now excited. Consequently one sees that the processes of charge transfer and direct excitation are coupled in an intricate manner so that calculating the one process without the other could lead to incorrect results.

To see how reliable are our calculated excitation cross sections we have compared them with those of Bates (see Bates 1962 pp. 589 and 590, figures 19 and 20) obtained by both the distortion approximation and the first Born approximation. For the 1s - 2p excitation cross sections our results agree well with the distortion approximation cross sections at 40, 50 and 800 keV. Beyond 50 keV our 1s - 2p cross sections fall below those of Bates reaching a maximum at about 200 keV. The 1s - 2p distortion cross sections of Bates also display a maximum at around 200 keV.

Beyond 200 keV our 1s - 2p excitation cross sections gradually approach from below those of Bates until 800 keV where good agreement is achieved again.

The case of the 1s - 2s excitation cross sections is different. Bates has remarked that 1s - 2s transitions are more likely to be affected by distortion than 1s - 2p transitions. The reason for this being that close encounters, where distortion is more effective, contribute relatively more to the 1s - 2s transitions than to the 1s - 2p transitions. It is therefore not surprising that our 1s - 2s excitation cross sections are much higher than those by Bates obtained using both the distortion approximation and the first Born approximation and tend to display the same behaviour as the Born approximation results at high energies.

Our 1s - 2s excitation cross sections show better agreement with Rapp's 1s - 2s results. For example: 400(8.05, 8.58); 200(11.98, 15.00); 50(5.31, 7.30); 25(1.79, 6.50) where the number outside the bracket indicates the energy in keV and the two numbers inside the bracket respectively represent the 1s - 2s excitation cross sections in units of $10^{-17}cm^2$ by Rapp and of this thesis. What conclusion can one draw from the picture we have depicted on the state of theoretically evaluated excitation cross sections? Not much indeed! The reader as an "external observer" is allowed some freedom of opinion for a change. However, it is imperative to point out that our calculations

including those by Rapp and more sophisticated than either the first Born approximation or the distortion approximation employed by Bates.

5.4. Ionization cross sections

In order to calculate ionization cross sections, a knowledge of continuum states is required. However, we do not know the continuum states in this case. Consequently we extract ionization cross sections from the knowledge of charge transfer cross sections and excitation cross sections obtained from coupling pseudo-states. We now illustrate the basis of the method. In the united atom limit ($R \to 0$, $\gamma_\alpha = \gamma_p$) Wilets and Gallaher (1966) have shown that for the H^+ - H collision $\sum_{n=1}^{\infty} | {}_{He^+}\langle 1s | ns \rangle_H |^2 = 0.76$ where $|1s\rangle_{He^+}$ and $|ns\rangle_H$ represent the bound states of the united atom and the hydrogen atom respectively. Therefore they concluded that there is little hope of simulating the collision process with a hydrogenic basis. Cheshire et al. (1970) then concluded that the remaining fraction comes from the hydrogenic continuum.

Pseudo-states are an approximation to the flux into all the open channels. In this case the open channels are charge transfer, excitation and ionization. Therefore we may calculate the total probability by coupling pseudo-states and eigenstates; the difference should give the fraction which goes into the continuum so that ionization cross sections may be estimated by using (5.1). The reasoning that

ionization may take place in the united atom limit $R \to 0$ and still be observed at $R \to \infty$ is consistent with the experimental measurements by Keever and Everhart (1966) who have attributed the oscillations in the total charge transfer probability versus impact evergy not to the accidentally resonant reaction $H(1s) + He^{2+} \to He^{+}(2s \text{ or } 2p) + H^{+}$ but to the $2p\sigma - 1s\sigma$ transition where $1s\sigma$ and $2p\sigma$ refer to the HHe^{2+} states (united atom). The experimental measurements are carried out at $R \to \infty$.

In figure 5.20 we have plotted the 2p polarization fraction P_o calculated from eigenstates, and the estimated ionization cross sections as a function of impact energy. The inner scale refers to polarization fractions and the outer to ionization cross sections. There are no experiments nor calculations available on either the 2p polarization fractions or ionization cross sections using α-particles as projectiles with which to compare our results. An explanatory note on the ionization cross sections is necessary.

The presentation of a graph with only four points on it should not be misconstrued. It should rather be considered as an attempt to obtain some idea about the behavior of ionization cross sections with impact energy, which follows from this hitherto untried concept of pseudo-states in the case of the He^{2+} - H collision. The main contribution to the ionization cross sections comes from the fraction

$$1 - \sum_{n=2}^{\infty} \left| < \overline{2p} \mid np > \right|^2_H = 0.8927, \text{ followed by}$$

$1 - \sum_{n=2}^{\infty} \left| {}_{He^+}\langle \overline{2p} \mid np \rangle_{He^+} \right|^2 = 0.2572$. The coefficient of $\sigma^{exch}_{1s-\overline{1s}}$ is small and therefore makes its contribution to the total ionization cross section quite small too. Below we present our estimate of ionization cross sections as a function of impact energy.

Impact energy (keV)	σ_{ion} ($X10^{-17}$ cm^2)
6.3	16.86
25	37.30
50	30.87
800	16.16

From the points on the graph in figure 5.20 one entertains the idea that ionization cross sections display a maximum around 20 keV and decay gradually as the impact energy increases beyond 1 Mev. Indeed the plot exhibits the same general behaviour as the ionization cross sections of the H atom by proton impact (see for example McDowell and Coleman 1970, p. 324, Fig. 7.2.1). Although there is no experiment nor calculation on ionization cross sections of the H atom by α-particle impact to contradict our estimated cross sections, nevertheless we are not satisfied with this calculation.

We have selected the radial part of our pseudo-states for the He^+ ion to have the following form (there are similar expressions for the H atom)

$$\overline{R}_{10} = 2\alpha^{3/2} e^{-\alpha\gamma}$$

$$\overline{R}_{20} = (A - B\gamma) e^{-\gamma}$$

where A and B are given in terms of the parameter α as

$$B = \frac{2}{\left[\frac{9}{(1+\alpha)^2} - \frac{9}{1+\alpha} + 3\right]^{\frac{1}{2}}}$$

and

$$A = \frac{3B}{1 + \alpha} \quad .$$

$$\overline{R}_{21} = 2\beta^{5/2}\gamma\, e^{-\beta\gamma} \quad .$$

The parameters α and β are different from each other and are chosen as follows

$$\alpha = (2.7 - 2)\, e^{-6R(t)} + 2$$

and

$$\beta = (1.4 - 1)\, e^{-6R(t)} + 1$$

In principle this choice is good since as $R(t) \to \infty$ the pseudo-states reduce to the ordinary atomic orbitals and as $R(t) \to 0$, they represent the intermediate states of $^5Li^{++}$ adequately. There are two main objections against the choice.

First, R(t), the internuclear separation, is a function of time. Therefore, there should be time derivatives arising from the $e^{-6R(t)}$ term in our coupled differential equations. However, noting that $e^{-6R(t)}$ is effective mainly at small R(t) whereas the contribution to both charge transfer and excitation cross sections comes from values of $\rho > 2$ Bohr radii in most cases, the terms arising from

$e^{-6R(t)}$ will always be small for all practical purposes. Difficulties arise however, when one attempts to compute the points for the Everhart curve which correspond at higher energies to very small values of ρ.

Second, according to Cheshire et al. (1970) the 2s state of hydrogen "... has a strong degeneracy coupling with the 2p state at moderate and large internuclear separations which affects the 2s and 2p excitation and exchange cross sections." Consequently these states (that is the 2s and 2p) ought to be included explicitly as eigenstates and the higher states selected as pseudo-states in our expansion of the electronic wave function. Therefore, the next step in our future calculations will be the retention of the 1s, 2s, and 2p hydrogenic states and the conversion of the 3s and/or 3p to pseudo-states.

The extraction of ionization cross sections in this fashion is a beautiful concept and ought to be pursued further. This is one way of calculating the three processes: charge transfer, excitation and ionization simultaneously; physically they are coupled channels.

5.5. Keever et al. curve

We have tried to obtain the points for the Keever et al. curve of total charge transfer probability as a function of impact energy without success. The curve is obtained by making use of the relationship connecting the kinetic energy of the incident α-particle with impact

parameter as well as with the angle of scattering . From Richtmyer et al. p. 145, equation (73a, b) we write

$$\rho = \frac{2Z\ e^2\ \cot(\theta/2)}{Mv^2} \tag{5.10}$$

where in this case Z = 1, e = 1 and E is the kinetic energy of the incident α-particle ($E = \frac{1}{2}Mv^2$). The impact parameter may be written in terms of E thus

$$\rho = \frac{\cot(\theta/2)}{E}$$

where E is in units of 27.2 eV. Therefore, the impact parameter may be obtained as a function of impact energy and hence of the incident α-particle velocity. Keever et al. have measured the total charge transfer probability for kinetic energies varying from 2keV to 100 keV at $\theta = 1.2°$ and 1.7°. Due to the difficulty of working with $^4He^{2+}$ beams, Keever et al. employed $^3He^{2+}$ ions for the experiment. The desired kinetic energy can then be obtained by scaling.

Our interest lies in obtaining the Keever et al. curve at $\theta = 1.2°$ to show how good or bad the atomic eigenfunction basis is in representing the collision at such small impact parameters. One sees from the above equation that as E increases from 2keV to 100 keV, ρ decreases proportionately (for example for E = 2 keV, ρ = 1.299 Bohr radii and for E = 100 keV, ρ = 0.026 Bohr radii). Consequently, from the nature of eigenfunctions, one does not expect good results from such a calculation.

Coupling four eigenstates, we obtained a few points and plotted them over the experimental points of Keever et al. Figure 5.21 shows our calculated values and the experimentally determined curve. For the results at 25 keV, and at 3 keV, unitarity preservation was satisfied to high accuracy (better than .1 per cent) and for the other points unitarity was conserved to better than 3 per cent. In fact, for energies greater than or less than about 25 keV it was not necessary to strive for high accuracy in the computation of the total charge exchange probability because it was obvious what we were up against. We obtained more points to prove our case beyond reasonable doubt. At 25 keV there is better agreement between our calculation and the experimental point. However, above and below 25 keV, our calculation drops far below the experimental points. This is not hard to explain. We have seen that charge transfer cross sections exhibit a maximum at around 25 keV. At high and low velocities charge transfer is confined to small values of the impact parameters. At small values of impact parameters, the atomic eigenfunction expansion basis we have employed is not adequate; it does not simulate accurately the collision at close encounters.

We then employed a pseudo-state expansion basis with an $e^{-6R(t)}$ dependence. For small impact energies (2 and 5 keV) where ρ is around one Bohr radius, we obtained values of the total charge transfer probability that were much

greater than the corresponding values obtained from the eigenstate basis and, therefore were closer to experimental values. As the energy increased, it became almost impossible to obtain a reasonable value for the total charge transfer probability without violating unitarity preservation considerably. This follows from the fact that $\rho \propto \frac{1}{E}$ and as pointed out before our choice of $e^{-6R(t)}$ is not sound at small values of ρ.

In the light of the preceding calculation on total charge transfer probability one ought to be careful about the conclusion one draws. The same eigenfunction expansion basis gave reasonable agreement with the experiments of Fite et al. on both total charge transfer cross sections and capture cross sections to the n=2 quantum level of the He^+ ion. Here the same basis gives hopeless results; there is no contradiction in terms, however. The expansion basis performed according to what it was designed to do. Therefore, a judicious choice of pseudo-states should bring better agreement with the experiments of Keever et al. This may be put in slightly different form as: a good agreement between the calculated results and the experiments of Keever et al. will reflect a good simulation of the collision process at close encounters.

Energy of He^{2+}(keV)	6.3	25	50	800
State of Capture				
$He^+(1S)$	0.59	3.14	6.38	0.41
$He^+(2S)$	22.87	24.03	33.03	0.02
$He^+(2P_o)$	23.50	48.40	28.16	0.17
$He^+(2P_1)$	19.93	36.60	26.68	0.20
$He^+(2P)$	43.42	84.99	54.84	0.37
$He^+(2)$	66.29	109.03	87.87	0.39
$He^+(1+2)$	66.87	112.16	94.25	0.80
P_o^{2P}	0.0274	0.047	0.0089	-0.028
State of Excitation				
$H(2S)$	3.18	10.92	11.14	5.03
$H(2P_o)$	5.69	14.41	14.47	7.88
$H(2P_1)$	0.65	2.73	3.99	10.10
$H(2P)$	6.34	17.14	18.46	17.98
$H(2)$	9.52	28.06	29.61	23.02
P_o^{2P}	0.315	0.263	0.044	-0.039

Table 5.1. Capture and excitation cross sections (in units of 10^{-17} cm^2) computed in the $\overline{1S}$, $\overline{2S}$, $\overline{2P}$ close coupling approximation. P_o^{2P} represent the 2P polarization fractions; H(2): excitation to the n=2 level; He^+ (2): capture to the n=2 level; He^+ (1+2): total capture to the n=1 and n=2 levels.

Energy of He^{2+}(keV)	6.3	10	15.81	20	25	40	50	100	200	400	800	3000	4000
State of Capture													
$He^+(1S)$	1.17	-	-	2.56	1.46	2.37	2.38	1.09	0.77	0.18	0.35	0.24	0.74
$He^+(2S)$	22.07	27.82	25.21	24.41	23.37	27.92	28.44	16.33	2.13	0.23	0.06	0.18	0.23
$He^+(2P_o)$	27.06	37.38	38.77	40.84	42.54	38.30	35.01	10.41	2.72	0.79	0.24	-	-
$He^+(2P_1)$	15.25	32.60	44.86	48.98	44.08	30.68	28.49	20.18	9.59	1.95	0.16	-	-
$He^+(2P)$	42.31	69.98	83.63	89.83	86.62	68.98	63.50	30.59	12.31	2.74	0.40	0.08	0.06
$He^+(2)$	64.38	97.80	109.84	114.23	109.99	96.90	91.94	46.92	14.44	2.97	0.46	0.26	0.29
$He^+(1+2)$	65.55	101.79	114.68	117.30	111.45	98.27	94.32	48.01	15.21	3.15	0.81	0.43	1.03
P_o^{2P}	0.097	0.023	-0.023	-0.029	-0.0058	-0.037	0.034	-0.097	-0.162	-0.126	0.068	-	-
State of Excitation													
H(2S)	-	-	-	-	6.50	6.34	7.30	15.17	15.00	8.58	4.70	5.50	4.28
$H(2P_o)$	-	-	-	-	11.80	6.80	10.62	20.19	22.29	16.19	13.13	-	-
$H(2P_1)$	-	-	-	-	2.70	5.02	6.46	7.83	14.59	18.20	15.64	-	-
H(2P)	-	-	-	-	14.50	11.82	17.08	28.02	36.88	34.39	28.77	2.46	1.95
H(2)	4.55	8.78	10.15	17.78	21.00	18.16	24.38	43.19	51.88	42.97	33.47	7.96	6.23
P_o^{2P}	-	-	-	-	0.239	0.051	0.084	0.160	0.072	-0.019	-0.028	-	-

TABLE 5.2. Capture and Excitation Cross Sections (in units of 10^{-17} cm^2) computed in the 1S, 2S, 2P close coupling approximation. P_o^{2P} represent the 2P polarization fractions; H(2): excitation to the n=2 level; $He^+(2)$: capture to the n=2 level; $He^+(1+2)$: total capture to the n=1 and n=2 levels.

State of Capture		Energy of He^{2+} (keV) 6.3	7.0	10.0	15.0	15.81	20.0	25.0	40.0	50.0	100	200	400	800
$He^+(2S)$	Q_M	9.07	-	17.10	-	25.80	25.10	24.10	19.20	15.30	11.30	5.00	1.21	0.18
	Q_R	-	21.67	29.50	38.74	-	-	27.31	-	26.69	12.61	2.55	0.43	-
	Q_P	22.07	-	27.82	-	25.21	24.41	23.37	27.92	28.44	16.33	2.13	0.23	0.06
$He^+(2P)$	Q_M	28.50	-	54.20	-	83.00	92.80	95.80	90.70	82.70	44.50	13.16	2.02	0.14
	Q_R	-	62.82	81.17	84.85	-	-	96.16	-	66.98	37.83	11.70	1.72	-
	Q_P	42.31	-	69.98	-	83.63	89.82	86.62	68.98	63.50	30.59	12.31	2.74	0.40
$He^+(2)$	Q_M	37.60	-	71.30	-	108.00	118.00	120.00	110.00	99.00	55.80	18.20	3.22	0.32
	Q_R	-	84.49	110.67	123.59	-	-	123.47	-	93.67	50.44	14.25	2.15	-
	Q_P	64.38	-	97.80	-	109.84	114.23	109.99	96.90	91.94	46.92	14.44	2.97	0.46
$He^+(1+2)$	Q_M	-	-	-	-	-	-	120.06	-	99.30	56.77	19.92	4.23	0.57
	Q_R	-	84.68	110.10	124.03	-	-	124.16	-	96.00	58.53	25.56	6.61	-
	Q_P	65.55	-	101.79	-	114.68	117.30	111.45	98.27	94.32	48.01	15.21	3.15	0.81

Table 5.3. Capture cross sections (in units of 10^{-17} cm^2). Q_M: Malaviya's five-state results; Q_R: Rapp's eight-state cross sections; Q_P: present four-state close-coupling calculations. $He^+(2)$ represent capture to the n=2 level of He^+ and $He^+(1+2)$ the total capture to both n=1 and n=2 levels of He^+.

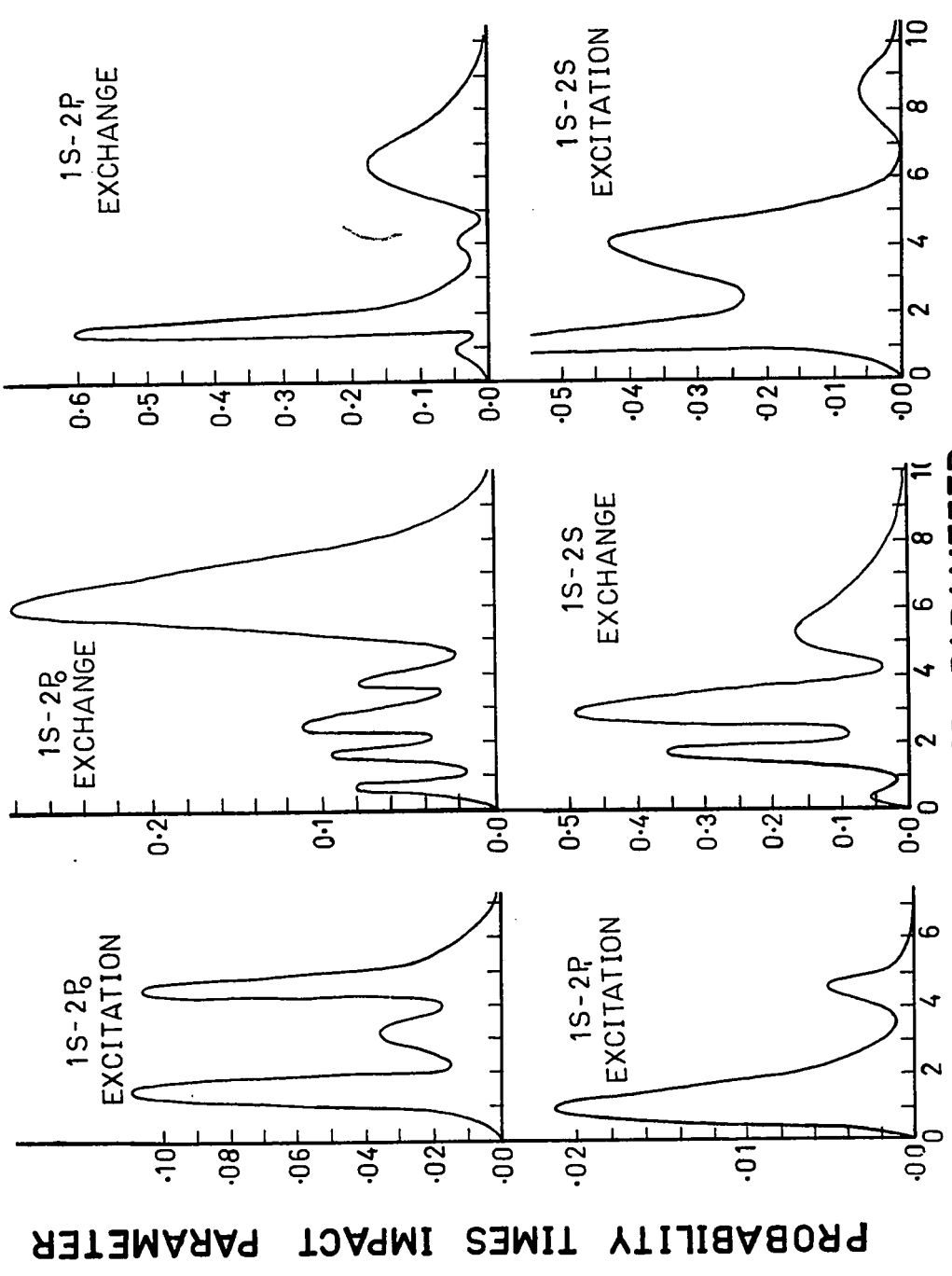

Fig. 5.1. Probability Times Impact Parameter Versus Impact Parameter For Excitation And Charge Exchange At 6.3keV. (pseudo)

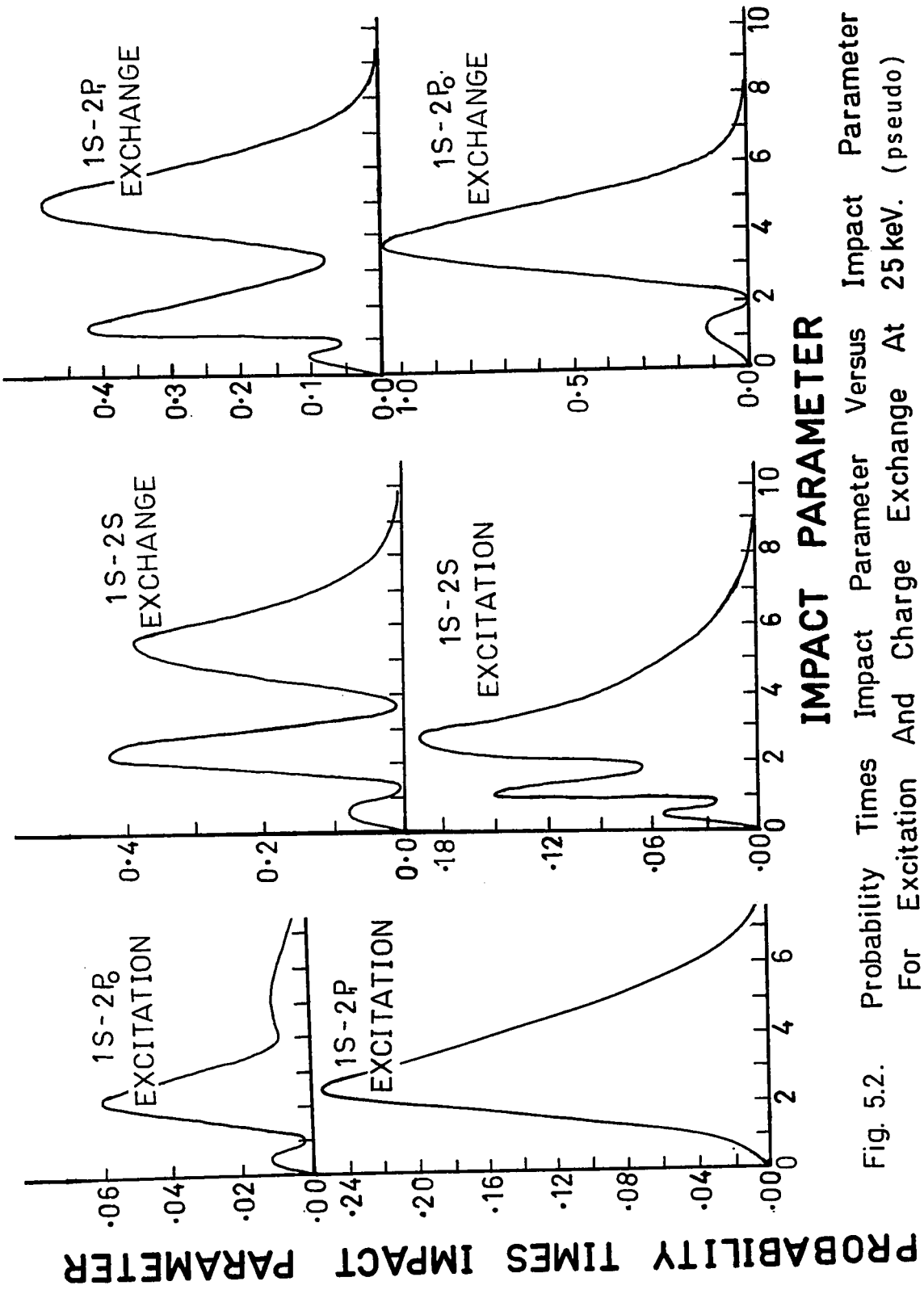

Fig. 5.2. Probability Times Impact Parameter Versus Impact Parameter For Excitation And Charge Exchange At 25 keV. (pseudo)

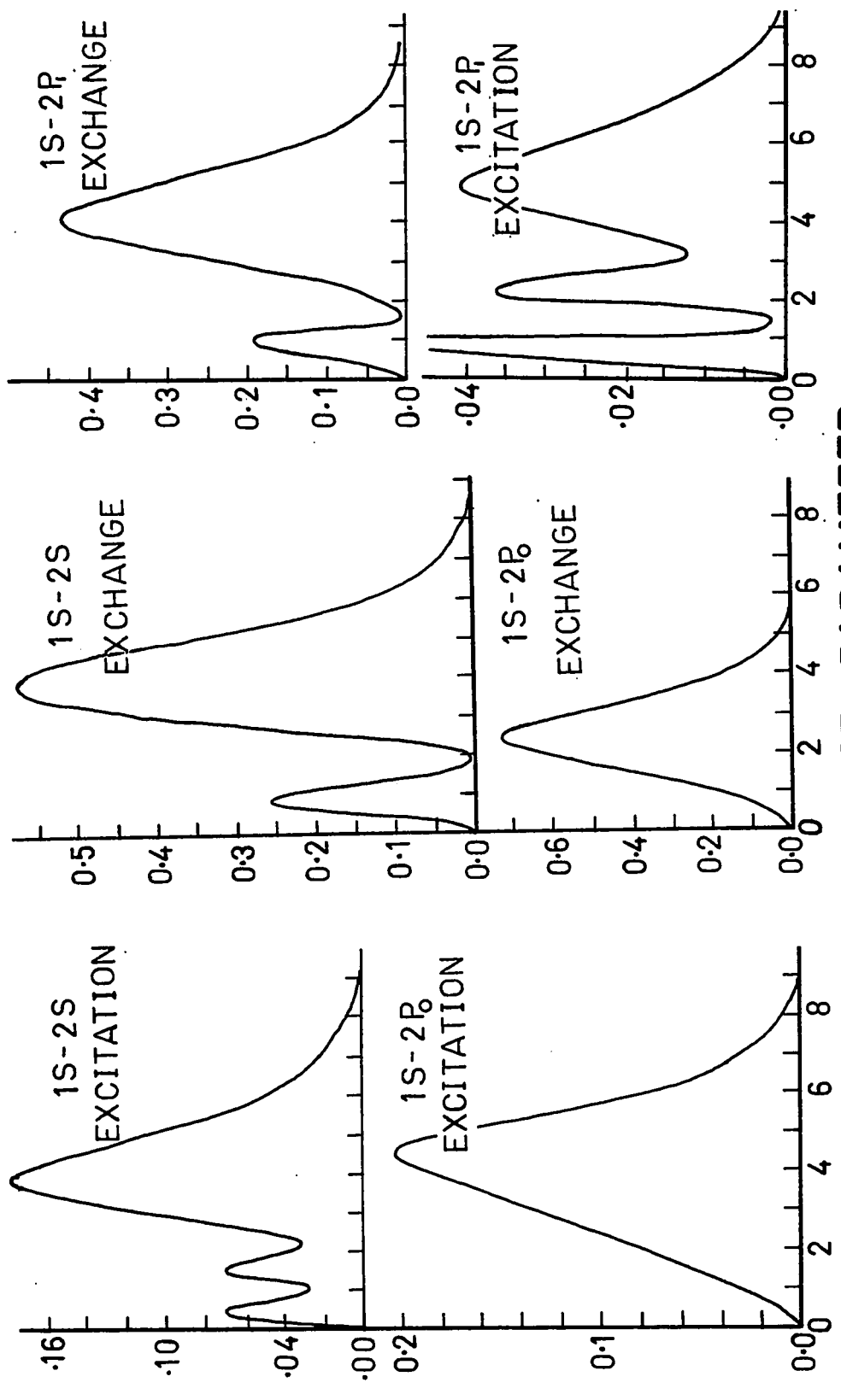

Fig. 5.3. Probability Times Impact Parameter Versus Impact Parameter For Excitation And Charge Exchange At 50 keV. (pseudo)

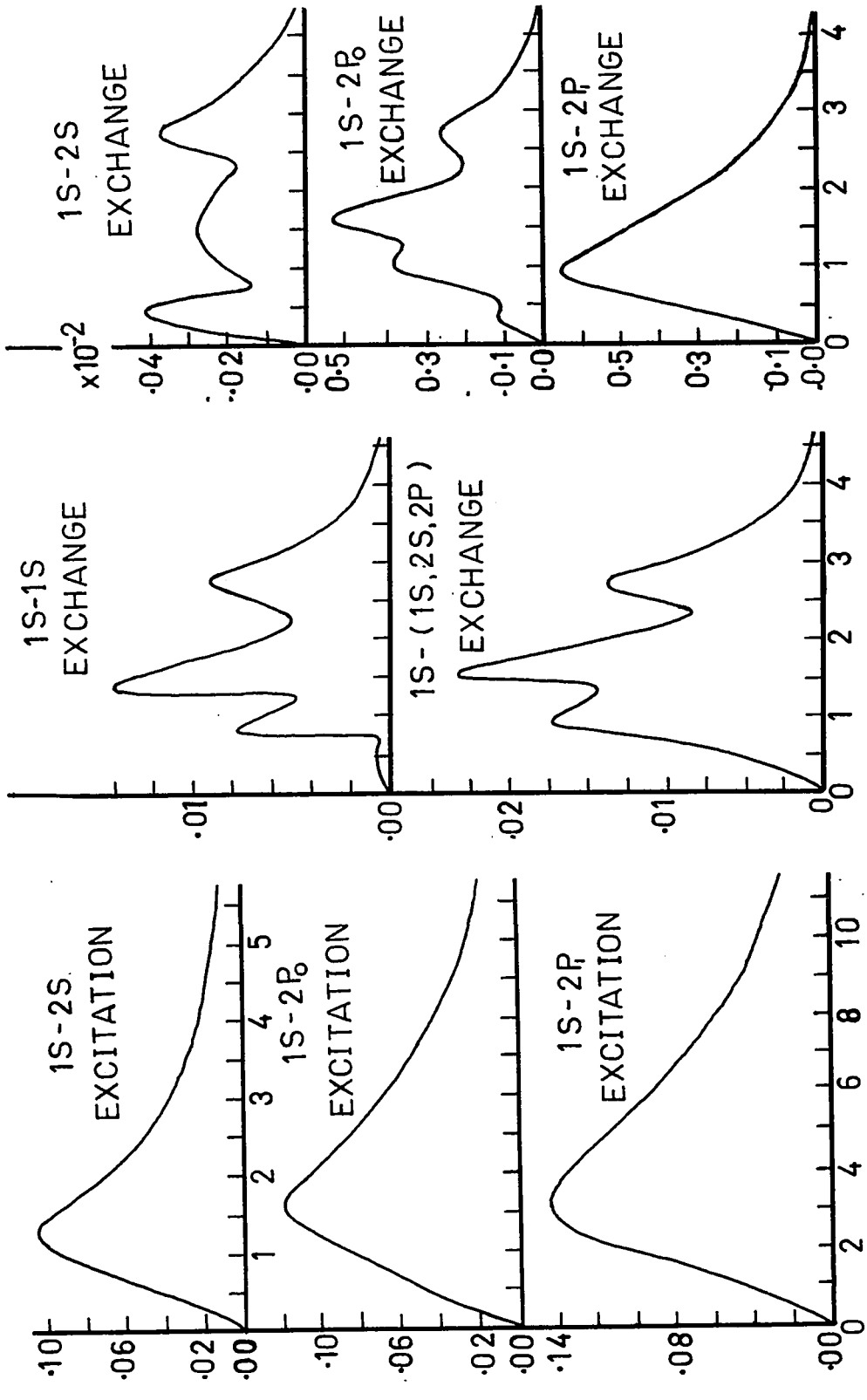

Fig. 5.4. Probability Times Impact Parameter Versus Impact Parameter For Excitation And Charge Exchange At 800 keV. (pseudo)

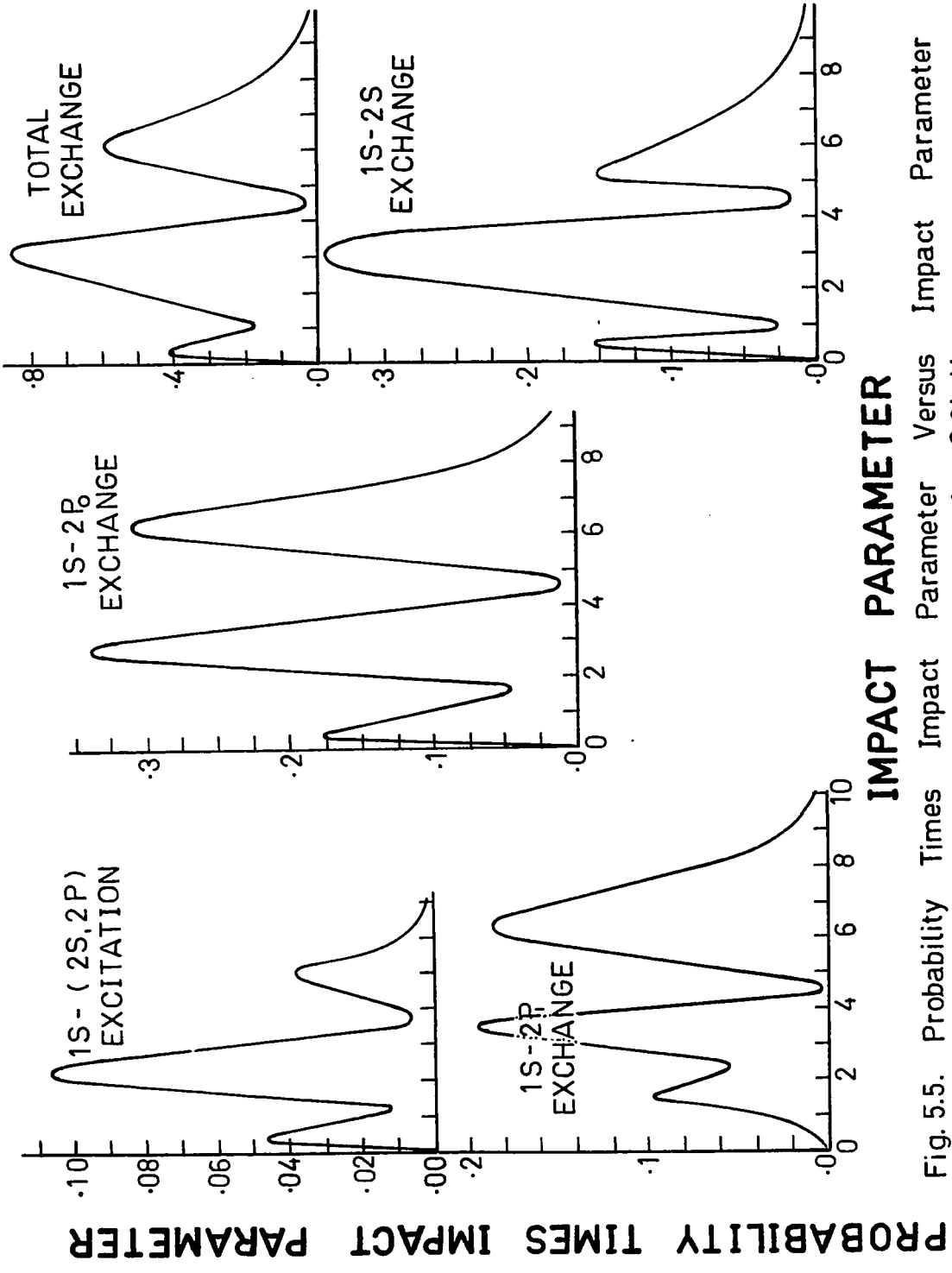

Fig. 5.5. Probability Times Impact Parameter Versus Impact Parameter For Excitation And Exchange At 6.3keV.

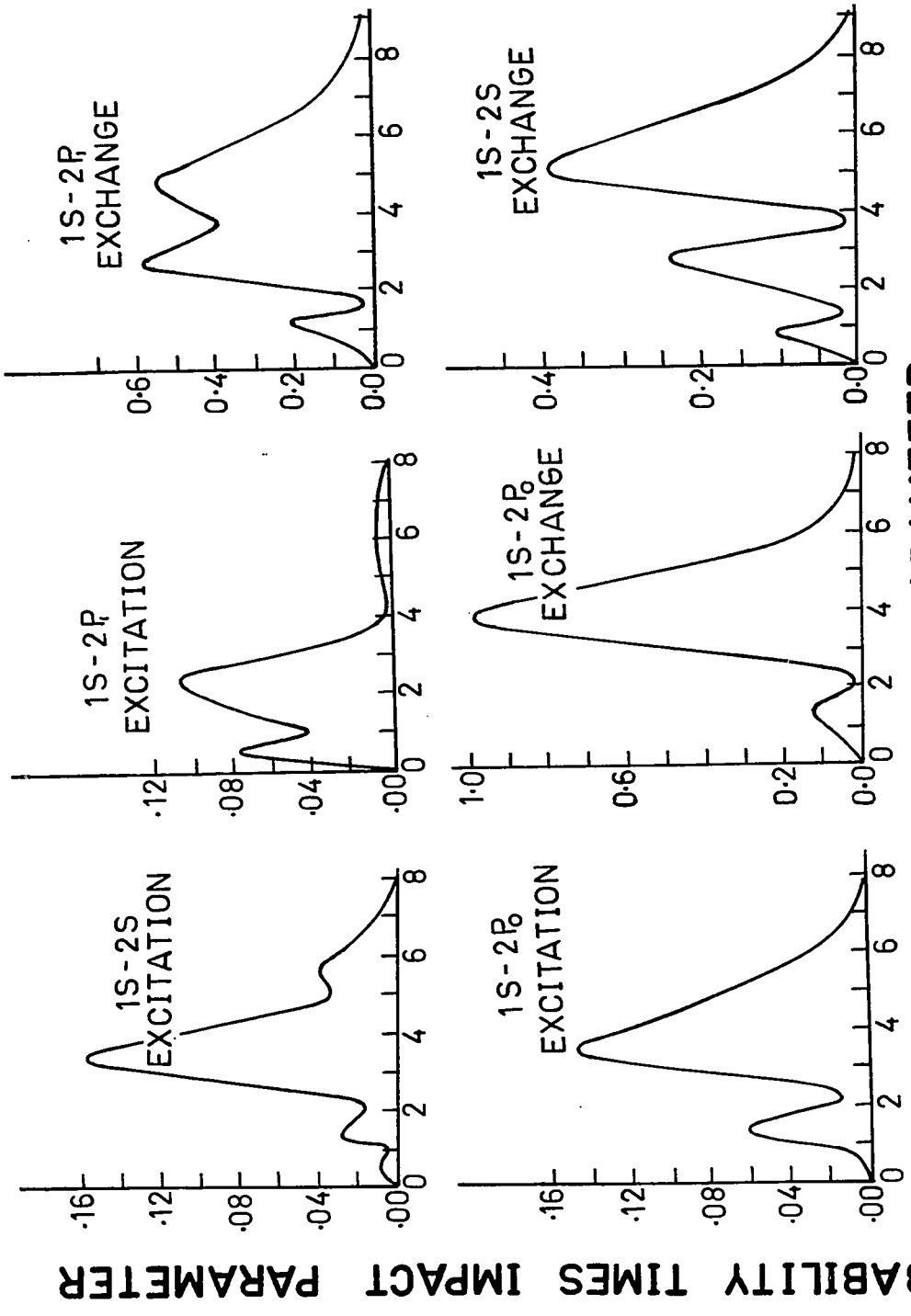

Fig. 5.6. Probability Times Impact Parameter Versus Impact Parameter For Excitation And Charge Exchange At 25 keV.

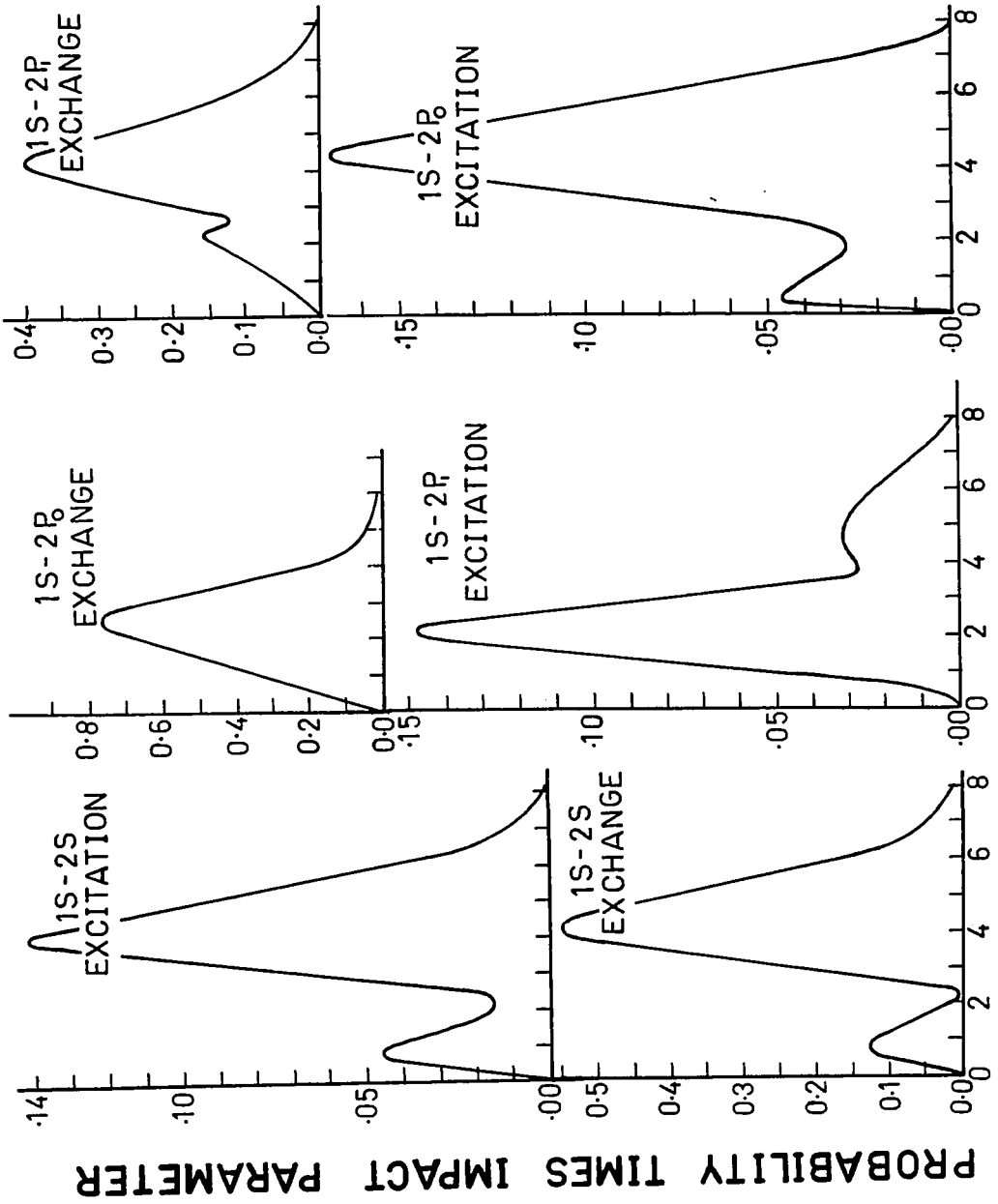

Fig. 5.7. Probability Times Impact Parameter Versus Impact Parameter For Excitation And Charge Exchange At 50keV.

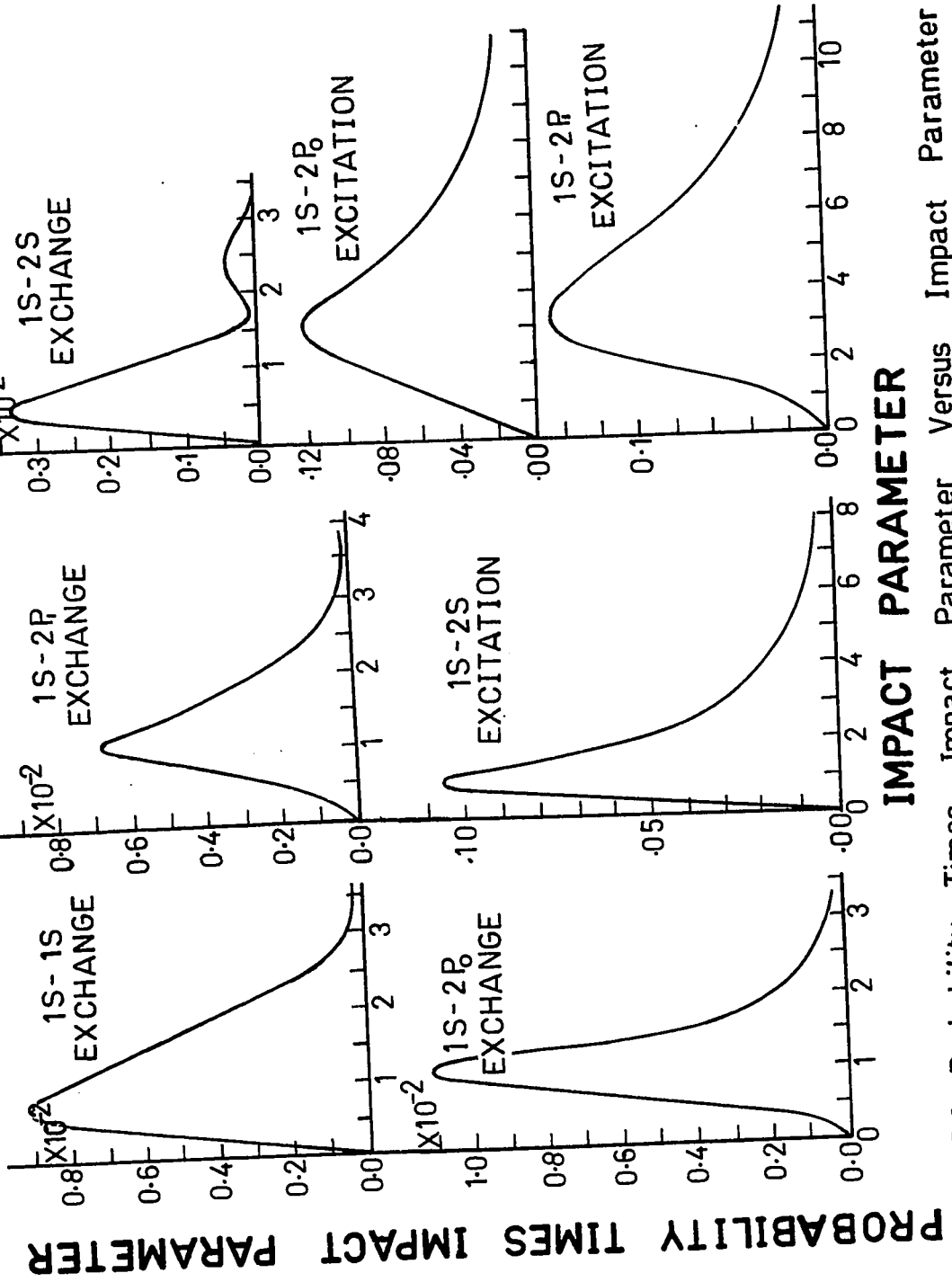

Fig. 5.8. Probability Times Impact Parameter Versus Impact Parameter For Excitation And Charge Exchange At 800keV.

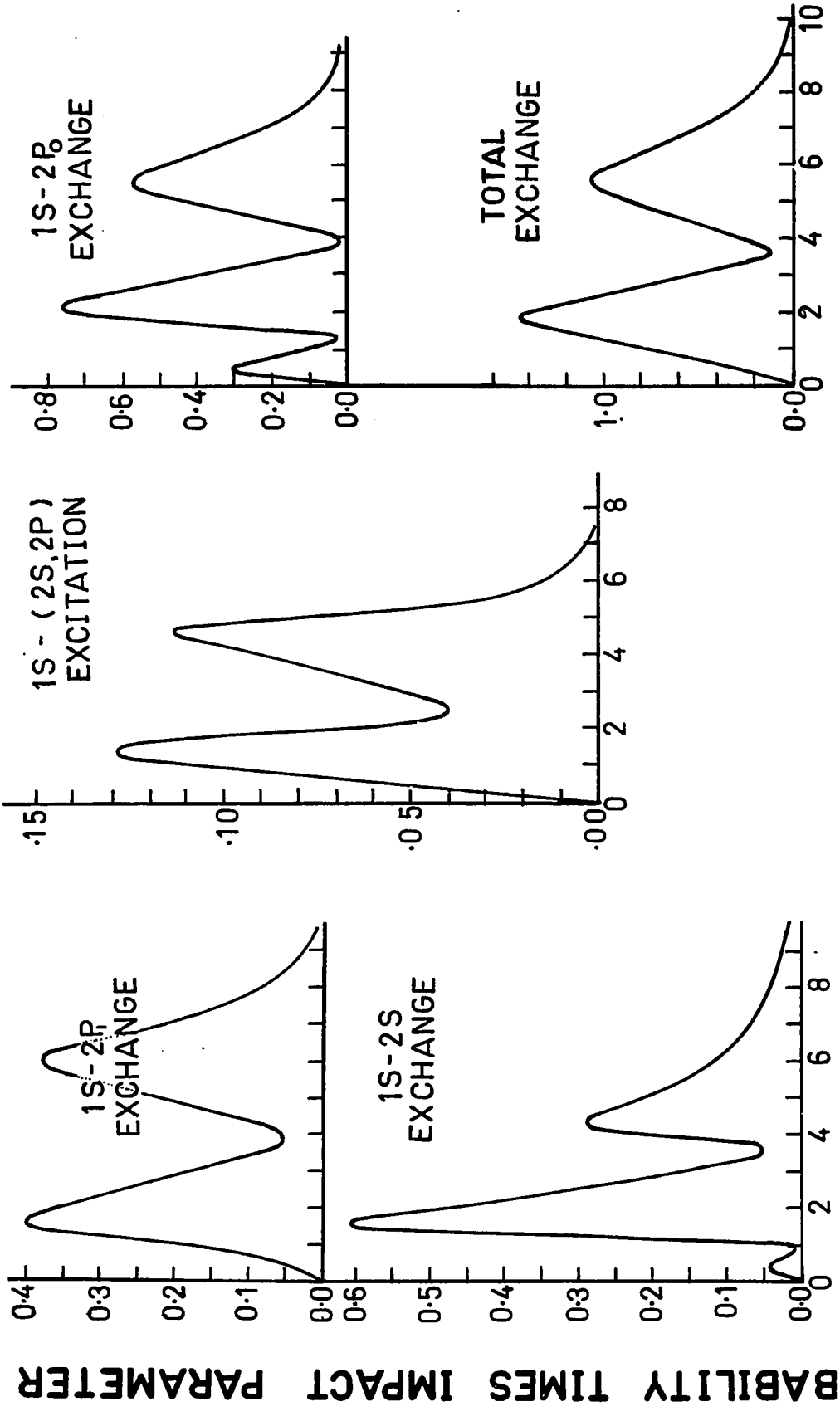

Fig. 5.9. Probability Times Impact Parameter Versus Impact Parameter For Excitation And Charge Exchange At 10keV

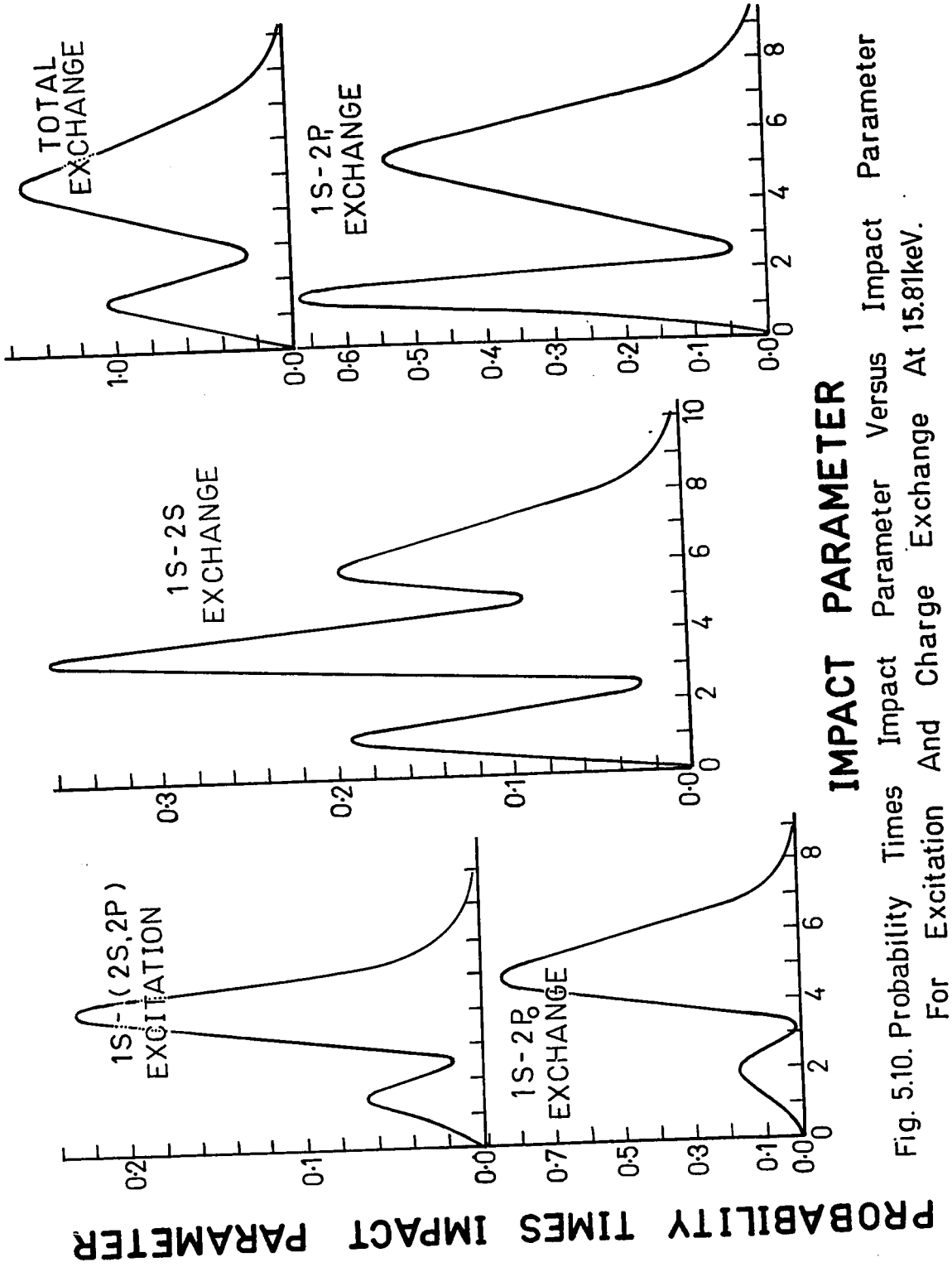

Fig. 5.10. Probability Times Impact Parameter Versus Impact Parameter For Excitation And Charge Exchange At 15.81keV.

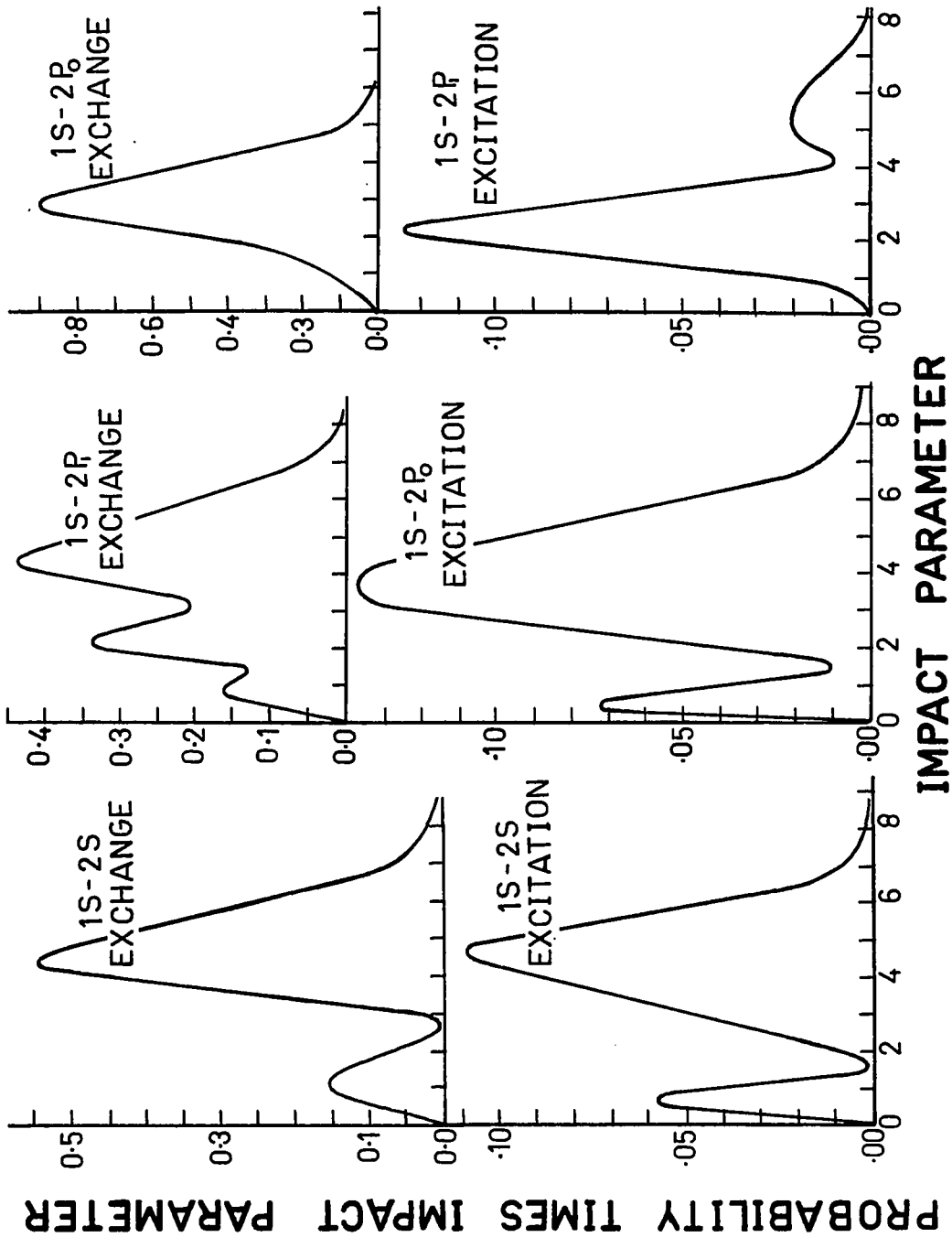

Fig.5.11. Probability Times Impact Parameter Versus Impact Parameter For Excitation And Charge Exchange At 40 keV.

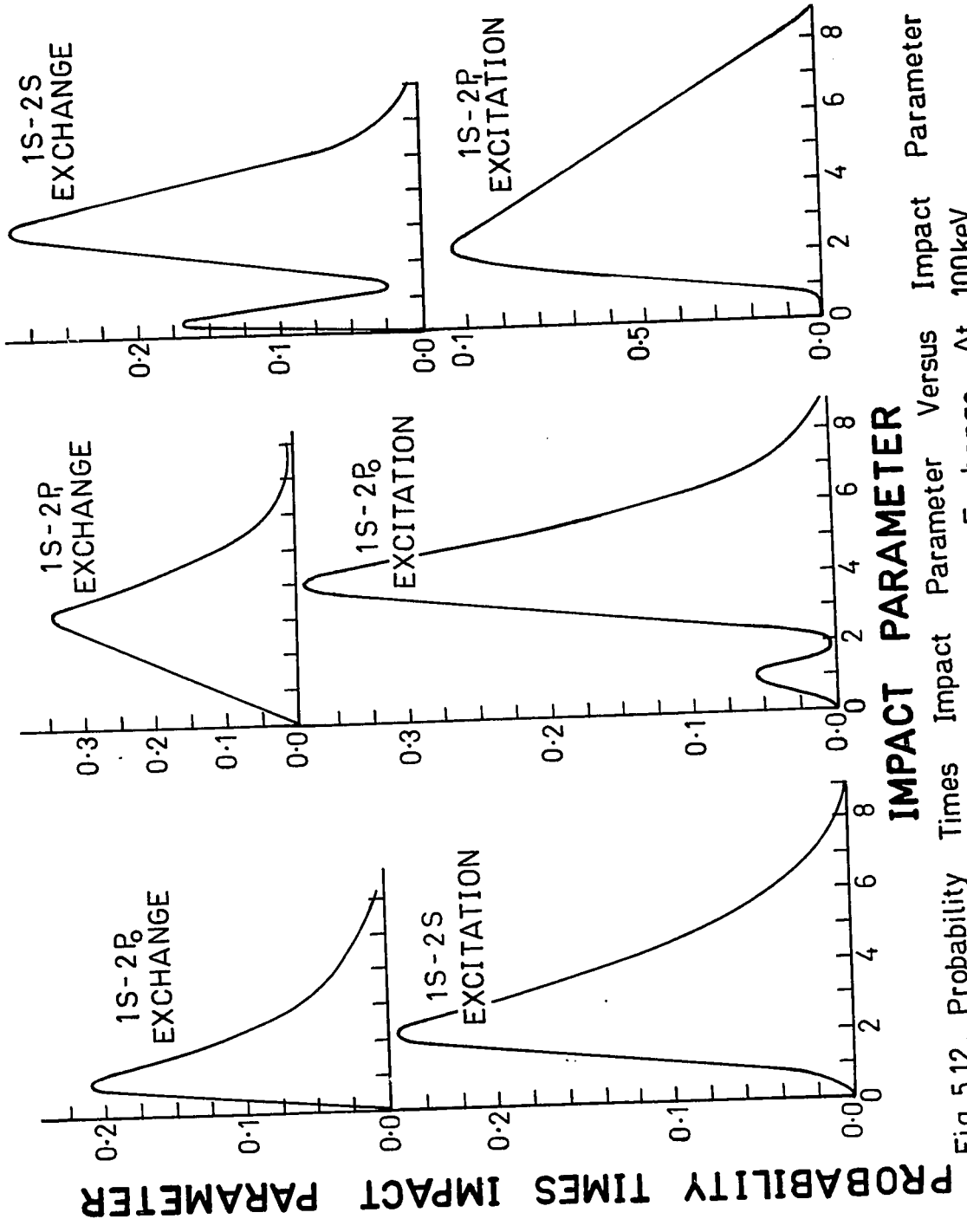

Fig. 5.12. Probability Times Impact Parameter Versus Impact Parameter For Excitation And Charge Exchange At 100keV.

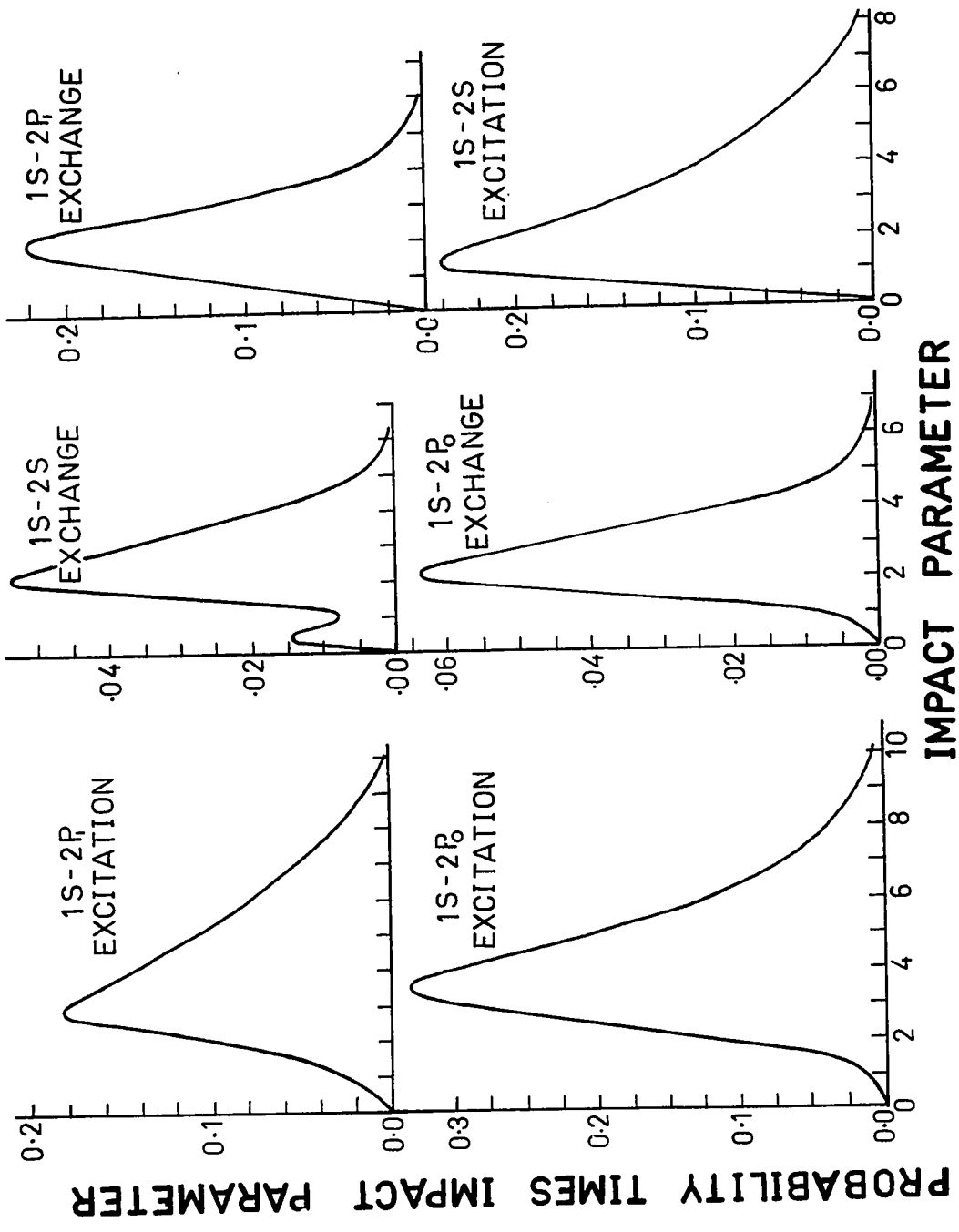

Fig. 5.13. Probability Times Impact Parameter Versus Impact Parameter For Excitation And Charge Exchange At 200keV.

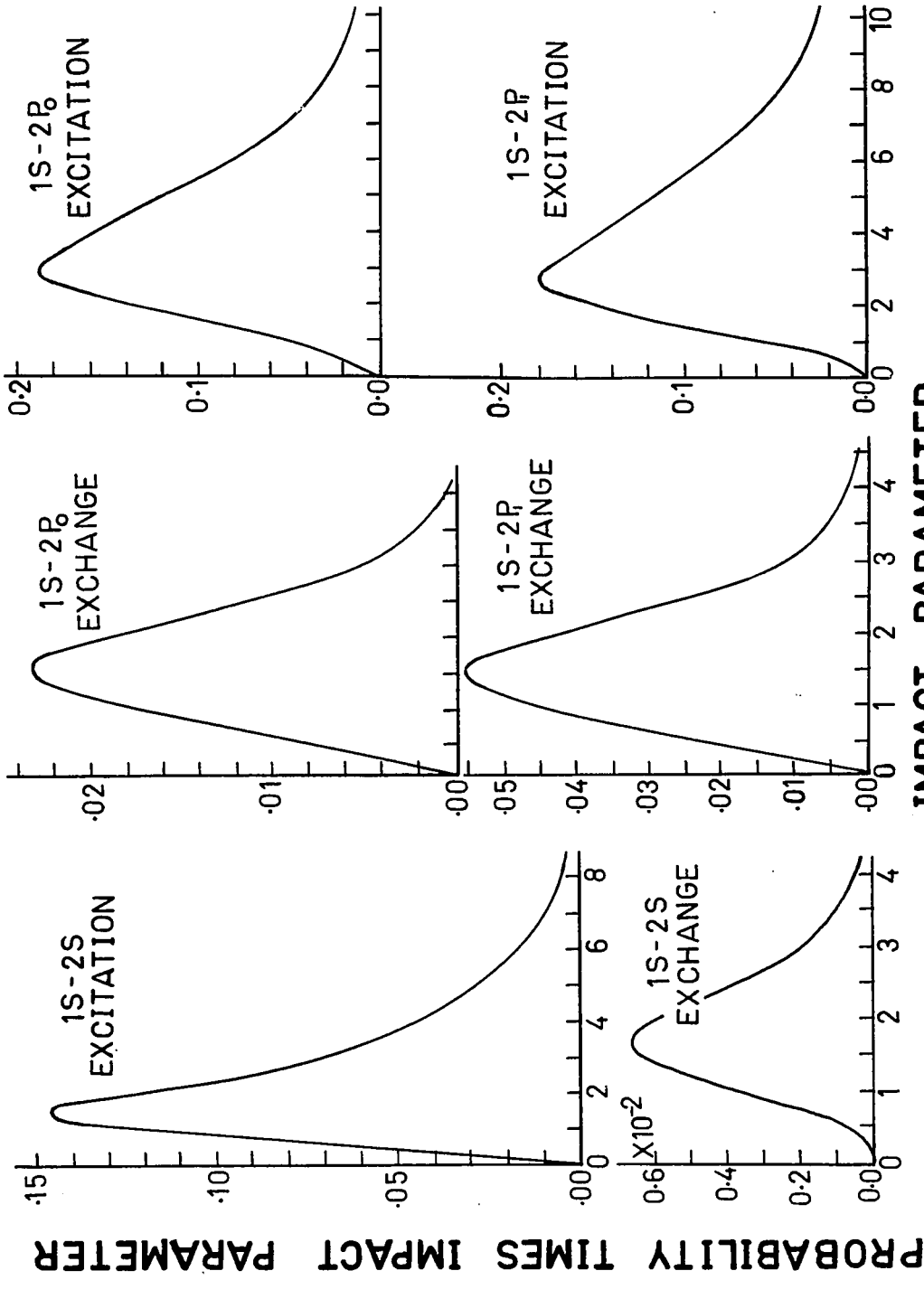

Fig. 5.14. Probability Times Impact Parameter Versus Impact Parameter For Excitation And Charge Exchange At 400keV.

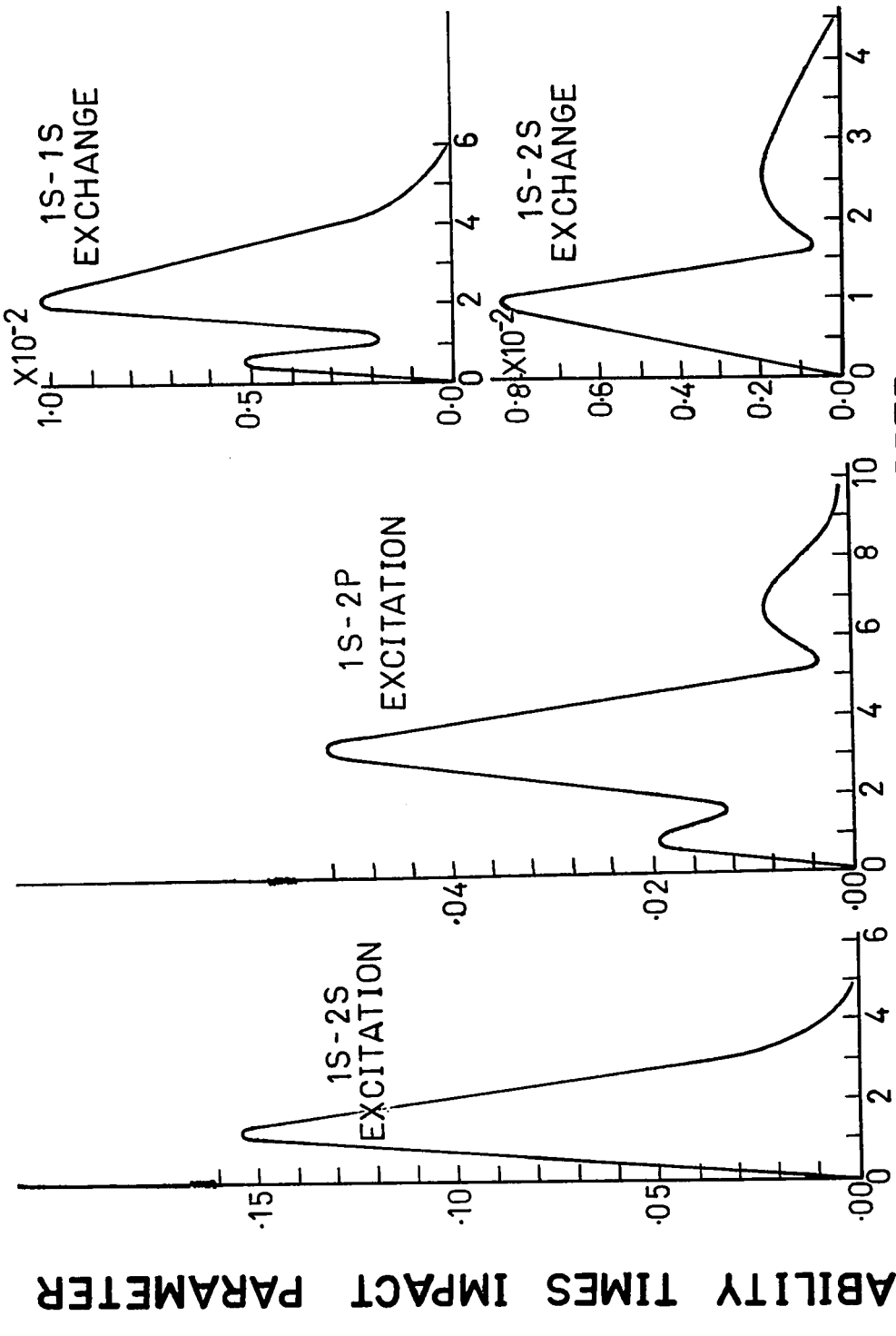

Fig. 5.15. Probability Times Impact Parameter Versus Impact Parameter For Excitation And Charge Exchange At 3000 keV.

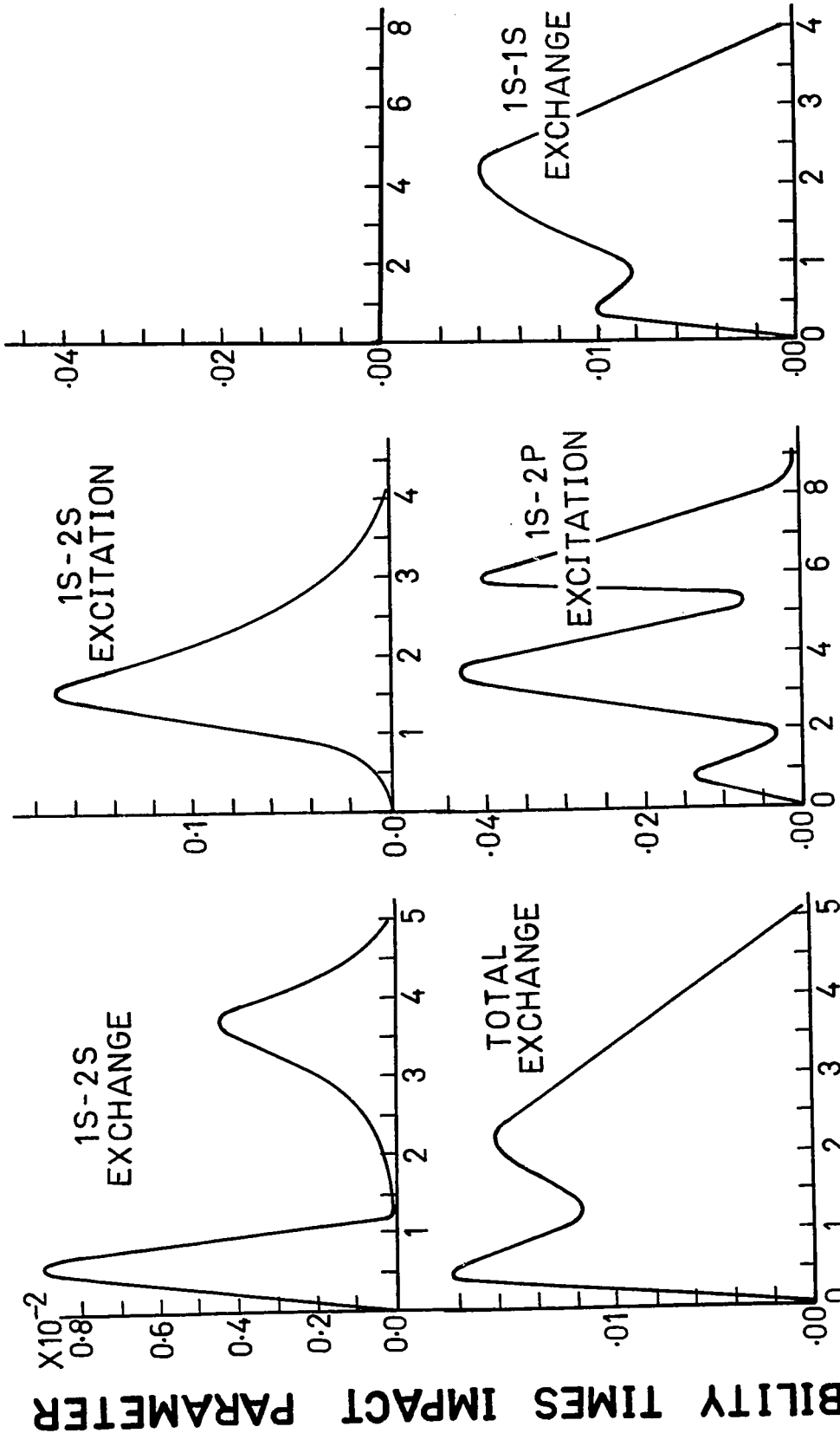

Fig. 5.16. Probability Times Impact Parameter Versus Impact Parameter For Excitation And Charge Exchange At 4000keV.

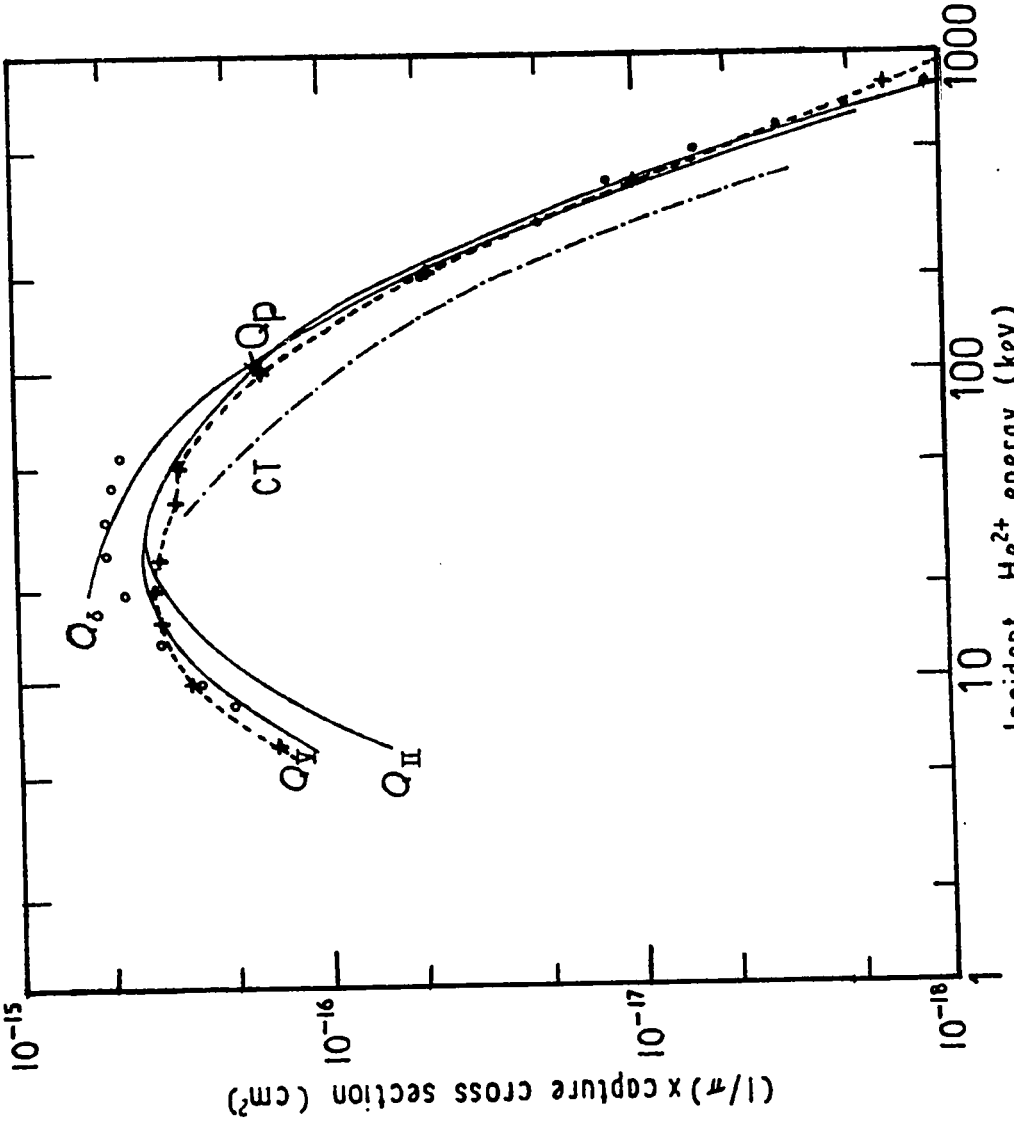

Fig. 5.17. Capture cross sections to the n=2 level of He^+. Q_δ, the two-state approximation of McElroy; Q_{II}, Q_V, two- and five-state approximation of Malaviya; CT, impulse approximation of Coleman and Trelease; Q_p, present four-state; experiments: O Fite et al.; ● Pivovar et al.

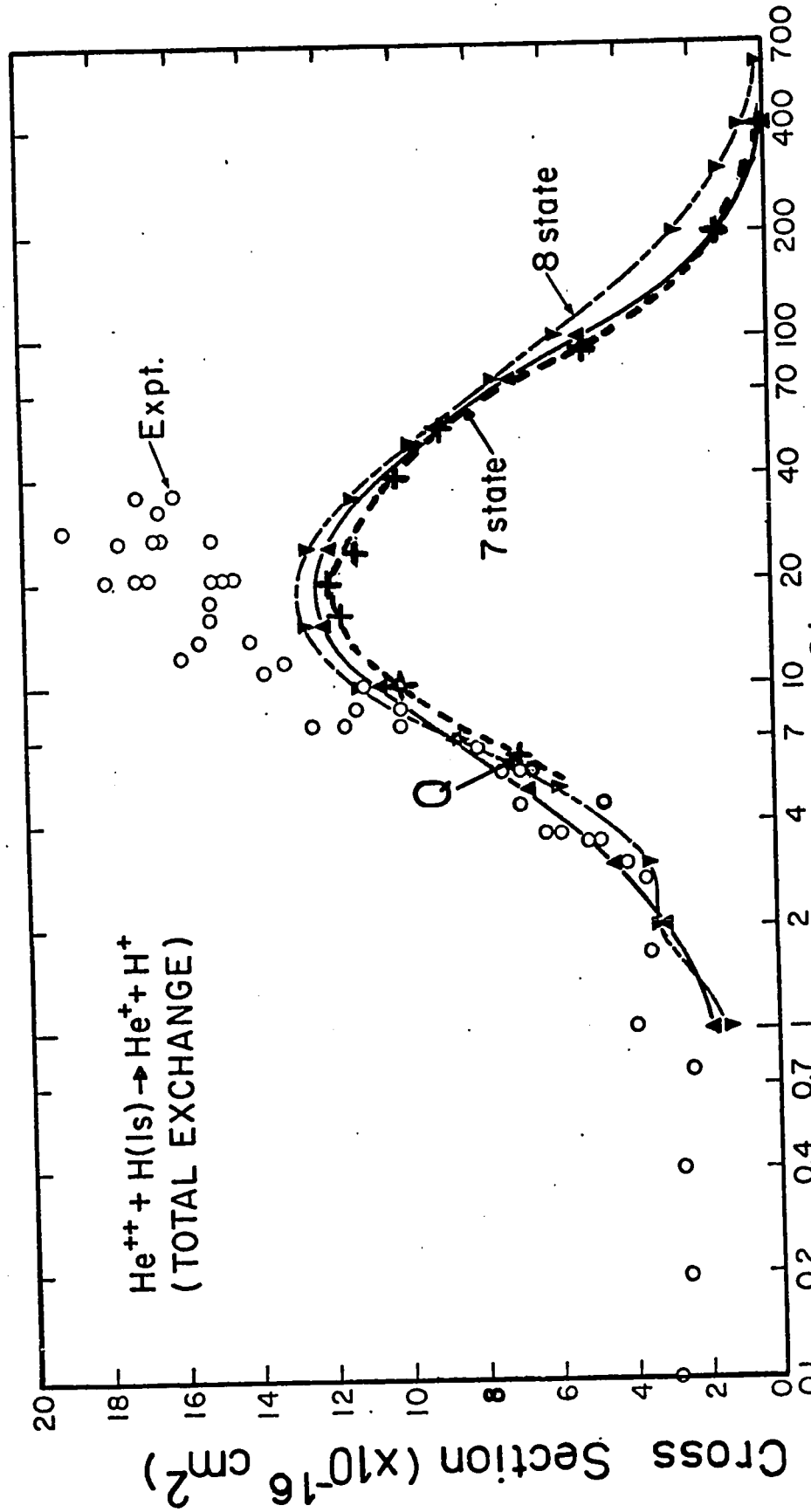

Fig. 5.18. Total capture cross sections. O Experiments of Fite et al.; ▼ eight-state and ▲ seven-state calculation by Rapp; + (Q) present four-state results.

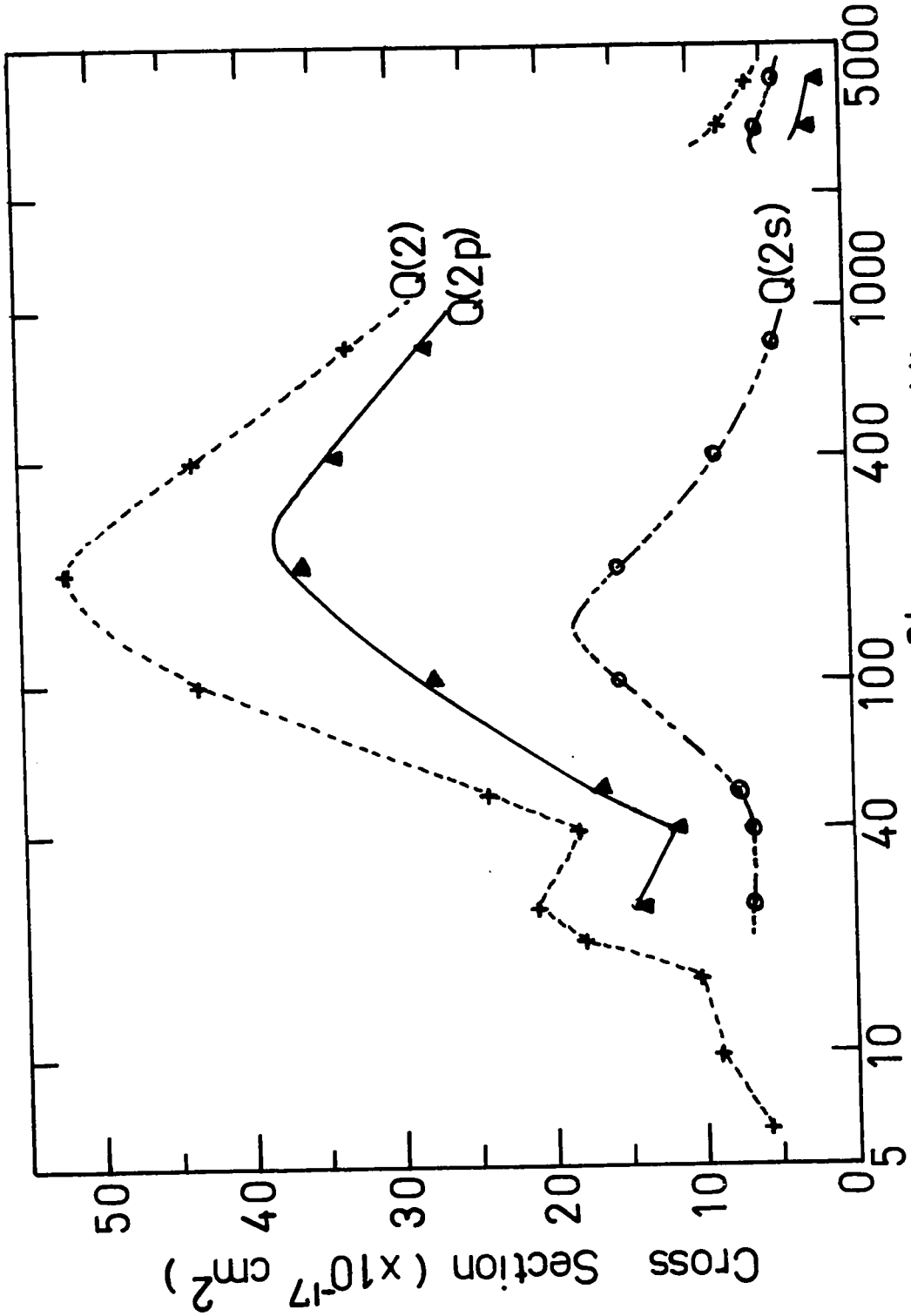

Fig. 5.19. Excitation cross sections: Q(2), excitation to 2S + 2P; Q(2P), excitation to 2P; Q(2S), excitation to 2S.

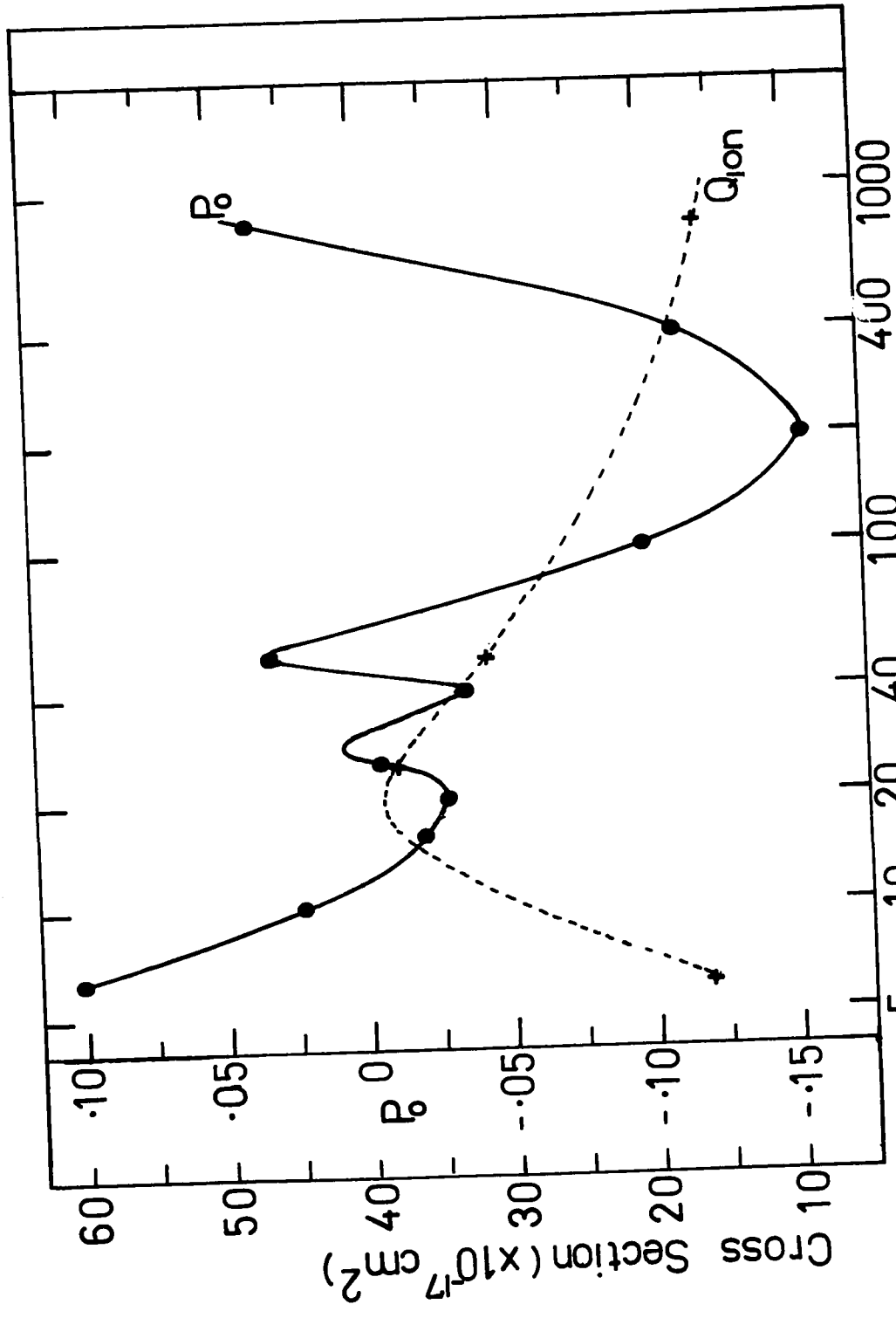

Fig. 5.20. Ionization cross sections, Q_{ion} and 2P Polarization fractions, P_o.

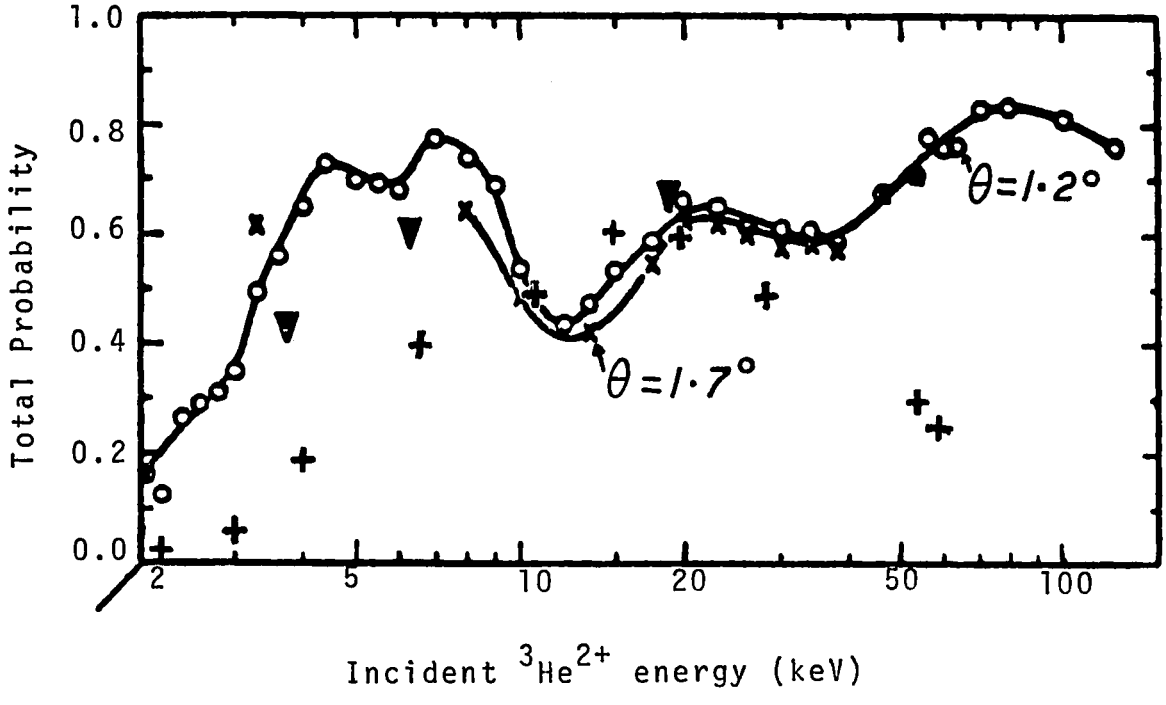

Fig. 5.21. Total charge transfer probability at θ = 1.2° and θ = 1.7° from the 1s state for the process $^3He^{2+}$-H collision. O and X represent the experimental measurements by Keever et al. (referred to as Everhart curve). Calculated points for θ = 1.2°: + eigenstates, ▼ pseudostates.

CHAPTER VI
CONCLUSION AND SUGGESTIONS

6.1. Conclusion

We have generalized the Wilets and Gallaher (1966) formulation for the collision between protons and hydrogen atoms to the collision of a heavy unstructured ion with atomic hydrogen which may be in the ground state or in any of its excited levels. We have then solved the resulting coupled differential equations and constructed a computer program to extract numerical results. Using this computer program, the theory has been tested by substituting an α-particle for the heavy ion to calculate both charge transfer and excitation cross sections. We also computed polarization fractions for 2p states and estimated ionization cross sections for the cases in which pseudo-states were employed.

In the first venture, that is the mathematical development we think we have succeeded, whereas in the second, only partly. If the mathematical treatment were incorrect, it would be virtually impossible to obtain any sensible results. In the application of the theory to the collision of an α-particle with atomic hydrogen we have established

that for α-particle energies less than about 15 keV the neglect of rotational coupling effects arising from the rotation of the internuclear line leads to incorrect results for charge transfer cross sections. The conclusion is supported by the calculation of Rapp (In the press) whose results are in good agreement with the experiments of Fite et al. (1962) in this energy range. For high energies of the incident α-particle we have shown that charge transfer cross sections to the $He^+(1s)$ level predominates over those to $He^+(2s)$ or $He^+(2p)$ and is further confined to a range of small values of the impact parameter. Again here our calculated conclusions are supported by those of Rapp. The high energy behaviour of the charge transfer cross sections follows the same trend as those of Malaviya (1969) except for some small differences in the numerical results.

The calculation of charge transfer at moderate energies of the α-particle is not that rosy. Although the theoretical calculations of total charge transfer do not differ that much, there is a discrepancy between theory and the experimental results of Fite et al. around 25 keV. This disagreement between the calculated and measured charge transfer cross sections is puzzling. Even the use of pseudo-states which tends to increase the cross sections at low and high energies does not bridge this gap. Before carrying out lengthy and costly computations on the charge transfer process coupling

more and more eigenstates or pseudo-states one ought perhaps to pause to question the accuracy of experimental measurements in this region of discrepancy.

The absence of experimental observations on excitation cross sections for the process He^{2+} - H collision leaves us with nothing to assess our success or failure. Charge transfer and excitation cross sections are calculated simultaneously in our method of computation. The sensitivity of excitation probabilities to variations in the unitarity condition is no more than that for the corresponding charge transfer probabilities. As pointed out before, our total charge transfer calculations compare well with those of Rapp at low energies and relatively high energies. The only available results on excitation of the H atom by α-particle impact are those by Rapp and by Bates (1962). There are no experimentally measured excitation cross sections on He^{2+} - H collisions. Our 1s - 2p excitation cross sections give good agreement with the distorted approximation results by Bates at 40, 50 and 800 keV. The closest agreement with Rapp's results on 1s - 2p excitation cross section is 34.39 compared with Rapp's 26.88 in units of 10^{-17} cm^2. Our 1s - 2s excitation cross sections give better agreement with those of Rapp and are much higher than those calculated by Bates.

Maybe our calculation of excitation and ionization cross sections together with the discrepancy between experiment and

the results of both Rapp and this calculation on charge transfer cross sections around 25 keV will stimulate more experimentation and theoretical computation on both charge transfer and excitation of the hydrogen atom by α-particle impact.

Finally, it ought not to be expected of us to have calculated every theoretical number conceivable pertaining to the He^{2+} - H collision. The limitations imposed by the availability of computing funds have curtailed our ambitions to investigate He^{2+} - H collisions more extensively.

From the attempt to reproduce the 1.2° Keever et al. curve of total charge transfer probability versus impact energy, we have discovered that it is almost impossible to achieve agreement with the experimentally measured points in a calculation employing a four-state approximation. We therefore believe that the hope of agreement between experimental measurements and theoretical calculations at very small impact parameters which are inherent in the experimental measurements of Keever et al. lies in a pseudo-state expansion basis.

The fact that we have generalized the Wilets and Gallaher (1966) formulation, devised numerical methods and constructed a corresponding computer program, as well as applied the program to the explicit case of an α-particle colliding with a hydrogen atom in our first attempt makes us feel more successful than defeated. Discrepancies in calculated results only attest to the difficulties inherent

in making this type of complex calculation.

6.2. Suggestions for future work

Future calculations on charge transfer and excitation might be carried out by abandoning the artifice of assuming a linear trajectory for the heavy ions in favour of more realistic hyperbolic trajectories. The major problem, however, in the calculation we have undertaken involves the computation of the momentum transfer terms. Their evaluation requires the use of both the Gauss-Legendre and Gauss-Laguerre quadrature methods. The Gauss-Legendre method is in general the more time consuming of the two. Consequently Gallaher (not yet tested) has devised an analytical scheme for the evaluation of the exchange matrix elements involving momentum transfer factors which eliminates the Gauss-Legendre method. If this scheme proves feasible the computation of the exchange type matrix elements should proceed very rapidly. The Bulirsch and Stoer formula employed by Gaussorgues and Salin (1971) for time integrating the amplitudes is supposed to be faster than the Adams-Moulton method employed in this thesis. Consequently, to speed up the calculations, these changes would have to be incorporated into our computer program. With these modifications we entertain the possibility of retaining the hydrogen 1s, 2s, 2p states and the He^+ 1s, 2s and 2p states and augmenting these with the 3s and 3p pseudo-states in the manner of Cheshire et al. (1970). Thus we should be able to carry out further

heavy ion-hydrogen atom collisions and obtain the Keever et al. curves at 1.2° and 1.7°.

In the near future we intend to carry out calculations involving the collisions of ions such as μ^+, π^+, d and Li^{3+} with atomic hydrogen, study rotational coupling effects upon charge transfer cross sections in a multi-state approximation and calculate differential cross sections for the He^{2+} - H collision.

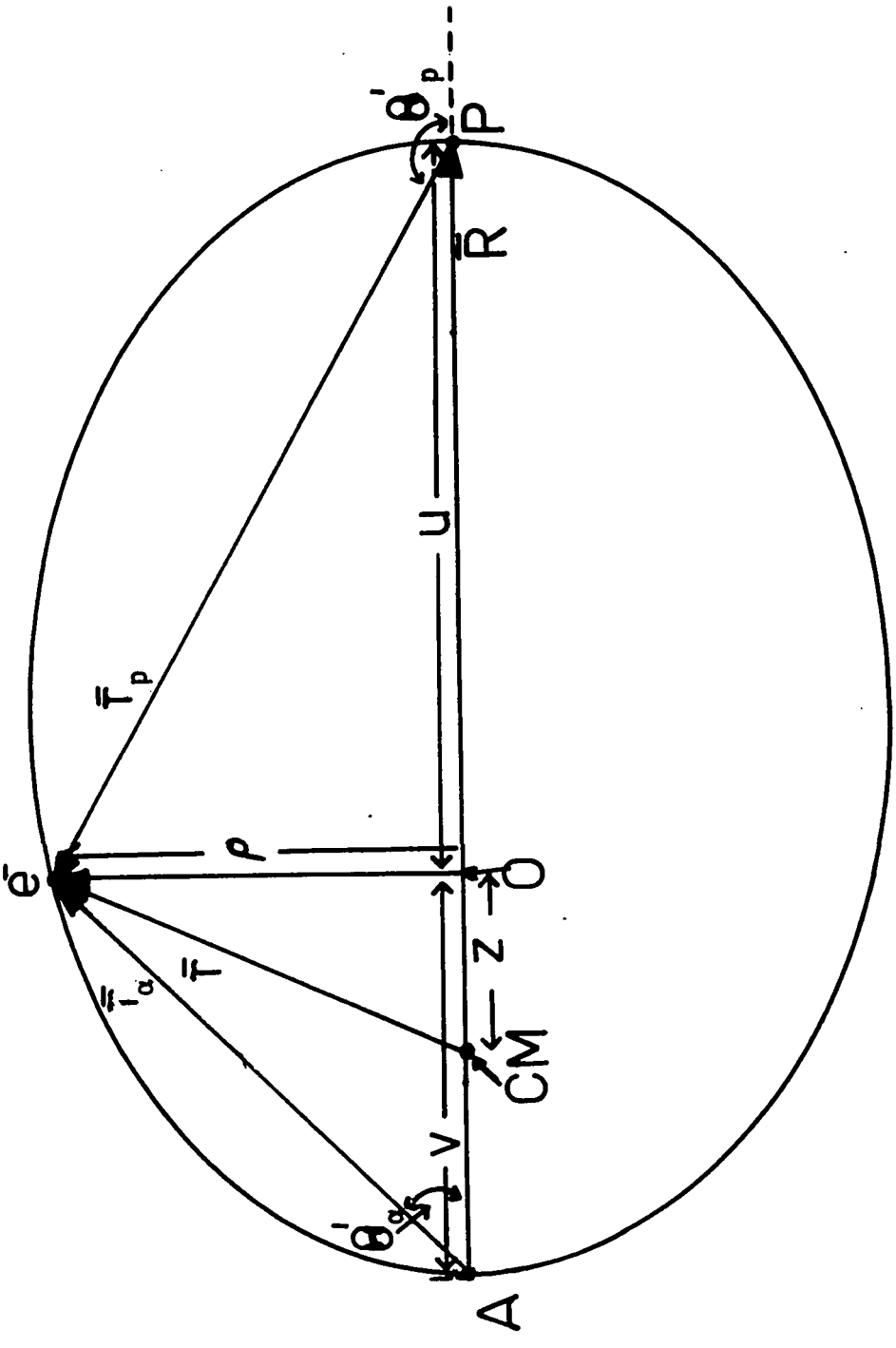

Fig. A.1. Confocal elliptic coordinates for the two-centre problem.

APPENDIX A

In this appendix we shall derive expressions for z', $\cos\theta'_\alpha$, $\cos\theta'_p$, $\rho' = \sqrt{x'^2 + y'^2}$ and the Jacobian $J(\rho', \phi', z' \to \xi, \phi', \eta)$ in terms of prolate elliptic coordinates. These quantities are required in the integration of the spatial matrix elements in (2.22a).

Let z be measured from CM (the centre of mass) to O, v from A to CM, u from P to CM and ρ from O to e^-. The rest of the symbols retain the same meaning as in Chapter II. Thus one writes

$$v = \frac{m_p}{M+m_p} R \equiv pR$$

$$u = \frac{M}{M+m_p} R \equiv qR$$

with $q + p = 1$.

From the figure

$$\rho^2 = \gamma_\alpha^2 - (v + z)^2$$

$$= \gamma_p^2 - (u - z)^2$$

so that

$$\gamma_\alpha^2 - (pR + z)^2 = \gamma_p^2 - (qR - z)^2$$

which reduces to

$$2Rz(q + p) = R^2(q^2 - p^2) + \gamma_\alpha^2 - \gamma_p^2 .$$

Expressing γ_α and γ_p in terms of prolate elliptic coordinates

as $r_\alpha = \frac{R}{2}(\xi + \eta)$ and $r_p = \frac{R}{2}(\xi - \eta)$, we obtain

$$2Rz = R^2(q - p) + [\tfrac{R}{2}(\xi + \eta)]^2 - [\tfrac{R}{2}(\xi - \eta)]^2$$

$$= R^2(q - p) + (\tfrac{R}{2})^2 4\xi\eta$$

which immediately leads to

$$z = \frac{R}{2}(q - p) + (\frac{R}{2})\ \xi\eta \tag{A.1}$$

Again from the figure, one writes

$$r_\alpha \cos\theta'_\alpha = v + z$$

so that

$$\cos\theta'_\alpha = \frac{pR + \frac{R}{2}(q-p) + \frac{R}{2}\xi\eta}{\frac{R}{2}(\xi + \eta)}$$

$$= \frac{1 + \xi\eta}{\xi + \eta} \tag{A.2}$$

and

$$\cos\theta'_p = -\frac{qR - z}{r_p}$$

$$= \frac{\frac{R}{2}(q-p) + \frac{R}{2}\xi\eta - qR}{\frac{R}{2}(\xi - \eta)}$$

$$= \frac{\xi\eta - 1}{\xi - \eta} \tag{A.3}$$

Using $\rho^2 = r_\alpha^2 - (v + z)^2$, one obtains

$$\rho^2 = (\tfrac{R}{2})^2(\xi + \eta)^2 - [pR + \tfrac{R}{2}(q - p) + \tfrac{R}{2}\xi\eta]^2$$

$$= (\tfrac{R}{2})^2(\xi + \eta)^2 - [\tfrac{R}{2} + \tfrac{R}{2}\xi\eta]^2$$

$$= (\tfrac{R}{2})^2(\xi^2 - 1)(1 - \eta^2)$$

Therefore, identifying ρ with ρ', we have

$$\rho' = \frac{R}{2}\sqrt{(\xi^2-1)(1-\eta^2)} \qquad (A.4)$$

Now $\tan\phi' = \frac{y'}{x'}$ and $\rho'^2 = x'^2 + y'^2$ so that

$$y' = \rho'\sin\phi' \quad \text{and} \quad x' = \rho'\cos\phi'$$

Thus one can write

$$x' = \frac{R}{2}\sqrt{(\xi^2-1)(1-\eta^2)}\ \cos\phi'$$

$$y' = \frac{R}{2}\sqrt{(\xi^2-1)(1-\eta^2)}\ \sin\phi' \qquad (A.5)$$

$$z' = \frac{R}{2}\xi\eta \ (= z - (\frac{R}{2} - pR) = z - (qR - \frac{R}{2}))$$

To obtain the Jacobian of the transformation, we have to calculate:

$$h_1^2 = (\frac{\partial x'}{\partial \xi})^2 + (\frac{\partial y'}{\partial \xi})^2 + (\frac{\partial z'}{\partial \xi})^2$$

$$h_2^2 = (\frac{\partial x'}{\partial \eta})^2 + (\frac{\partial y'}{\partial \eta})^2 + (\frac{\partial z'}{\partial \eta})^2$$

and

$$h_3^2 = (\frac{\partial x'}{\partial \phi'})^2 + (\frac{\partial y'}{\partial \phi'})^2 + (\frac{\partial z'}{\partial \phi'})^2$$

From (A.5)

$$\frac{\partial x'}{\partial \xi} = \frac{R}{2}\frac{\xi(1-\eta^2)}{\sqrt{(\xi^2-1)(1-\eta^2)}}\ \cos\phi'$$

$$\frac{\partial x'}{\partial \eta} = -\frac{R}{2}\frac{\eta(\xi^2-1)}{\sqrt{(\xi^2-1)(1-\eta^2)}}\ \cos\phi'$$

$$\frac{\partial x'}{\partial \phi'} = -\frac{R}{2}\sqrt{(\xi^2-1)(1-\eta^2)}\ \sin\phi'$$

Similar expressions may be obtained for the variables y' and z' from (A.5). h_1^2, h_2^2 and h_3^2 can now be calculated and they are found to be

$$h_1^2 = \left(\frac{R}{2}\right)^2 \frac{(\xi^2-\eta^2)}{\xi^2-1}$$

$$h_2^2 = \left(\frac{R}{2}\right)^2 \frac{(\xi^2-\eta^2)}{1-\eta^2}$$

and

$$h_3^2 = \left(\frac{R}{2}\right)^2 (\xi^2 - 1)(1 - \eta^2) \ .$$

Therefore, the Jacobian, J which is given by

$$J = h_1 \, h_2 \, h_3$$

becomes in terms of ξ and η

$$J(\rho', \phi', z', \rightarrow \xi, \phi', \eta)$$

$$= \left(\frac{R}{2}\right)^3 (\xi^2 - \eta^2) \qquad \text{(A.6)}$$

REFERENCES

Abramowitz, M., and Stegun, I. A., Handbook of Mathematical Functions with Formulas, Graphs, and Mathematical Tables (U.S. Government Printing Office, Washington, D.C., 1970).

Basu, D., Bhattacharya, D.M., and Chatterjee, G., 1967, Phys. Rev., 163, 8.

Bates, D. R., 1958, Proc. Roy. Soc. A, 247, 294.

Bates, D. R., Atomic and Molecular Processes (Academic Press, New York, 1962).

Bates, D. R., and Lynn, N., 1959, Proc. Roy. Soc. A, 253, 141.

Bates, D.R., and McCarroll, R., 1962, Adv. Phys., 11, 39.

Brinkman, H. C. and Kramers, H. A., 1930, Proc. Acad. Sci. Amst., 33, 973.

Burke, P. G., Atomic and Molecular Collisions (H. M. Stationery Office, U. K., 1967).

Cheshire, I. M., 1968, J. Phys., B: Atom. Molec. Phys., 1, 428.

Cheshire, I. M., Gallaher, D. F., and Taylor, A. J., 1970, J. Phys. B: Atom. Molec. Phys., 3, 813.

Coleman, J. P., and Trelease, S., 1968, J. Phys. B (Proc. Phys. Soc.), [2], 1, 172.

Condon, E. U., and Shortley, G. H., The Theory of Atomic Spectra (University Press, Cambridge, 1935) p. 115.

Fite, W. L., Smith, A. C. H., and Stebbings, R. F., 1962, Proc. Roy. Soc. A, 268, 527.

Gallaher, D. F., 1967, Ph.D. Thesis, University of Washington, Seattle.

Gallaher, D. F., and Wilets, L., 1968, Phys. Rev. 169, 139.

Gallaher, D. F. (not yet published).

Gaussorgues, C. and Salin, A., 1971, J. Phys. B: Atom. Molec. Phys., 4, 503.

Geltman, S., Topics in Atomic Collision Theory, (Academic Press, New York, 1969).

Goldstein, H., Classical Mechanics (Addison-Wesley, Reading, Mass., 1950) p. 83.

Green, T. A., 1965, Proc. Phys. Soc. (London) 86, 1017.

Hildebrand, F. B., Introduction to Numerical Analysis (McGraw-Hill, New York, 1956).

Hyllerraas, E. A., Mathematical and Theoretical Physics, Vol. I, (Wiley - Interscience, New York, 1970), p. 57.

Jackson, J. D., Classical Electrodynamics (John Wiley & Sons, Inc., New York, 1962), pp. 71 and 72.

Jahnke, F., and Emde, E., Tables of Functions, Fourth Edition (Dover, New York, 1945), p. 125.

Keever, W. C., and Everhart, E., 1966, Phys. Rev., 150, 43.

Macomber, H. K., and Webb, T. G., 1967, Proc. Phys. Soc., 92, 839.

Malaviya, V., 1969, J. Phys. B: Atom. Molec. Phys., 2, 843.

McCalla, T. R., Introduction to Numerical Methods and Fortran Programming (John Wiley & Sons, Inc., New York, 1967).

McCarroll, R., and McElroy, M. B., 1962, Proc. Roy. Soc. A, 266, 422.

McDowell, M. R. C., and Coleman, J. P., Introduction to the Theory of Ion-Atom Collisions (North-Holland Publishing Company, Amsterdam, 1970), p. 192.

McElroy, M. B., 1963, Proc. Roy. Soc. A, 272, 542.

Milne, W. E., Numerical Solution of Differential Equations (John Wiley & Sons, Inc., New York, 1962).

Mott, N. F., and Massey, H. S. W., The Theory of Atomic Collisions (Oxford University Press, 1965).

Msezane, A., and Gallaher, D. F., Twenty-Fifth Annual Gaseous Electronics Conference, London, Canada, 1972.

Oppenheimer, J. R., 1928, Phys. Rev., 51, 349.

Percival, I. C., and Seaton, M. J., 1958, Phil. Trans. Royal Soc., 251, 113.

Pivovar, L. I., Novikov, M. T., and Tubaev, V. M., 1962, Sov. Phys. - JETP, 15, 1035.

Ralston, A., and Wilf, H. S., Mathematical Methods for Digital Computers, Vol. I (John Wiley & Sons, Inc., 1960), p. 110.

Rapp, D., (in the press).

Richtmyer , F. K., Kennard, E. H., and Lauritsen, T., Introduction to Modern Physics, 5th Edition (McGraw-Hill Book Company, Inc., 1955), p. 211.

Schiff, H., 1954, Can. J. Phys., 32, 393.

Schiff, L. I., Quantum Mechanics, 2nd Edition (McGraw-Hill, New York, 1955), p. 85.

Tuan, T. F., and Gerjuoy, E., 1960, Phys. Rev., 117, 756.

Wilets, L. and Gallaher, D.F., 1966, Phys. Rev., 147, 13.